# Redox Reactions and Sorption of Quinones and Natural Organic Matter at Iron Mineral/Fe(II) Interfaces

**Dissertation**
der Mathematisch-Naturwissenschaftlichen Fakultät
der Eberhard Karls Universität Tübingen
zur Erlangung des Grades eines
Doktors der Naturwissenschaften
(Dr. rer. nat.)

vorgelegt von
M.Sc. Zhengrong Xue
aus Shanghai, China

Tübingen
2017

Tag der mündlichen Qualifikation:    09.02.2018
Dekan:                               Prof. Dr. Wolfgang Rosenstiel
1. Berichterstatter:                 Prof. Dr. Stefan B. Haderlein
2. Berichterstatter:                 Dr. Silvia Orsetti

献给我所挚爱的家人

Dedicated to my beloved family

Für meine geliebte Familie

# Table of Contents

# Abstract

Redox reactions in soils and groundwater, especially at iron mineral surfaces, often play a major role in biogeochemical processes, including transformation of organic pollutants and thus are determining factors for water quality. Previous studies have shown that under anoxic conditions, ferrous iron bound to iron mineral phases forms highly reactive species and, together with redox active natural organic matter (NOM), is an important player in electron transfer processes across the mineral-water interface. On one hand, organic ligands' sorption on iron hydroxides might compete with the formation of highly reactive Fe(II) surface sites. Alternatively, redox active organic solutes might enhance the electron-transfer across the mineral surfaces. Therefore, my work focused on elucidating the dual role of sorptive organic matter regarding electron transfer at iron mineral surfaces.

To this purpose, batch experiments under anoxic conditions were conducted in suspensions containing goethite, dissolved Fe(II) and 2-hydroxy-1,4-naphthoquinone (Lawsone) as a redox probe representing important structural and functional properties of natural organic matter macromolecules. My findings indicate that the sorption behavior of the naphthoquinone lawsone on goethite is significantly altered by its redox state, as well as the amount and type of highly reactive Fe(II) sites bound to goethite surface. Reversible electron transfer processes were observed to take place at goethite surface, including the reduction of quinone (oxidize state) by Fe(II) associated with goethite and oxidation of hydroquinone (reduced state) by Fe(III) at the goethite surface. Furthermore, on the basis of dissolved equilibrium lawsone speciation, the apparent reduction potential of reactive iron species at goethite was assessed at pH 7 to be -150 ± 23 mV vs SHE. In comparison with the earlier observation on the apparent redox potential measurements by the non-sorbing quinone AQDS (anthraquinone-2,6-disulfonate), these results demonstrate that significant quinone/hydroquinone sorption does not change the apparent redox potential of the Fe(II)/Fe(III) goethite surface sites.

While quinones are well defined in structure, natural organic matter is undoubtedly more complicated due to heterogeneous functional groups. My work described a systematic study with regard to sorption and electron transfer processes of organic matter in anoxic Fe(II)/iron mineral system using Aldrich Humic Acid (AHA) as a model NOM. The obtained sorption isotherms illustrated that the redox state of AHA does not affect its sorption behavior on goethite. Also, the sorption dataset indicated that the abundance and speciation of Fe(II) sorbed to goethite can strongly enhance the redox-active organic matter sorption onto goethite depending on its redox state (i.e. untreated and electrochemically reduced AHA). Furthermore, electron transfer

reactions occur between the goethite/Fe(II) surfaces and humic acid at neutral pH, due to the significant difference between the redox potential of reactive Fe(II) associated with goethite and dissolved humic acid. Therefore, we can predict that the strong sorption ability and electron transfer process of organic matter might block the mineral surface and exhaust the redox capacity of reactive Fe(II) sorbed to the iron mineral surface, and thus limiting the reduction of organic pollutants at the iron mineral/Fe(II) interface.

To this end, sorption of quinones and humic acid on goethite has been investigated by batch experiments. Yet the bonding mechanism at molecular level still remains unclear. To identify the surface species and thus to explore the sorption mechanism, UV-Vis analysis together with in-situ flow cell measurements of attenuated total reflectance Fourier-transform infrared (ATR-FTIR) spectroscopy was conducted. First, the flow cell of the ATR-FTIR setup has been successfully established and then validated by exploring the sorption mechanism of catechol on goethite as a bidentate surface complex, consistent with the literature. The UV-Vis results indicated that the naphthoquinone lawsone can not form binary complexes with dissolved ferrous/ferric iron in the aqueous phase and also the FTIR and batch sorption data indicate the lack of significant sorption of oxidized Lawsone to goethite only. Furthermore, ATR-FTIR technique was used to investigate the sorption kinetics mechanism of organic matter (i.e, humic acid) at goethite. The spectroscopic dataset stated clearly that the carboxyl and phenol functional groups in humic acid structure form a surface complex at the goethite surface. Thus, we suggest that the high sorption of organic matter at iron mineral-aqueous interface is due to electrostatic attraction and surface complexation. However, the flow cell of ATR-FTIR measurements for the reduced species such as reduced state of lawsone and goethite-Fe(II) system need to be further evaluated.

Summarized, the combined approach and datasets of batch experiments and ATR-FTIR technique depicts a clear picture of surface reaction of redox reactive organic matter across the iron mineral/Fe(II) interface. It may be a first step to predict the effects of sorptive organic matter on pollutant fate in heterogeneous systems.

# Zusammenfassung

Redoxreaktionen in Böden und Grundwässern, vor allem an Eisenmineraloberflächen, spielen oft eine wichtige Rolle für biogeochemischen Prozesse, wie z.B. von Transformationsprozessen von organischem Schadstoff und sind entscheidend für die Wasserqualität. Bisherige Untersuchungen haben gezeigt, dass zweiwertiges Eisen (FeII), das an Eisenmineralphasen gebunden ist, unter anoxischen Bedingungen hochreduktive Spezies bildet und zusammen mit redoxaktiver, natürlicher, organischer Substanz (NOM) ein wichtiger Akteur für Elektronentransferprozesse an der Mineral/Wassergrenzfläche ist. Einerseits kann die Sorption von organischen Liganden an Eisenhydroxiden mit der Bildung hochreaktiver Fe(II)-Oberflächen konkurrieren. Andererseits könnten redoxaktive, organische, gelöste Substanzen den Elektronentransfer über die mineralischen Oberflächen verstärken. Folglich fokussiert sich diese Arbeit auf die Untersuchung der doppelten Rolle der sorptiven, organischen, Substanz bezüglich Elektronentransfer auf Eisenmineraloberflächen.

Zu diesem Zweck wurden Batch-Experimente unter anoxischen Bedingungen in Suspensionen mit Goethit, gelöstem Fe(II) und 2-Hydroxy-1,4-naphthochinon (Lawsone) als Redox-Sonde durchgeführt, die wichtige strukturelle und funktionelle Eigenschaften von Makromolekülen natürlicher organischer Substanzen darstellen. Meine Ergebnisse zeigen, dass das Sorptionsverhalten von Lawsone auf Goethit anhängt von seinem Redox-Zustand sowie von der Menge und Typ der hoch reaktiven Fe(II)-Stellen, die an die Goethitoberfläche gebunden sind. Des Weiteren wurde nachgewiesen, dass der reversible Elektronentransfer auf der Goethitoberfläche, einschließlich der Reduktion von Chinon (oxidierter Zustand) durch Fe(II), verbunden mit Goethit und Oxidation von Hydrochinon (reduzierter Zustand) durch Fe(III) an der Goethitoberfläche stattfinden. Ferner wurde basierend auf der Gleichgewichtsspeziierung von Lawsone in Lösung das beobachtete Reduktionspotential von reaktiven Eisenspezies bei Goethit in einem weiten Bereich von -150 ± 23 mV gegen SHE ermittelt. Im Vergleich zur früheren Redoxpotentialmessungen durch das nicht sorbierende Chinon AQDS (Anthrachinon-2,6-disulfat) zeigen diese Ergebnisse, dass das Vorhandensein einer signifikanten Chinon/Hydrochinon Sorption den Elektronentransferprozess über die Fe(II)/Fe(III)-Goethitoberflächen nicht beeinflusst.

Während Chinone in der Struktur gut definiert sind, ist natürliche organische Substanz zweifellos komplizierter aufgrund ihrer heterogenen funktionellen Gruppen. Diese Arbeit stellt eine systematische Untersuchung der Sorptions- und Elektronenübertragungsprozesse von organischem Material in anoxischem Fe(II)/Eisenmineralsystem dar anhand von Aldrich Huminsäure (AHA) als

Modellverbindung. Die erhaltenen Sorptionsisothermen zeigen, dass der Redoxzustand von Huminsäure dessen Sorptionsverhalten auf Goethit nicht messbar beeinflusst. Auch zeigen die Sorptionsdaten, dass die Spezies von Fe(II) an Goethit, die redox-abhängige Sorption der organischen Substanz (d.h. unbehandelte und elektrochemisch reduzierte AHA), erheblich beeinflussen können. Des Weiteren treten aufgrund von signifikanten Unterschieden zwischen den Redoxpotentialen von an Goethit gebundenem reaktivem Fe(II) und gelöster Huminsäure bei neutralem pH Elektronentransferreaktionen zwischen Goethit/Fe(II)-Grenzflächen und Huminsäuren auf. Die starke Sorption an und die Elektronenübertragung von AHA mit der Mineraloberfläche erschöpfen die Redoxreaktivität von reaktivem Fe (II), dass an der Eisenmineraloberfläche sorbiert ist. Dies vermindert die Umsetzung von organischen Schadstoffen an der Eisen-Mineral/Fe(II) –Grenzfläche.

Die bisherigen Untersuchungen zum Sorptionsverhalten von Chinonen und Huminsäure auf Goethit wurden mittels Batch-Experimente durchgeführt. Der Bindungsmechanismus auf molekularer Ebene ist aber noch unklar. Um die Oberflächenspezies zu identifizieren und so den Sorptionsmechanismus aufzuklären wurden UV-Vis-Analysen in Kombination mit in-situ Durchflusszellenmessungen von Attenuiertem Totalreflexions-Fourier-Transform-Infrarot (ATR-FTIR) Spektroskopie Messungen durchgeführt. Zunächst wurde die Flusszelle des ATR-FTIR-Aufbaus erfolgreich etabliert und validiert, indem der Sorptionsmechanismus von Catechol auf Goethit als zweizähniger Oberflächenkomplex in Übereinstimmung mit der Literatur untersucht wurde. Die UV-Vis-Ergebnisse zeigen, dass das Naphthochinon-Lawsone keine binären Komplexe mit gelöstem Eisen / Eisen (III) -Ionen in der wässrigen Phase bildet. Diese Ergebnisse stehen im Einklang mit den Resultaten der Batch und ATR-FTIR-Messungen, die deren vernachlässigbare Sorption an Goethit belegen. Darüber hinaus wurde die ATR-FTIR-Technik verwendet, um die sorptive Wechselwirkung von organischen Stoffen, die reich an verschiedenen funktionellen Gruppen, sind mit Goethit hinsichtlich ihrer Reaktionskinetik zu untersuchen. Die spektroskopischen Daten zeigen, dass die Carboxyl- und Phenol-funktionellen Gruppen in der Huminsäurestruktur stark an der Goethitoberfläche haften können unter Ausbildung von Oberflächenkomplexen. Die starke Sorption von AHA an der Eisenmineral-Wasser-Grenzfläche ist daher auf elektrostatische Anziehung und Oberflächenkomplexierung zurückzuführen. Allerdings muss die Eignung der Durchflusszelle des ATR-FTIR-Systems noch für Untersuchungen unter reduzierenden Bedingungen optimiert werden.

Zusammengefasst zeigt Kombination von Batch-Experimenten und ATR-FTIR-Technik ein klares Bild der Oberflächenreaktion von redoxreaktiver organischer Substanz an der Eisenmineral/Fe(II)-Grenzfläche. Dies ist ein erster Schritt, die Auswirkungen von sorptiver organischer Substanz auf das Schadstoff-Verhalten in heterogenen Systemen zu prognostizieren.

# Chapter 1

## General Introduction

# 1.1 Background

Redox reactions in soils and groundwater, especially at iron mineral surfaces, play an important role in determining the overall biogeochemical conditions in aqueous systems and thus are key factors for water quality. This subject is of increasing significance as the fluxes of Natural Organic Matter (NOM) are affected by the type of land use and are expected to alter with future climate change which in turn will affect the function of aquatic systems as field scale reactors for pollutant attenuation. In recent years, a large number of studies have shown that ferrous iron- (Fe(II)) associated with iron mineral surfaces plays a significant role in transformation reactions of organic and inorganic pollutants in soils and groundwater.[1-4]

In natural systems, however, iron mineral surfaces are inevitably in contact with NOM. As NOM can react with a number of pollutants,[5-7] it is likely that sorbed organic matter affects the reduction process of the contaminants at mineral interfaces due to its interactions with iron both in aqueous solution and at the solid phase (see Figure 1.1).[2, 6, 8, 9] On one hand, NOM sorption at iron hydroxides may interfere with the formation of reactive Fe(II) surface sites. On the other hand, NOM contains redox active quinone moieties and may act as a mediator enhancing the electron-transfer across the mineral surface. Even though redox reactions of iron mineral or NOM with pollutants have been studied extensively in binary systems in the past,[1, 2, 7, 10-12] little is known about the effects of NOM sorption at iron minerals-Fe(II) interfaces. In this work, the effect of redox-active organic matter such as quinones and humic substances on redox reactions and sorptive properties of iron minerals has been investigated.
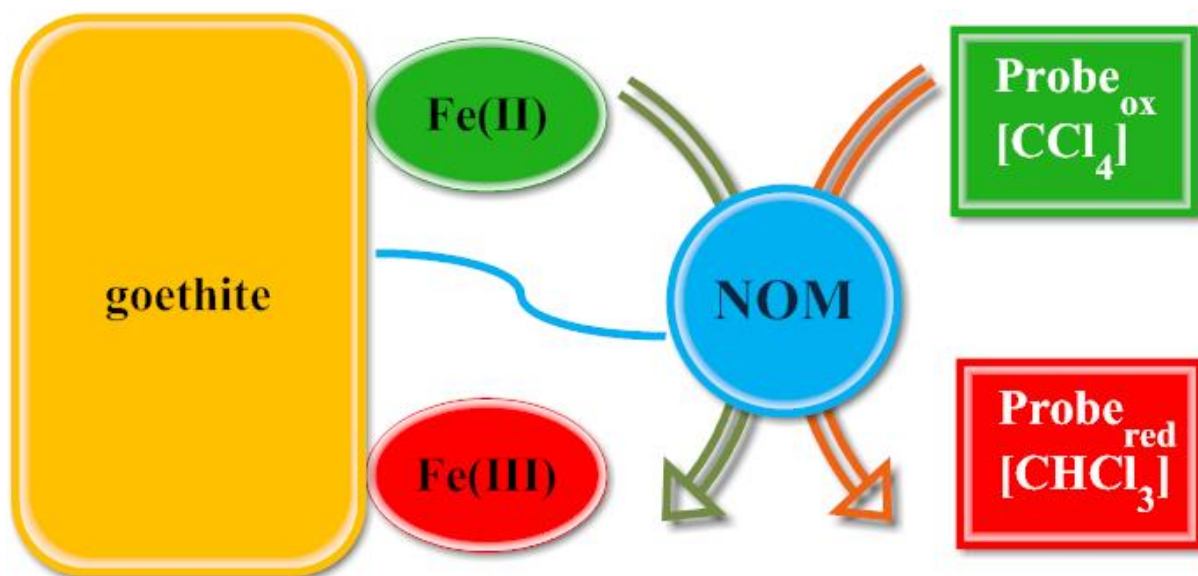


**Figure 1.1.** Scheme of effect of NOM on the contaminant degradation in the iron mineral (goethite)/Fe(II) system.

*Iron Minerals*. Iron (Fe) is one of the most abundant rock-forming elements, constituting about 5% of the Earth's crust.[13] Iron (hydr)oxides, such as goethite, lepidocrocite, hematite and magnetite, are common and major minerals in soils and aquifer sediments.[13] Goethite has a diaspore structure with hexagonal close packing of anions and is also a thermodynamically stable iron oxide at ambient temperature. The goethite structure, with the octahedral double chains, is shown in Figure 1.2.
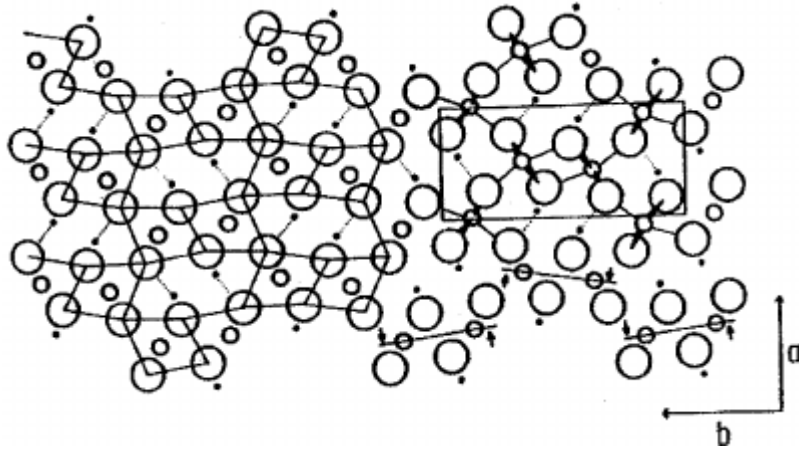


**Figure 1.2.** Goethite structure with octahedral double chains.[14] Iron atoms are represented by small, open circles; oxygen atoms by large, open circles; hydrogen atoms by small, close circles.

Specific surface area as well as surface charge of iron minerals can significantly affect the sorption ability and surface reactivity.[13] The surface charge of an iron mineral is highly pH dependent due to the release or uptake of protons by the mineral surface, and thus characterized by the pH values at the point of zero charge of the surface ($pH_{pzc}$). At conditions below the $pH_{pzc}$, the surfaces are more protonated and thus positively charged. On the other hand, the surface is negatively charged when the pH is above the $pH_{pzc}$. The $pH_{pzc}$ of goethite ranges between 7.5 – 9.5.[13] Thus, high specific surface area and PZC enables goethite surface to attract metal cations, (such as Fe(II))[15, 16] as well as organic and inorganic anions (e.g. carboxylic or humic acids, phosphate).[17-24]

Ferrous iron is one of the common metal species naturally present in the oxygen free environments. The sorption of Fe(II) to ferric iron mineral such as goethite can form an inner-sphere complex with surface hydroxyl group.[15, 25] Such surface bound Fe(II) has been reported to be bulk reductant with a lower redox potential and more reactive than aqueous Fe(II).[2, 26-29] Through their high reducing capacity, Fe(II) associated with iron mineral can catalyze the electron transfer in the reductive transformation of various contaminants (e.g. chlorinated hydrocarbons, nitroaromatic compounds [1, 30]).

*Quinones.* Quinones are oxidized derivatives of aromatic compounds and are usually formed from reactive aromatic materials with electron-donating substituents such as phenols.[31-33] In biochemistry, quinones play an important role in the redox reaction chains and serve as mediators in electron transport processes. It has been reported that quinones and dissolved organic matter can affect the reduction of nitrobenzenes and chlorinated hydrocarbons by zero-valent iron or Fe(II) associated with iron oxides.[2, 9, 34] Also, hydroquinones as well as humic substances have the ability of reducing hexachloroethane or nitroaromatic compounds without any bulk reductant.[7, 10] However, the effect of quinones and organic matter on the surface reactivity of iron minerals remains although unclear. Inhibition as well as stimulation of contaminant degradation was observed depending on the type of organic matter, its concentration, and the type of iron mineral as well as the geochemical conditions.[9, 35]

Figure 1.3 represents the structure of some quinones with different properties. By uptake of two electrons and two protons, the oxidized quinone gets reduced to hydroquinone. These quinone/hydroquinone couples dominate the redox activity of NOM (e.g. Aeschbacher et al[36]). Covering a range of redox potentials, these model quinones should also serve as indicator for the redox properties of the mineral surface. Determining the ratio of quinone/hydroquinone formed during the contact with goethite-Fe(II) enables to calculate the redox potential of the mineral surface by the Nernst Equation.[27] Furthermore, the quinones differ with respect to their pH speciation. For instance, lawsone is deprotonated at neutral pH (pK$_a$ =3.9). We therefore expect significantly different sorption behavior of quinones to goethite and goethite-Fe(II) mineral surfaces.



**AQDS**
$E_H^0{}_{(W)}$ = -210 mV
pKa$_{R1}$=8.1, pKa$_{R2}$=10.5

**Lawsone**
$E_H^0{}_{(W)}$ = 152 mV
pKa = 3.9
pKa$_{R1}$=8.6, pKa$_{R2}$=10.7

**Juglone**
$E_H^0{}_{(W)}$ = 29 mV
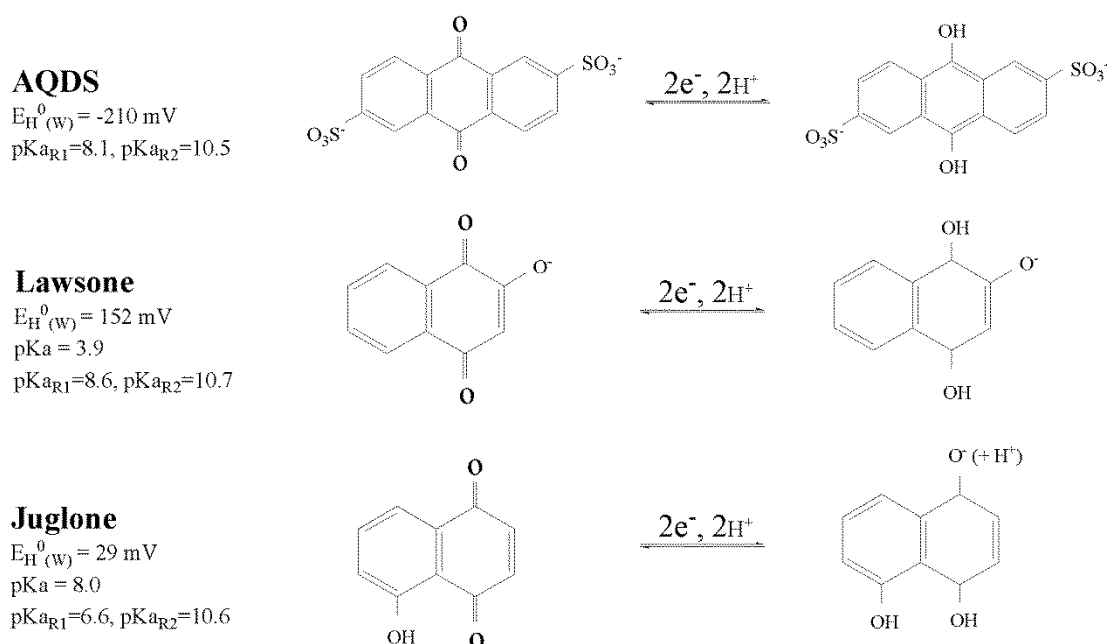pKa = 8.0
pKa$_{R1}$=6.6, pKa$_{R2}$=10.6

**Figure 1.3.** Structures of the quinones/hydroquinones couples of AQDS, lawsone and juglone. Illustrated are the dominant species at pH 7.

*Natural organic matter.* Natural organic matter (NOM) stems from the decomposition of plants and animals and is ubiquitously present in ecosystems.[37, 38] Its functions are mainly related to nutrient availability for plants, as well as to be carbon source for heterotrophic microorganisms. The basic structures of NOM are created from its precursors lignin, cellulose and tannin, as well as various proteins, lipids and sugars.[39-41] It comprises a variety of compound classes (e.g. carboxylic acids, carbohydrates, amino acids), among which the humic substances contribute with 40-60%.[39] Humic substances can be further divided into three forms: the highly aromatic macromolecular humic acids (HA), the highly soluble fulvic acids (FA) and the insoluble, refractory humin.[40]

A very important characteristic of humic substances is their redox activity, as they can act as electron donors or acceptors. It has been shown that humic substances play an important role in redox reactions with organic pollutants,[7] as well as redox sensitive elements in soil such as metal ions (Fe, Mn and Hg[8, 42, 43]), and also may serve as "electron shuttle" in many microbialy driven redox reactions.[42, 44] The redox activity of humic substances primarily arises from the presence of quinone functional groups.[34, 36, 45] Hence, quinone may serve as a model and proxy for redox active natural organic matter.

*Sorptive interactions of NOM with iron minerals.* In soils and sediments, natural organic matter can be strongly adsorbed to mineral surfaces. Many studies about NOM adsorption on iron oxides have been published, focusing on several different aspects: stabilization of organic matter, pH influence, ionic strength, solute composition, surface complexation, size distribution and functional groups.[17, 18, 20, 21, 46] It has been indicated that sorption to fine-grained mineral surfaces is well considered as an important element in the preservation of organic matter in sediments and soils.[47] Also some experimental studies have been carried out to show that humic acids (HA) bind very strongly to the mineral surface. This adsorption behavior can be described by the Langmuir model and is also pH dependent.[18, 20, 21, 46] The adsorption process is the binding between the adsorbing species (e.g. HA) and the surface hydroxyl groups on the iron oxide (e.g. goethite). On the oxide surface, the hydroxyl group can be protonated depending on the pH conditions. The adsorbing species is then attached on the oxide surface to form a complex. This pattern is consistent with a ligand-exchange mechanism, which is described by Figure 1.4.
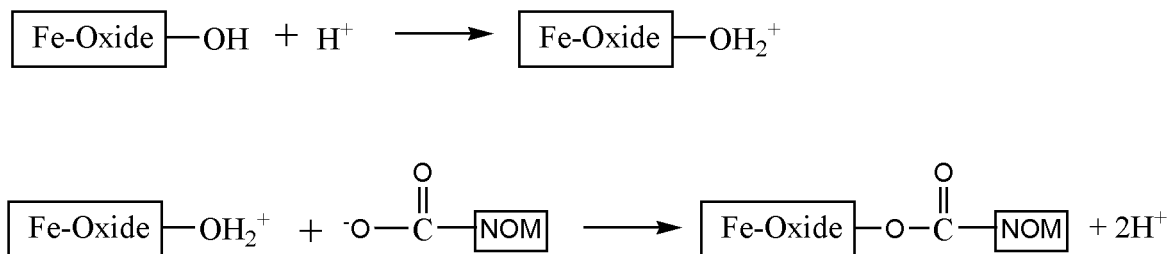


**Figure 1.4.** Mode of ligands exchange interactions between iron oxide and NOM (modified from Gu et al, 1994).

Furthermore, organic matter adsorbed onto the solid surface can still exhibit the physical and chemical characteristics of these organic ligands.[21, 46] The adsorbed humic substances may strongly affect the mobility of mineral particles as well as the interaction and transport of environmental contaminants.[10, 21] Such humic-coating of minerals also affects heavy metal ($Pb^{2+}$, $Zn^{2+}$, $Cu^{2+}$) sorption-desorption processes, and therefore influence their mobility and bioavailability.[48-51] In this work, one important objective is to investigate the sorption behavior of humic acids on the Fe(II)/goethite mineral surface.

*Electron transfer between NOM and iron mineral/Fe(II).* Under reducing conditions, natural organic matter especially humic acid may accept electrons directly from the bound Fe(II) on the mineral surface depending on the redox capacity of HA. Previous studies have demonstrated that the redox properties of HA are largely determined by their quinone-hydroquinone moieties.[45, 52] Their redox properties can be characterized by Electron Accepting (EAC) and Donating (EDC) Capacities, quantified by chemical or electrochemical approaches.[36, 45, 53, 54] Additionally, humic substances have been reported to comprise a wide distribution of redox potentials from -0.3 to 0.8 V vs SHE.[36, 45, 54] However, the goethite associated with Fe(II) has been experimentally investigated to have a lower redox potential,[27, 55, 56] compared to quinone/HA. Thus, it is expected that Fe(II) at goethite surface may reduce humic substances due to their redox potential difference.

For a comprehensive understanding of electron transfer processes in organic matter-Fe(II)-iron mineral systems, more detailed investigations with regard to the importance of the redox state of sorbing humic acid as well as quinones are essential. The overall electron transfer in heterogeneous Fe(II)/Fe(III) systems may be controlled by the reactivity of the Fe(II) species and the redox properties of the input of sorbing organic matter in the system.

## 1.2 Objectives

Aside of determining the sorption of organic matter to the mineral surfaces, of particular interest is to identify the redox reactions between quinones/NOM and iron mineral-Fe(II) surfaces. Therefore speciation of the organic matter as well as of the mineral surfaces needs to be characterized and modeled.

In detail, the specific objectives of the present thesis are:

i)  To determine sorption isotherms for model quinones (e.g. lawsone)/NOM at iron mineral surface as well as Fe(II)-mineral phases at given geochemical conditions such as pH. The sorption studies will be complemented under various redox states to improve the mechanistic understanding of the sorption and complexation behavior of selected quinone/NOM.

ii) To identify the redox speciation of quinones/organic matter in contact with Fe(II)-mineral phases and to characterize the redox potential of the mineral surface based on the quinone speciation.

iii) To perform spectroscopic investigations of the iron speciation and the effects of sorbed DOM on reactive iron species at the mineral surface with various spectroscopic techniques (FTIR and UV-Vis). The spectroscopic studies will be complemented by modeling of the quinone and iron speciation to establish an electron balance.

iv) To acquire a framework of the multiple interactions between natural organic matter and iron minerals at various geochemical conditions in order to provide a mechanistic basis for the prediction of redox processes with natural and anthropogenic compounds.

## 1.3 Thesis Organization

*Chapter 1.* This chapter is a general introduction introducing background, objectives, and structure of this study.

*Chapter 2.* This chapter presents results of the sorption and electron transfer reactions of the model quinone with goethite/Fe(II) interfaces. With the aim of estimating the redox potential of the goethite-Fe(II) system, a spectroscopic study has been conducted in order to obtain the speciation of quinone. The UV-Vis spectra of dissolved quinone species were obtained, using electrochemical reduction in anoxic conditions (glovebox) to achieve different redox states of the quinone of interest to obtain suitable reference spectra of well-defined species. The pH was adjusted so that all acid-base forms were spectrally characterized and these could serve as reference spectra. The electrochemical set-up followed the method of Aeschbacher et al,[36] and allowed not only modifying quantitatively the model quinones redox speciation but also determining the amount of electrons transferred.

Batch experiments were then conducted, where the effects of sorbed Fe(II) concentration on redox speciation of quinones were studied. Different amounts of quinone were added to aliquots of a goethite-Fe(II) suspension. After equilibration, the UV-Vis spectra of the supernatant was obtained. Using the reference spectra previously obtained, the sample spectra were deconvoluted into individual components and the ratio of quinone/hydroquinone consequently derived. With this information, the redox potential of the reactive mineral surface was estimated from the Nernst equation.

*Chapter 3.* The work presented in this chapter describes a systematic study of the sorption and electron transfer process of organic matter at iron mineral/Fe(II) surface by introducing Aldrich humic acid (AHA) as a model compound. Batch experiments under anoxic conditions in suspensions containing goethite, Fe(II) and AHA were conducted. Sorption experiments with defined mineral suspensions and geochemical conditions were set up (partially under anoxic conditions in the glove box) and defined amounts of organic matter added. After some

equilibration time the resulting DOC concentration was determined by a TOC analyzer as well as UV-Vis spectroscopy. The obtained sorption isotherms were used as input data for the comparison with the model quinone lawsone. The geochemical conditions were systematically varied by adjusting the pH in a range from 6-8 and also the effect of Fe(II) concentrations was studied.

*Chapter 4*. This chapter focuses on the spectroscopic investigations of aqueous iron-quinone by UV-Vis and the sorbed quinone/humic acid species at the iron mineral surface by Fourier transform infrared techniques. UV-Vis spectra were taken to assess whether aqueous iron-quinone (e.g.lawsone) complexes exist by spiking quinone/hydroquinone into Fe(II)/Fe(III) solution in the pH range of 2-7. Attenuated Total Reflectance-Fourier Transform Infrared (ATR-FTIR) measurements were performed with a flow through setup to study the sorbed quinone species at the iron mineral-Fe(II) interfaces. The ATR-FTIR analysis was firstly operated on aqueous catechol and its interaction with iron mineral surface and the obtained results were compared with the published literature for the validation of the setup.[57, 58] Then the same ATR-FTIR setup was utilized for target compound lawsone to better understand its sorption mechanism at iron mineral-Fe(II) surface. Finally, the ATR-FTIR technique was applied to explore the sorption mechanism of humic acid with more complicated structure on goethite.

*Chapter 5* provides a general conclusion and suggestions for future research

# Chapter 2

**Effects of Sorbed Quinone/Hydroquinone on Electron Transfer and Apparent Redox Potential of Goethite**

# Abstract

Redox reactions at iron minerals play an important role in determining the biogeochemical conditions in the subsurface. Fe(II) associated with iron mineral phases forms highly reactive surfaces and, together with sorbed redox active Natural Organic Matter (NOM), is key to understand electron transfer processes across the mineral-water interface. Here we investigate the role of sorptive and redox active organic matter on the surface chemistry and electron transfer at goethite in the absence and presence of Fe(II) using lawsone (2-hydroxy-2,4-naphthoquinone) as a model compound. To this end, we conducted batch experiments under anoxic conditions in suspensions containing goethite, dissolved Fe(II) and quinone model compounds. The results indicated that sorption of the naphthoquinone lawsone (i.e. in its oxidized form: $LAW_{ox}$) is consistent with surface-complex formation involving Fe(II) surface sites as it affected the abundance and type of reactive Fe(II)-sites at goethite as well as the regeneration of such sites after oxidation by re-adsorption of Fe(II) from solution. The sorption isotherm of the reduced form of LAW ($LAW_{red}$) on the goethite-Fe(II) surface was consistent with the Langmuir model, but not related to initial Fe(II) loading. Also, electron transfer processes occurred between quinone and the reactive goethite-Fe(II) surface, accompanied by sorption processes. The apparent reduction potentials of the goethite-Fe(II)-(hydro)quinone surface were evaluated by measuring dissolved quinone/hydroquinone redox couples and spanned a wide range of $-150 \pm 23$ mV vs SHE. By comparison with $E_H$ measurements using the non-sorbing quinone AQDS (anthraquinone-2,6-disulfonate), we conclude that the presence of sorbed quinone/hydroquinone does not significantly alter the redox potential of the goethite/goethite-Fe(II) surface.

## 2.1 Introduction

Redox reactions at iron mineral surfaces play an important role in controlling biogeochemical processes, especially in the presence of diurnal, seasonal or long-term variations in redox conditions of natural porous media such as sediments, soils and aquifers. Previous studies have shown that ferrous iron associated with iron mineral phases is an extremely reactive reductant and, together with redox active natural organic matter, is a key player in electron transfer processes across the mineral-water interface.[1, 3, 4, 7, 12, 30, 34]

Iron (oxy)(hydr)oxides, such as goethite, ferrihydrite, lepidocrocite, hematite and magnetite, are common and major minerals in soils and aquifer sediments. Sorption capacities and surface reactivities of these iron minerals are largely determined by their specific surface area as well as surface charge.[13]

Due to the high specific surface area and point of zero charge, goethite exhibits a high sorption capacity for organic and inorganic anions (e.g. carboxylic or humic acids, phosphate) and despite electrostatic repulsion as well as cations can be strongly adsorbed to its surface.[18, 21, 22] The adsorption process includes the interaction of the adsorbing species and the surface hydroxyl groups on the goethite surface. The sorbed species may influence surface charge and surface properties.

Under anoxic conditions, ferrous iron - which primarily stems from microbial iron reduction - is one of the most important naturally occurring bulk reductants. The sorption of Fe(II) to e.g. goethite significantly alters the mineral surface by complexation and formation of secondary mineral phases.[15, 26, 28] Such surface bound ferrous iron is characterized by a lower redox potential and has been shown to be exceedingly more reactive than aqueous Fe(II), catalysing the reductive transformation of numerous contaminants (e.g. chlorinated hydrocarbons, nitroaromatic compounds).[1, 35] The presence of various organic sorbents seems to modulate the reactivity of surface-bounded Fe(II) species in aqueous systems by different types and arrangements of ligands. On one hand, organic solutes such as quinones and humic acids may act as mediators enhancing the electron-transfer across the mineral surface.[7] On the other hand, uptake of organic ligands on iron hydroxides may involve competition with highly reactive Fe(II) surface sites and the complexation of ferrous iron by organic ligands may cause desorption of surface bound ferrous iron and decrease electron transfer to the oxidants at the surface. In this case, the availability of reactive surface sites may become limiting. Although interactions between organic matter and iron minerals have been widely studied with regard to sorption,[17, 18, 21] redox reactions [59, 60] and electron shuttling to microbes,[42, 44] systematic investigations on the combined effects of these processes on the redox properties of the mineral surface are scarce.

Natural organic matter (NOM), especially humic acids, comprises of a wide range of redox potentials (-300 mV ~ +800 mV vs SHE).[61, 62] The redox properties of NOM are largely determined by their quinone moieties,[45, 52] which facilitate electron transfer between NOM

and various redox active species including potential determining geochemical components such as $O_2$, iron oxides, Fe(II) or $H_2S$ [36, 60, 63] as well as various redox sensitive contaminants.[4, 9, 11, 12, 30, 34, 35, 64] However, inhibition as well as stimulation of contaminant degradation was observed depending on the type and concentration of organic matter, type of iron mineral as well as the geochemical conditions. Thus it is currently difficult to foresee the overall effect of organic sorbents on the surface reactivity of iron mineral in the presence of bound ferrous iron.

In order to elucidate the dual role of redox active organic matter regarding electron transfer process and also its sorption behaviour at iron mineral surfaces, we chose 2-hydroxy-1,4-naphthoquinone (lawsone, $E_{H(pH7)}$ = -152 mV) as a model for redox active natural organic matter (see Figure 2.1).[38] Lawsone can provoke various biological processes through chelating metals due to its catechol-like structure.[65-70]
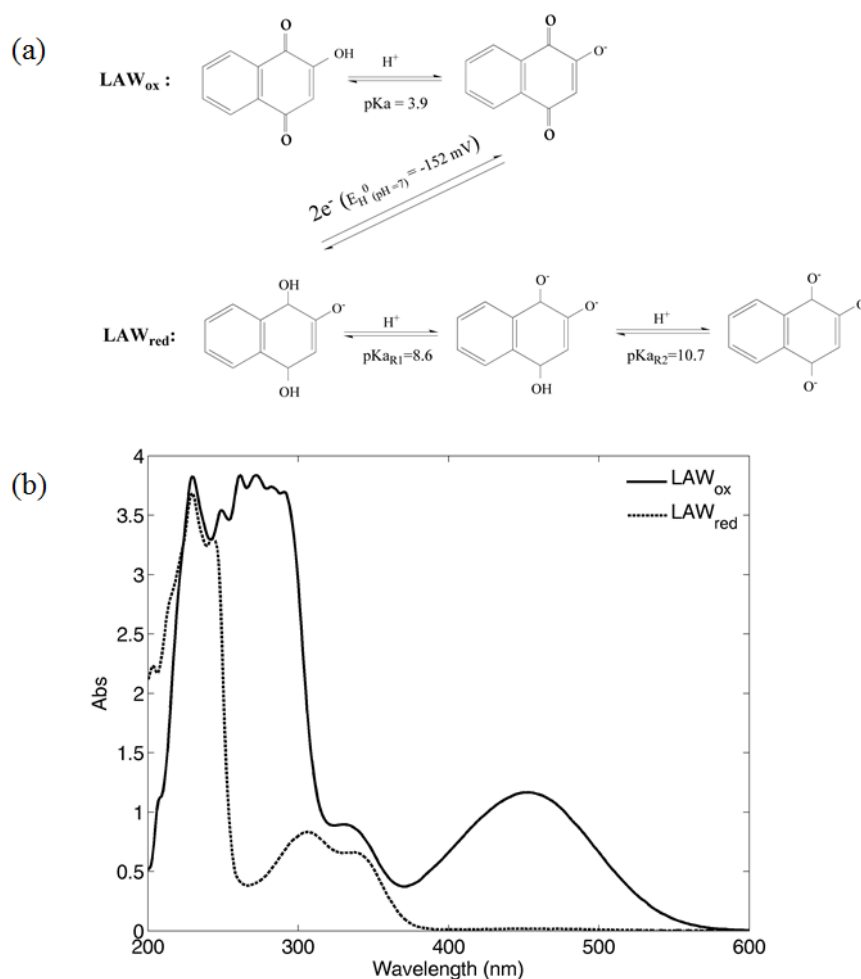


**Figure 2.1.** Speciation of the quinones/hydroquinones couples of lawsone (a). Absorbance spectra of the dominant species at pH 7 (b).

This study aims towards a better understanding of the multiple interactions between quinone model compounds and iron minerals at various geochemical conditions in order to provide a mechanistic basis for the prediction of redox processes with natural organic compounds. The major objectives are: (i) to investigate the sorption behaviour of quinone and hydroquinone at the goethite mineral surface under various redox conditions; (ii) to investigate whether electron transfer reactions of the sorbed quinone/hydroquinone on goethite occur in the presence and absence of initially added ferrous iron; (iii) to probe the redox properties of goethite-Fe(II) surfaces via quinone redox speciation (Orsetti et al. 2013). To this end we conducted batch experiments to elucidate how the presence of quinone modifies the reactivity of the mineral surface towards electron transfer processes.

## 2.2 Materials and Methods

**Chemicals.** 2-hydroxy-2,4-naphthoquinone (lawsone, 97%) and sodium hydroxide were purchased from Sigma-Aldrich. Hydrochloric acid (HCl), boric acid ($H_3BO_4$) and zinc chloride ($ZnCl_2$) were from Merck. Potassium chloride (KCl), acetic acid ammonium salt ($NH_4COOCH_3$, 98%) and Ferrozine (98%) were obtained from Acros Organics. Zincon monosodum salt was provided by Fluka. All aqueous solutions were prepared with Millipore water. Goethite ($\alpha$-FeOOH, Bayferrox 920Z) was received from Lanxess; specific surface area ($N_2$-BET) = 9.2 $m^2$/g; $pH_{pzc}$ = 6.5.[35]

Fe(II) stock solution (0.5 M in 1M HCl) was prepared according to Buchholz et al.[35] Zn(II) stock solution (0.5 M) was prepared by dissolving $ZnCl_2$ (s) into Millipore water.

**Preparation of GT, GT-Fe(II), GT-Fe(II)+$O_2$ and GT-Zn(II) Stock Suspensions**. Goethite suspensions with a final goethite surface area of 100 $m^2$/L were prepared in a serum glass bottle. The detailed preparation procedures of goethite (GT) and GT-Fe(II) stock suspensions were described by Orsetti et al.[27] In the case of GT-Fe(II)+$O_2$ suspensions, a defined amount of air ($O_2$ = 0.15 or 0.3mM, $CO_2$ < 1 $\mu$M) was injected into previously prepared goethite-Fe(II) suspensions through the butyl rubber stopper, stirred under repeated pH adjustment for seven hours in the glove box and stored for one day .

To prepare GT-Zn(II) suspensions, the goethite suspension was purged with $N_2$ and transferred into the glovebox, adjusting its pH to 7.0 $\pm$ 0.1 with NaOH or HCl. Zn(II) was added from the stock solution under continuous stirring, achieving a final total Zn(II) concentration of approximately 3 mM, followed by pH readjustment to 7.0 and equilibration for three days.

**LAW$_{ox}$ and LAW$_{red}$ Stock Solution**. Oxidized lawsone (LAW$_{ox}$) stock solutions were prepared by dissolving lawsone in Millipore water and adjusting its pH to 7 to enhance solubility, followed by filtration through 0.45 $\mu$M membrane filters (mixed cellulose ester, Whatman). In order to obtain reduced lawsone (LAW$_{red}$) stock solutions, electrochemical reduction of LAW$_{ox}$ in the presence of 0.1 M KCl was performed inside the anoxic glovebox

using a 200 ml bulk electrolysis cell, an Ag/AgCl reference electrode, a glassy carbon working electrode and a platinum-wire as counter electrode. A reduction potential of -450 mV vs SHE was applied with an Autolab PGSTAT101 potentiostat (Metrohm, Germany) and pH was adjusted to 5-7 by titrating with HCl discontinuously during the reduction. After complete reduction of $LAW_{red}$, the pH was readjusted to 7.0 with NaOH or HCl prior to use in the experiments.

**Experimental Procedure**. All oxygen-susceptible procedures were carried out inside an Unilab anoxic glovebox (M. Braun, Germany, $O_2 < 1ppm$, 100% $N_2$). Nine different batch experimental setups were designed in order to investigate (i) whether $LAW_{ox/red}$ is adsorbed on the goethite/Fe(II) surface and (ii) whether electron transfer processes between adsorbed quinone/hydroquinone and the goethite/Fe(II) surface are possible. The detailed initial conditions and compositions are listed in Table 2.1.

**Table 2.1**. Compilation of experimental conditions and setups (goethite loading: 50 m$^2$/L; solid density: 5.43 g/L, GT = goethite; LAW = Lawsone)

| Experiment | Condition | pH[a] | Initial Concentration[b] | | | | |
|---|---|---|---|---|---|---|---|
| | | | Fe(II)$_{aq}$ (mM) | Fe(II)$_{tot}$ (mM) | Fe(II)$_{sorb}$ (mM) | Zn(II)$_{aq}$ (mM) | Zn(II)$_{tot}$ (mM) |
| GT+LAW$_{ox}$ | oxic | 7.0 $\pm$ 0.1 | - | - | - | | |
| GT-Zn(II)+LAW$_{ox}$ | anoxic | 7.0 $\pm$ 0.1 | - | - | - | 1.20 $\pm$ 0.01 | 1.51 $\pm$ 0.02 |
| GT-Fe(II)+LAW$_{ox}$ | anoxic | 6.8 $\pm$ 0.2 | 1.02 $\pm$ 0.01 | 1.51 $\pm$ 0.01 | 0.49 $\pm$ 0.01 | | |
| GT-Fe(II)+LAW$_{red}$ (I) | anoxic | 7.0 $\pm$ 0.1 | 1.04 $\pm$ 0.01 | 1.56 $\pm$ 0.01 | 0.52 $\pm$ 0.01 | | |
| GT-Fe(II)+LAW$_{red}$ (II) | anoxic | 7.0 $\pm$ 0.1 | 0.33 $\pm$ 0.01 | 0.79 $\pm$ 0.01 | 0.46 $\pm$ 0.01 | | |
| GT-Fe(II)+LAW$_{red}$ (III) | anoxic | 7.0 $\pm$ 0.1 | < 1 µM | 0.20 $\pm$ 0.01 | 0.20 $\pm$ 0.01 | | |
| GT-Fe(II)+O$_2$+LAW$_{red}$ (I) | anoxic | 7.0 $\pm$ 0.1 | 0.83 $\pm$ 0.01[c] | 1.36 $\pm$ 0.01[c] | 0.53 $\pm$ 0.01 | | |
| GT-Fe(II)+O$_2$+LAW$_{red}$ (II) | anoxic | 7.0 $\pm$ 0.1 | 0.51 $\pm$ 0.01[c] | 0.98 $\pm$ 0.01[c] | 0.47 $\pm$ 0.01 | | |
| GT+LAW$_{red}$ | anoxic | 7.0 $\pm$ 0.1 | < 1 µM | < 1 µM | < 1 µM | | |

[a] no buffer and background electrode added, pH adjusted by HCl and NaOH addition.
[b] initial Fe(II)$_{aq/tot}$ and Zn(II)$_{aq}$ concentration were experimentally determined. Fe(II)$_{sorb}$ = Fe(II)$_{tot}$ − Fe(II)$_{aq}$
[c] concentrations after purging air into GT-Fe(II) and then equilibrium 7 hrs. Initial concentrations of Fe(II)$_{tot}$ and Fe(II)$_{aq}$ of the GT-Fe(II) systems were 1 and 1.5 mM, respectively.

General Procedure: aliquots of 25 ml of either GT, GT-Fe(II), GT-Fe(II)+O$_2$ or GT-Zn(II) stock suspensions were pipetted into 50 ml brown serum bottles. LAW$_{ox}$ or LAW$_{red}$ were equilibrated with these suspensions in a 1:1 dilution for about 20 hours, resulting in initial lawsone concentrations from 0 to 800 μM and a goethite content of 5.43 g/L (50 m$^2$/L). The pH was adjusted to 7.0 ± 0.1 with NaOH or HCl. After shaking overnight, the suspensions were passed through 0.45 μm syringe filters and the absorbance spectra of the supernatants were recorded using 1 cm air tight quartz cuvettes and UV-Vis spectrophotometer (photoLab 6600, WTW, Germany) under strictly anoxic conditions. Aqueous LAW$_{ox}$, LAW$_{red}$ and LAW$_{tot}$ concentrations were further quantified by UV-Vis absorbance (see analytic method details below). Also, final aqueous Fe(II) and Zn(II) were determined by colorimetric methods (see below). Fe(II) control treatments consisted of goethite suspension and Millipore water in the absence of quinone. In addition, further controls containing LAW$_{red}$ and Millipore water were prepared to check for oxygen contamination during the course of experiments and whether the LAW concentration was influenced by the filtration process. All experiments were done in duplicate.

**Fe(II)$_{aq}$, Fe(II)$_{tot}$ and Zn(II)$_{aq}$ Determination.** Fe(II) was determined photometrically at 562 nm using the ferrozine assay.[71] The samples for Fe(II)$_{aq}$ were measured in the filtrate (0.45 μm). Fe(II)$_{tot}$ was measured in unfiltered samples after 24 hrs storage in 1M HCl to desorb/extract Fe(II) from goethite. Aqueous Zn(II)$_{aq}$ was measured photometrically at 620 nm after reaction with zincon (2-carboxy-2'-hydroxy-5'-sulfoformazylbenzene) as described elsewhere.[72] All analytical measurements were performed in duplicates.

**LAW$_{ox,aq}$ and LAW$_{red,aq}$ Quantification.** Dissolved LAW$_{ox}$ and LAW$_{red}$ speciation both exhibit acid-base speciation (see Figure 2.1). Detailed reference absorbance spectra of LAW$_{ox}$ and LAW$_{red}$ are shown in Figures S2.1 and S2.2. At neutral pH, LAW$_{ox}$ and LAW$_{red}$ bear one negative charge, and their absorption spectra partially overlap. While spectrophotometric quantification of LAW$_{ox}$ at 453 nm is possible also in mixtures with LAW$_{red}$, direct quantification of the latter requires further treatment of the samples:

In the presence of low aqueous Fe(II) (< 50 μM), LAW$_{red}$ was quantified from the difference of the absorbance peak at 453 nm (LAW$_{ox}$) before and after re-oxidation of the samples in the presence of MOPS buffer (30 mM, pH 7) ('GT-Fe(II)+LAW$_{red}$ (III)' and 'GT+LAW$_{red}$' systems). Higher ferrous iron concentrations (> 0.5 mM), however, interfere significantly with the absorbance spectra of LAW$_{ox}$. Thus, a 'MOPS + EDTA' method was developed for aqueous LAW$_{ox}$ and LAW$_{tot}$ determination in such cases (applied in experiment 'GT-Fe(II)+LAW$_{ox}$'), which is described in Supporting Information for Chapter 2. In addition, Dissolved Organic Carbon (DOC) was determined using a high TOC Analyzer (Hanau, Germany) for comparison and good agreement with the absorbance data was obtained (see examples in Supporting Information Figure S2.13).

**Sorption Isotherms.** A generic Langmuir model was applied to describe the sorption isotherms of $LAW_{ox}$ and $LAW_{red}$ on goethite-Fe(II), shown in eq.(2.1):

$$[LAW_i]_{sorb} = \frac{K_{L,i} \cdot [LAW_i]_{sorb,max} \cdot [LAW_i]_{aq}}{K_{L,i} \cdot [LAW_i]_{aq} + 1} \tag{2.1}$$

Here, $K_{L,i}$ is the Langmuir constant [L/µmol], $[LAW_i]_{sorb,\,max}$ is the apparent maximum uptake [µmol/g]; $[LAW_i]_{aq}$ is the aqueous concentration of LAW [µmol/L], $[LAW_i]_{sorb}$ represents the sorbed concentration of LAW [µmol/g] and I represents either $LAW_{red}$ or $LAW_{ox}$. Resulting parameters are summarized in Table S2.2.

## 2.3 Results and Discussion

Multiple types of interactions may occur between quinone and goethite, depending on redox speciation of the quinone and the mineral. Sorbed Fe(II) at goethite is a reductant and potentially forms complexes with the reduced quinone, which presents two catechol-like neighboring –OH groups. The presence or absence of redox reactions and the extent and type of sorptive interaction between quinone and the mineral are summarized in the Table 2.2.

Even though the exact surface speciation of quinone/hydroquinone on the mineral surface is unknown and out of the scope of the present work, the obtained results indicate specific interactions of LAW with Fe(II)-goethite and a distinct speciation of sorbed LAW. $LAW_{ox}$ can act as an electron acceptor in the goethite-Fe(II) system (reducing conditions), while $LAW_{red}$ can be oxidized by goethite in the absence or at very low concentrations of added Fe(II) ($GT+LAW_{red}$ and $GT-Fe(II)+LAW_{red}$ (III) at lowest Fe(II) loading).

**Table 2.2.** Compilation of interactions between Lawsone and Goethite as examined by the various experimental setups.

| Experiment | Processes | |
|---|---|---|
| | **Electron transfer** | **Sorption** |
| GT+LAW$_{ox}$ | no | Negligible |
| GT-Zn(II)+LAW$_{ox}$ | no | Linear (Langmuir) |
| GT-Fe(II)+LAW$_{ox}$ | GT-Fe(II)+LAW$_{ox}$ → GT-Fe(III)+LAW$_{red}$ | LAW$_{red}$: Langmuir 'Excess'(LAW$_{ox}$): Langmuir |
| GT-Fe(II)+LAW$_{red}$ (I) | no | Langmuir |
| GT-Fe(II)+LAW$_{red}$ (II) | no | Langmuir |
| GT-Fe(II)+LAW$_{red}$ (III) | GT-Fe(III)+LAW$_{red}$ → GT-Fe(II)+LAW$_{ox}$ | LAW$_{red}$: Langmuir LAW$_{ox}$: Negligible |
| GT-Fe(II)+O$_2$+LAW$_{red}$ (I) | no | Langmuir |
| GT-Fe(II)+O$_2$+LAW$_{red}$ (II) | no | Langmuir |
| GT+LAW$_{red}$ | GT-Fe(III)+LAW$_{red}$ → GT-Fe(II)+LAW$_{ox}$ | LAW$_{red}$: Langmuir LAW$_{ox}$: Negligible |

## 2.3.1 Sorption Isotherms of Quinone and Hydroquinone

Figure 2.2 shows sorption isotherms of LAW$_{ox}$ and LAW$_{red}$ onto goethite under various redox conditions. The adsorption isotherm of LAW$_{red}$ on goethite-Fe(II) showed an initial steep slope and reached a plateau at approximately 14 μmol/g uptake indicating a high affinity of reduced lawsone for GT-Fe(II) surface sites. The sorption data was fitted to a Langmuir model (see Figure 2.2 and 2.3)[21, 73] and the obtained parameters [LAW$_{red}$]$_{sorb,max}$ and K$_{L,red}$ were 14.5 μmol/g and 0.11 L/μmol respectively.
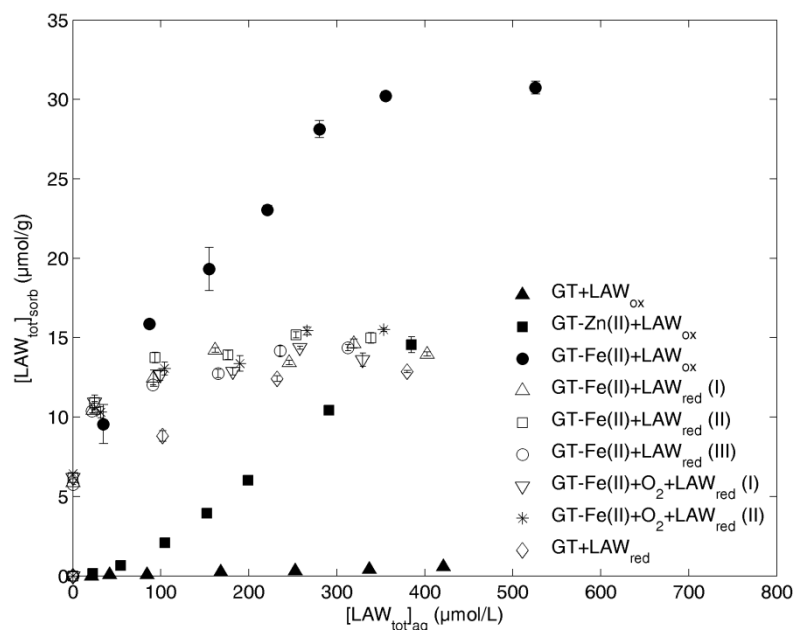
**Figure 2.2.** Sorption behavior of $LAW_{tot}$ under different redox conditions. Data points refer to mean values of two independent experiments with error bars representing the lowest and highest values. Error bars are smaller than symbols.

Goethite has a certain capacity to accommodate delocalized electrons within its crystal structure which must be exceeded in order to form localized Fe(II) surface sites.[15] Experiments with GT-Fe(II) with lower amount of initial Fe(II) loading were conducted to investigate this hypothesis (0.8 and 0.2 mM instead of 1.6 mM). In the case of 0.2 mM Fe(II) as total initial ferrous iron (GT-Fe(II)+$LAW_{red}$ (III)), no significant amount of aqueous ferrous iron was found due to complete uptake (and partial oxidation) of Fe(II) by goethite. The obtained adsorption isotherm of total lawsone in this circumstance presented no significant differences from the total lawsone isotherm on GT-Fe(II)+$LAW_{red}$ (I) (1.6 mM initial Fe(II) loading) (see Figure 2.3), even though electron transfer occurred at some extent between the iron and the quinone (details in Table 2.3b). Lawsone sorption isotherm on GT-Fe(II) using an intermediate initial Fe(II) loading (0.8 mM) also did not show significant differences from the two previous described isotherms; no evidence of electron transfer between iron and quinone was found in this case. These results would indicate that the type of surface sites generated at the lowest initial Fe(II) loading used in this study is no significantly different from those at high initial Fe(II) values (0.2 and 1.6 mM, respectively).
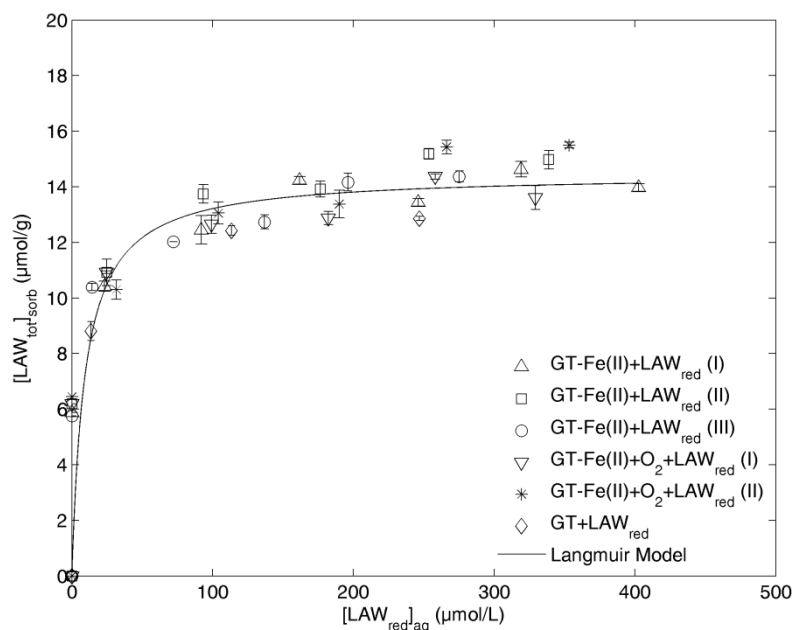
**Figure 2.3.** Sorption of total lawsone vs aqueous $LAW_{red}$. Solid line represents a Langmuir model (eq.2.1) with $[LAW_{red}]_{sorb,max}$ = 14.5 µmol/g and $K_{L,red}$ = 0.11 L/µmol. Data points refer to mean values of two independent experiments with error bars representing the low and high values.

Furthermore, to study how the type of Fe(III) surface sites formed by oxidation of Fe(II) at goethite compare with those at pristine goethite regarding the sorption of reduced lawsone, experimental setups GT-Fe(II)+$O_2$+$LAW_{red}$ (I) and (II) were designed. Here, oxidation of defined amounts of Fe(II) at goethite was achieved by injecting controlled quantities of air equivalent to 200 and 500 µM electrons. It is worth mentioning that sorption of the $CO_2$ present in such air volume is negligible. The resulting conditions are comparable to those of the setups GT-Fe(II)+$LAW_{red}$ (I) and (II) in terms of initial Fe(II) loadings. No significant difference regarding lawsone sorption was found between the two types of setups. Sorption of $LAW_{red}$ was consistent in all of these systems, (see Figure 2.3), which suggests that surface sites formed by oxidation of Fe(II) exhibit the same properties as those at pristine goethite, consistent with findings of Larese-Casanova et al. (2012). They showed that extensive and repetitive Fe(II) sorption and oxidation on goethite results in surface remodeling and epidictic growth of goethite with similar structural properties as the template mineral under geochemical conditions comparable to our study.[74]

Considering its molecular structure, $LAW_{red}$ (a catechol-like quinone) consists of neighboring phenol function groups (see Figure 2.1). Many experimental studies demonstrate significant complex formation between catechol and both Fe(II) and Fe(III) in aqueous solution but also at the surfaces on iron oxides.[58, 75-78] Unfortunately, data on potential complex formation between iron and lawsone are scarce. Padhye et al. showed by Mössbauer and EPR spectroscopy that a Fe(II)-lawsone complex [$Fe^{II}(Lawsone)_2(H_2O)_2$] formed in a methanolic

solution of lawsone and $FeSO_4 \cdot 7H_2O$ at pH 6.[66] However, our UV-Vis spectroscopic study (data not shown), showed no evidence of Fe(II)/Fe(III)-$LAW_{red}$ complexes in aqueous solution at pH values ranging from 2 to 7. Spectroscopic studies showed that catechol forms inner-sphere complexes at iron oxides surfaces for pH = 7, which might also be expected for $LAW_{red}$.[57, 58]

When $LAW_{red}$ was added to GT-Fe(II), [Fe(II)$_{aq}$] remained constant (Figure 2.4), which indicates no significant ternary GT-Fe(II)-$LAW_{red}$ surface complexes formation.
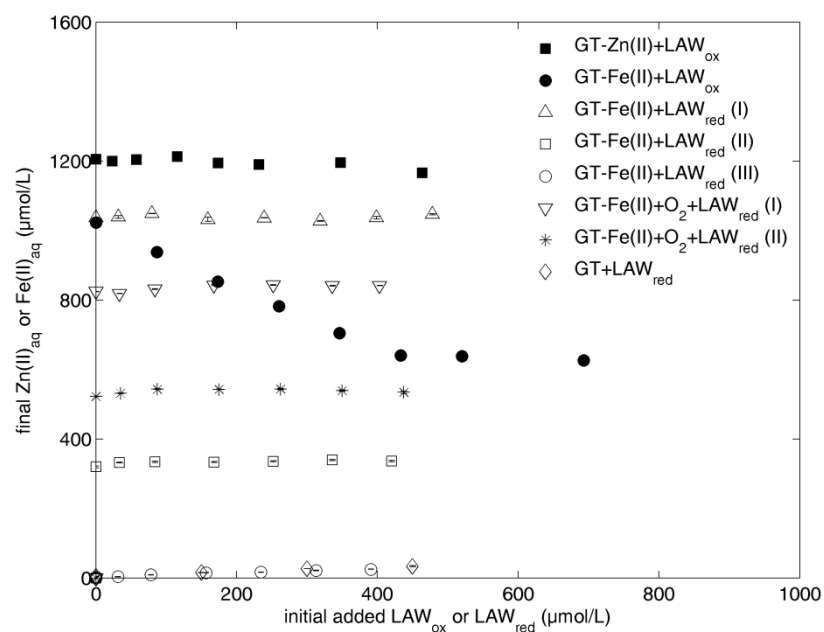


**Figure 2.4.** Aqueous equilibrium concentrations of Fe(II) or Zn(II) in goethite suspensions under different experimental conditions. Data points refer to mean values of two independent experiments with error bars representing the low and high values. Error bars are smaller than symbols.

Under oxic conditions (i.e. GT+$LAW_{ox}$, no Fe(II) present), uptake of $LAW_{ox}$ on goethite was negligible. As both the goethite used in this work (pH$_{pzc}$ = 6.5[27, 35]) and $LAW_{ox}$ carry a slightly negative charge at neutral pH, the lack of sorption can be rationalised by electrostatic repulsion and the absence of significant specific interactions (complex formation) between these species. Although the ketone-group of e.g. quinolone antibiotics was shown to play a role in their surface complexation process to goethite,[79-81] the weaker sorption of $LAW_{ox}$ than $LAW_{red}$ can be explained by the smaller reactivity of the ketone-group of $LAW_{ox}$ than the hydroxy-group of $LAW_{red}$. The latter is able to e.g. undergo ligand substitution with goethite surface –OH groups.[57, 58]

Due to inevitable electron transfer between goethite-Fe(II) and $LAW_{ox}$, sorption of $LAW_{ox}$ to goethite-Fe(II) cannot be studied without concomitant redox reaction, i.e. reduction of $LAW_{ox}$ to $LAW_{red}$. To circumvent this limitation, we studied sorption of $LAW_{ox}$, at GT-Zn(II). Zn(II) was not redox active and mimicked the surface charge of the GT-Fe(II) system to investigate potential electrostatic interactions between $LAW_{ox}$ and GT-Fe(II). As expected, no reduction of $LAW_{ox}$ by GT-Zn(II) occurred. However, uptake of $LAW_{ox}$ was significantly higher in the presence of sorbed Zn(II) than on pure goethite (see Figure 2.2). The adsorption isotherm of $LAW_{ox}$ at GT-Zn(II) was linear without reaching saturation in the concentration of Zn(II) applied. Since $Zn(II)_{aq}$ concentration remained constant in the filtered fractions (see Figure 2.4), ternary GT-Zn(II)-$LAW_{ox}$ surface complexes formation may be neglected. Therefore, this increase in $LAW_{ox}$ adsorption in the presence of Zn(II) is consistent with a less negative or even positive surface charge of GT due to sorbed Zn(II), thus enhancing the electrostatic contribution to the sorption of $LAW_{ox}$. As uptake of Zn(II) by goethite was much lower than uptake of Fe(II) (0.3 instead of 0.5 mM), $LAW_{ox}$ sorption to GT-Fe(II) is expected stronger than to GT-Zn(II).

When $LAW_{ox}$ was added to GT-Fe(II), the total amount of sorbed lawsone was almost twice the uptake in GT-Fe(II)+$LAW_{red}$ systems (see Figure 2.2). In this case, both specific and non-specific (electrostatic) mineral-lawsone interactions may be responsible for the high adsorption. Furthermore, reduction of $LAW_{ox}$ at GT-Fe(II) occurred, as evidenced by the presence of aqueous $LAW_{red}$ as well as the concomitant decrease in aqueous Fe(II) content, which indicates a loss of surface Fe(II) by oxidation causing subsequent adsorption of dissolved Fe(II) to re-establish the Fe(II) adsorption equilibrium. It is worth mentioning that aqueous Fe(II) cannot reduce $LAW_{ox}$ in the conditions of our experiments (data not shown).

The sorbed amount of $LAW_{red}$ can be estimated using the Langmuir isotherm obtained from fitting the data of GT-Fe(II)+$LAW_{red}$ (I) experiment (eq.2.1) according to the aqueous concentration of $LAW_{red}$ at each data point, as sorption of $LAW_{red}$ at GT-Fe(II) did not vary with different Fe(II) loadings and oxidation of Fe(II) at goethite. Based on this observation, we conclude that the "excess" sorption occurring in the GT-Fe(II)+$LAW_{ox}$ system can be attributed to $LAW_{ox}$ only (i.e. the amount of sorbed $LAW_{tot}$ sorbed which cannot be explained by sorbed $LAW_{red}$). The observed significant "excess" sorption at $LAW_{ox}$-GT-Fe(II) was quantified as the difference between the sorbed reduced lawsone and the sorbed total lawsone, expressed by (eq.2.2):

$$[excess]_{sorb} = [LAW_{tot}]_{sorb} - [LAW_{red}]_{sorb} = [LAW_{ox}]_{sorb} \tag{2.2}$$

This "excess" sorption was thus fitted by using a second Langmuir isotherm (eq.2.1) for $LAW_{ox}$ on goethite-Fe(II) surfaces (see Figure 2.5c). When comparing the fitted Langmuir parameters, $K_L$ ($LAW_{red}$) is one order of magnitude higher than $K_L$ ($LAW_{ox}$) in the goethite-Fe(II) system, whereas the maximum uptake of $LAW_{red}$ is approximately 4 μmol/g lower than that of $LAW_{ox}$.
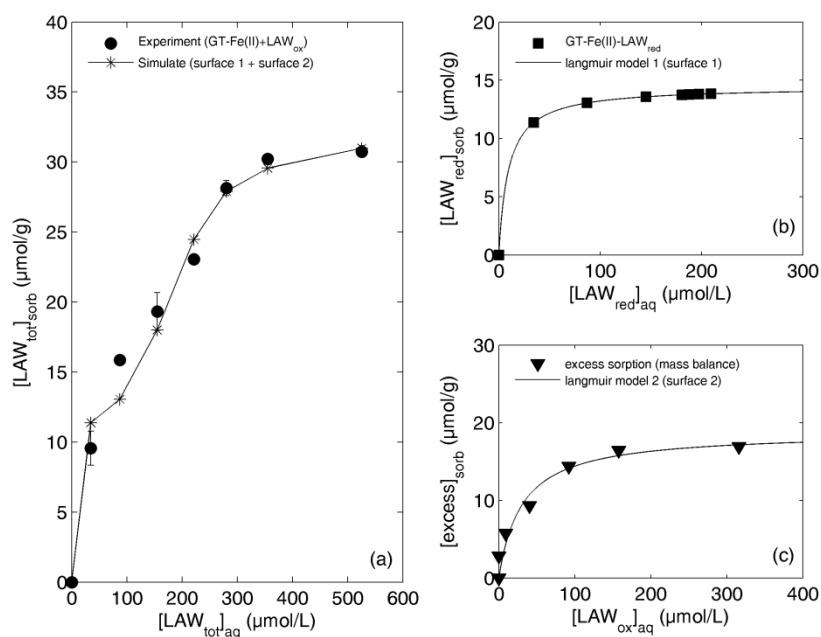
**Figure 2.5.** (a) Comparison of experimental uptake data for lawsone on goethite-Fe(II)-LAW$_{ox}$ with a model using two surface species. Filled circles represent mean values of two independent experiments with error bars representing the low and high values. Line with star markers represent the sum of two Langmuir models at each data point.(b) Line represents simulation of surface species 1 using a Langmuir model (eq.2.1) with [LAW$_{red}$]$_{sorb, max}$ = 14.5 μmol/g and K$_{L,red}$ = 0.11 L/μmol. Filled squares represent the sorbed amount of LAW$_{red}$ estimated using the Langmuir isotherm obtained from fitting the data of GT-Fe(II)+LAW$_{red}$ (I) experiment (eq.2.1) according to the aqueous concentration of LAW$_{red}$ at each data point.(c) Line represents fitting of 'excess sorption' involving a second Langmuir model (eq.2.1) with [LAW$_{ox}$]$_{sorb, max}$ = 18.8 μmol/g and K$_{L,ox}$ = 0.033 L/μmol. Filled triangles represent the observed significant "excess" sorption at LAW$_{ox}$-GT-Fe(II) quantified as the difference between the sorbed reduced lawsone and the sorbed total lawsone (eq.2.2).

The nature of the quinone-mineral interaction for the "excess" sorption can only be explained if specific sorption is taken into account (i.e., surface complex formation between LAW$_{ox}$ and Fe(II)/Fe(III) surface sites). The electrostatic interactions of LAW$_{ox}$ with the mineral surface are equal or less than those of LAW$_{red}$. Considering that both LAW$_{red}$ and LAW$_{ox}$ carry a negative charge at pH 7 (being of similar size), non-specific sorption should be similar for both. Surface saturation was achieved for GT-Fe(II)+LAW$_{red}$ systems (I) and (II), in the absence of redox reaction with a [LAW$_{red}$]$_{sorbed,max}$ around 14 μmol/g. Thus, this surface loading can be considered as a maximum limit for the electrostatic component (even though we assume that specific sorption is also occurring between LAW$_{red}$ and the surface).

In order to study the "backward" reaction (e.g. oxidation of LAW$_{red}$ by Fe(III) in GT, no Fe(II) initial added), different concentrations of LAW$_{red}$ were added to GT suspensions. Both reaction products (LAW$_{ox}$ and Fe(II)) were detected in aqueous solution after equilibration

33

time. These findings indicate that $LAW_{red}$ was oxidized by lattice-bound Fe(III) of goethite forming GT-Fe(II) surface sites and releasing Fe(II) to the aqueous phase, which enhances the sorption of remaining $LAW_{red}$ and, potentially newly formed $LAW_{ox}$.

For the lowest initial $LAW_{red}$ concentrations studied (150 μM), total sorption of LAW to GT was lower compared to the GT-Fe(II) experiments discussed so far (Figure 2.2), presumably because the amount of formed Fe(II) was too low to result in formation of significant quantities of Fe(II)/Fe(III) surface sites. However, our results shown so far suggest that $LAW_{red}$ sorption is much less dependent of Fe(II) loading than $LAW_{ox}$, whose sorption is almost insignificant in the absence of Fe(II). Thus we can assume that $LAW_{ox}$ sorption is negligible in the 'GT+$LAW_{red}$' system due to the limited Fe(II)/Fe(III) surface sites, so that the sorbed $LAW_{tot}$ is exclusively $LAW_{red}$. Therefore, it could be more representative when sorption is plotted as a function of $LAW_{red,aq}$ instead of $LAW_{tot,aq}$ ($LAW_{tot,sorbed}$ vs $LAW_{red,aq}$, see Figure 2.3). Here, we can observe that all sorption data are consistent and they can be described with a single sorption isotherm; individual fitting of each system showed no significant differences in the obtained Langmuir parameters (see Table S2.3). This confirms that $LAW_{ox}$ sorption is negligible when no enough goethite-Fe(II) surface sites are present.


## 2.3.2 Electron Transfer between Goethite and Lawsone

According to previous research, redox reactions occurred between dissolved anthraquinone (AQDS) and Fe(II) associated with goethite, in the absence of quinone sorption.[27] In the present study with lawsone (a sorbing quinone) electron transfer between the mineral and the quinone was observed in general, showing that the sorption of lawsone does not prevent the electrons from being transferred. Table 2.3 shows the results for the systems in which an electron transfer reaction was observed.

GT-Fe(II)+$LAW_{ox}$. The extent of $LAW_{ox}$ reduction at given initial Fe(II) loadings varied with the amount of $LAW_{ox}$ initially added. $LAW_{ox}$ was completely reduced up to about 200 μM initial quinone loading. For higher initial $LAW_{ox}$ loadings, a maximum $LAW_{red}$ concentration of 200 μM was observed indicating an electron transfer capacity of the GT-Fe(II) mineral of about 400 μM electrons at the given conditions (pH 7; 1.5 mM total initial Fe(II)).

Due to the absence of aqueous phase redox reactions, changes in aqueous Fe(II) concentration provide indirect information about changes of sorbed Fe(II) such as oxidation of surface bound Fe(II) by quinones and subsequent adsorption of dissolved Fe(II) at the new Fe(III) surface sites, as previously demonstrated by using a non-sorbing quinone (AQDS).[27] In our systems, direct determination of sorbed Fe(II) is not possible due to the presence of sorbed quinone. Since the exact stoichiometry of the Fe(II) re-adsorption process is unknown, we consider the decrease of aqueous Fe(II) as a lower estimate of oxidized sorbed Fe(II). Our results show that the decrease of dissolved Fe(II) was consistent with the measured increase of $LAW_{red}$ in solution (see Figure 2.3 and Table 2.3a).

GT+LAW$_{red}$. The oxidation of LAW$_{red}$ by ferric iron associated with GT (i.e., the "backward" reaction) was studied by adding fully reduced quinone (LAW$_{red}$) to anoxic goethite suspensions without initial added Fe(II). LAW$_{red}$ was oxidized to some degree (depending on the initial quinone concentration), and only a fraction of the Fe(II) product appeared in the aqueous phase (Table 2.3b). The oxidizing capacity of the goethite was not exhausted in the studied range of concentrations of quinone, since no plateau in LAW$_{ox}$ concentration was achieved.

GT-Fe(II)+LAW$_{red}$. Three different initial Fe(II) concentrations were studied (1.5, 0.8 and 0.2 mM). While no electron transfer reaction was observed at high Fe(II) loadings (1.5 and 0.8 mM), LAW$_{ox}$ was found in the aqueous phase when only 0.2 mM Fe(II) was initially present (GT-Fe(II)+LAW$_{red}$ (III)). In this scenario, no significant aqueous Fe(II) was present before quinone addition; an increase in the Fe(II)$_{aq}$ was observed as shown in Table 2.3c, reaching up to 25 μM when about 40 μM LAW$_{ox}$ was produced (aqueous phase). A maximum of about 40 μM LAW$_{ox}$ was produced, i.e. four times less than during the oxidation of LAW$_{red}$ in the GT+LAW$_{red}$ system. This observation is compatible with the more oxidizing redox potential of the mineral (higher E$_{H,GT-Fe(II)}$) due to the absence of initial Fe(II).

Furthermore, an electron balance was estimated based on the previously described assumptions concerning the redox speciation of sorbed lawsone. Sorbed Fe(II) content was estimated considering the reduction or oxidation of lawsone, depending on the system (i.e. loss of Fe(II) corresponding to twice the produced LAW$_{red}$, or increment of Fe(II) corresponding to twice the oxidation of LAW$_{red}$) (see Table 2.3).

## 2.3.3 Redox Potential of Goethite-Fe(II) (E$_{H, GT-Fe(II)}$)

Assuming redox equilibrium between solution and mineral, the redox potential of the Fe(II) associated with goethite can be estimated from the redox speciation of the quinone in the aqueous phase (eq.2.3).[28]

$$\Delta E = E_{H,lawsone(aq)} - E_{H,GT-Fe(II)} \qquad (2.3)$$

Here, E$_{H,lawsone(aq)}$ and E$_{H,GT-Fe(II)}$ represent the reduction potential of the aqueous quinone and the ferrous iron associated with the mineral at given experimental conditions.

The redox potential at the goethite/Fe(II)/water interface was estimated for each experiment with detectable concentrations of aqueous quinone and hydroquinone, using equations S2.1 and S2.3 (Table 2.3) (for details see Supporting Information for Chapter 2). E$_{H,GT-Fe(II)}$ values for GT-Fe(II)+LAW$_{ox}$ ranged from -127 to -173 mV vs SHE (Table 2.3a) while more reducing potentials were measured for GT-Fe(II)+LAW$_{red}$ systems (-173 to -196 mV, Table 2.3b). Lower potentials (higher reducing conditions) occurred in systems with a higher total Fe(II) concentration, as expected.

When GT and $LAW_{red}$ reacted in the absence of initial Fe(II), Fe(II) formed in situ from oxidation of $LAW_{red}$ by structural Fe(III) of goethite and the corresponding $E_{H,GT-Fe(II)}$ values ranged from -139 to -161 mV (Table 2.3c). However, for the lowest initial $LAW_{red}$ added (150 µM) only 13% remained reduced, resulting in a low $LAW_{red}$ concentration involving a higher uncertainty when determining its value (by difference in $LAW_{ox}$ concentration, as previously described). In any case, sorption behavior of Fe(II) differs significantly from the case where it was added prior to LAW addition (GT-Fe(II) experiments) and the case where it was formed in situ (GT+$LAW_{red}$ experiment). Results shown in Table 2.3 indicate an important difference in the nature of the surface in both scenarios when it comes to sorption of Fe(II) and quinone, which would explain the difference in $E_{H,GT-Fe(II)}$ values for similar Fe(II) sorbed concentrations.

**Table 2.3.** Aqueous redox species and calculated reduction potentials ($E_{H,GT-Fe(II)}$, according to equations S2.1 and S2.3) for Lawsone added in different redox states to anoxic Fe(II)-goethite systems. All potentials are expressed vs SHE.

**a) GT-Fe(II)+LAWₒₓ system (pH = 6.8 ±0.2; Fe(II)$_{tot, initial}$ = 1.5 mM, Fe(II)$_{sorb, initial}$ = 0.5 mM)**

| initial added LAW$_{ox}$ (μM) | LAW$_{red}$ (aq) produced (μM) | LAW$_{ox}$ (aq) remaining (μM) | LAW$_{tot}$(aq) (μM) | LAW$_{red}$(aq)/ LAW$_{tot}$(aq) (%) | LAW$_{red}$ (sorb) (μM)[a] | 'excess' (sorb) (μM)[b] | LAW$_{ox}$ (aq)/ LAW$_{red}$ (aq) | pH | $E_{H,GT-Fe(II)}$ (mV) | Fe(II)$_{aq}$ final (μM) | Electrons transferred (μM)[c] | Fe(II)$_{sorb}$ final (μM)[e] |
|---|---|---|---|---|---|---|---|---|---|---|---|---|
| 86.6 | 34.7 ±6.6 | <1 | 34.7 ±6.6 | 100.0 | 61.8 | <1 | 0.00 | 6.95 | - | 939 ±4.3 | 192 | 379 |
| 173.2 | 87.0 ±1.5 | <1 | 87.0 ±1.5 | 100.0 | 70.9 | 15.3 | 0.00 | 6.95 | - | 853 ±2.2 | 316 | 341 |
| 259.8 | 149.7 ±6.6 | 9.6 ±3.7 | 159.3 ±2.9 | 94.0 | 73.9 | 31.0 | 0.07 | 6.81 | -173 ±5.1 | 782 ±8.3 | 439 | 289 |
| 346.4 | 180.7 ±0.7 | 40.6 ±0.7 | 221.2 ±1.5 | 81.7 | 74.6 | 50.5 | 0.22 | 6.80 | -156 ±2.2 | 705 ±1.4 | 511 | 294 |
| 433.0 | 188.0 ±5.2 | 92.2 ±2.2 | 280.2 ±2.9 | 67.1 | 74.8 | 78.0 | 0.49 | 6.76 | -143 ±1.5 | 640 ±0.4 | 526 | 344 |
| 519.6 | 197.6 ±1.5 | 157.8 ±2.9 | 355.5 ±1.5 | 55.6 | 74.9 | 89.1 | 0.80 | 6.77 | -137 ±1.2 | 638 ±1.1 | 545 | 327 |
| 692.8 | 209.4 ±7.4 | 316.4 ±5.2 | 525.8 ±2.2 | 39.8 | 75.1 | 91.8 | 1.51 | 6.74 | -128 ±1.1 | 626 ±8.7 | 569 | 315 |

**b) GT-Fe(II)+LAW$_{red}$ (III) system (pH = 7.0 ±0.1; Fe(II)$_{tot, initial}$ = 0.2 mM, Fe(II)$_{sorb, initial}$ ~ 0.2 mM)**

| initial added LAW$_{red}$ (μM) | LAW$_{ox}$ (aq) produced (μM) | LAW$_{red}$ (aq) remaining (μM) | LAW$_{tot}$(aq) (μM) | LAW$_{ox}$(aq)/ LAW$_{tot}$(aq) (%) | LAW$_{red}$ (sorb) (μM)[a] | 'excess' (sorb) (μM)[b] | LAW$_{ox}$ (aq)/ LAW$_{red}$ (aq) | pH | $E_{H,GT-Fe(II)}$ (mV) | Fe(II)$_{aq}$ final (μM) | Electrons transferred (μM)[d] | Fe(II)$_{sorb}$ final (μM)[f] |
|---|---|---|---|---|---|---|---|---|---|---|---|---|
| 31.3 | <1 | <1 | <1 | - | 31.3 | <1 | - | 7.14 | - | 3.7 ±0.5 | <1 | 396 |
| 78.1 | 7.4 ±0.4 | 14.4 ±0.4 | 21.7 ±0.7 | 33.9 | 56.4 | <1 | 0.51 | 7.12 | -173 ±1.0 | 8.9 ±0.4 | 14.8 | 406 |
| 156.3 | 18.9 ±0.0 | 72.1 ±0.0 | 91.0 ±0.0 | 20.8 | 69.5 | <1 | 0.26 | 7.12 | -180 ±2.7 | 15.2 ±0.8 | 37.8 | 423 |
| 234.4 | 28.4 ±0.4 | 136.9 ±1.1 | 165.3 ±1.4 | 17.2 | 73.5 | <1 | 0.21 | 7.10 | -185 ±2.1 | 16.5 ±0.2 | 56.8 | 440 |
| 312.6 | 39.6 ±1.1 | 196.1 ±0.7 | 235.6 ±1.8 | 16.8 | 74.9 | 2.0 | 0.20 | 7.12 | -191 ±1.2 | 21.3 ±0.9 | 79.2 | 458 |
| 390.7 | 37.5 ±0.4 | 275.2 ±0.7 | 312.7 ±1.1 | 12.0 | 75.9 | 2.1 | 0.14 | 7.18 | -196 ±0.8 | 24.8 ±0.6 | 75.0 | 450 |

| | | | | **c)** | **GT+LAW$_{red}$ system (pH = 7.0 $\pm$0.1; no initial Fe(II) loading)** | | | | | | | |
|---|---|---|---|---|---|---|---|---|---|---|---|---|
| initial added LAW$_{red}$ ($\mu$M) | LAW$_{ox}$ (aq) produced ($\mu$M) | LAW$_{red}$ (aq) remaining ($\mu$M) | LAW$_{tot}$(aq) ($\mu$M) | LAW$_{ox}$(aq)/ LAW$_{tot}$(aq) (%) | LAW$_{red}$ (sorb) ($\mu$M)$^a$ | 'excess' (sorb) ($\mu$M)$^b$ | LAW$_{ox}$ (aq)/ LAW$_{red}$ (aq) | pH | E$_{H,GT-Fe(II)}$ (mV) | Fe(II)$_{aq}$ final ($\mu$M) | Electrons transferred ($\mu$M)$^d$ | Fe(II)$_{sorb}$ final ($\mu$M)$^f$ |
| 150.0 | 88.5 $\pm$1.8 | 13.6 $\pm$0.4 | 102.1 $\pm$1.5 | 13.3 | 46.4 | < 1 | 6.52 | 7.06 | -139 $\pm$0.7 | 15.3 $\pm$0.3 | 177 | 162 |
| 300.0 | 118.9 $\pm$2.2 | 113.4 $\pm$3.3 | 232.4 $\pm$1.1 | 48.8 | 72.5 | < 1 | 1.05 | 7.02 | -160 $\pm$1.2 | 27.1 $\pm$0.1 | 238 | 211 |
| 450.0 | 132.9 $\pm$0.7 | 247.1 $\pm$0.4 | 380.0 $\pm$0.4 | 65.0 | 75.6 | 1.4 | 0.54 | 6.93 | -161 $\pm$1.9 | 33.4 $\pm$1.5 | 266 | 233 |

$^a$ LAW$_{red(sorb)}$ was simulated by eq. (2.1).

$^b$ 'excess'$_{(sorb)}$ = LAW$_{initial\ added}$ − LAW$_{tot(aq)}$ − LAW$_{red(sorb)}$.

$^c$ In GT-Fe(II)+LAW$_{ox}$ system, electrons transferred = 2$\times$(LAW$_{red(aq)}$+LAW$_{red(sorb)}$);    LAW$_{red(aq)}$ concentration was experimental determined and LAW$_{red(sorb)}$ was simulated by eq. (2.1).

$^d$ In GT-Fe(II)+LAW$_{red}$ (III) & GT+LAW$_{red}$ systems, electrons transferred = 2$\times$LAW$_{ox(aq)}$;    LAW$_{ox(aq)}$ concentration was experimental determined.

$^e$ In GT-Fe(II)+LAW$_{ox}$ system, Fe(II)$_{sorb,final}$ = Fe(II)$_{tot,\ initial}$ − Fe(II)$_{transferred\ to\ Fe(III)}$ (electrons) − Fe(II)$_{aq,\ final}$.

$^f$ In GT-Fe(II)+LAW$_{red}$ (III) & GT+LAW$_{red}$ systems, Fe(II)$_{sorb,final}$ = Fe(II)$_{tot,\ initial}$ + Fe(II)$_{produced\ from\ Fe(III)}$ (electrons) − Fe(II)$_{aq,\ final}$.

The correlation between the $E_{H,GT-Fe(II)}$ values and the amount of transferred electrons, final sorbed Fe(II) concentration and sorbed $LAW_{red}$ is shown in Figure 2.6. There is a strong correlation between $E_{H,GT-Fe(II)}$ and the amount of transferred electrons for the three type of experiments (Figure 2.6a), following the expected effect: lower $E_{H,GT-Fe(II)}$ for the higher amounts of sorbed Fe(II). In the case of GT-Fe(II)+$LAW_{ox}$, a transfer of electrons translates into a loss of ferrous iron in the system, therefore the slope is positive. For the GT-Fe(II)+$LAW_{red}$ (III) case (low Fe(II) initial loading) the hydroquinone is oxidized, resulting in more Fe(II) with increasing amounts of transferred electrons. The same situation applies for GT+$LAW_{red}$, presenting both a negative slope.

The effect of sorbed Fe(II) on the potential is not as clear (Figure 2.6b); a more reducing potential is obtained with more sorbed Fe(II), valid from a concentration around $300\,\mu M$. However, for lower sorbed Fe(II) concentrations no correlation between these factors occurs between the redox potential and the amount of sorbed $LAW_{red}$ (Figure 2.6c).
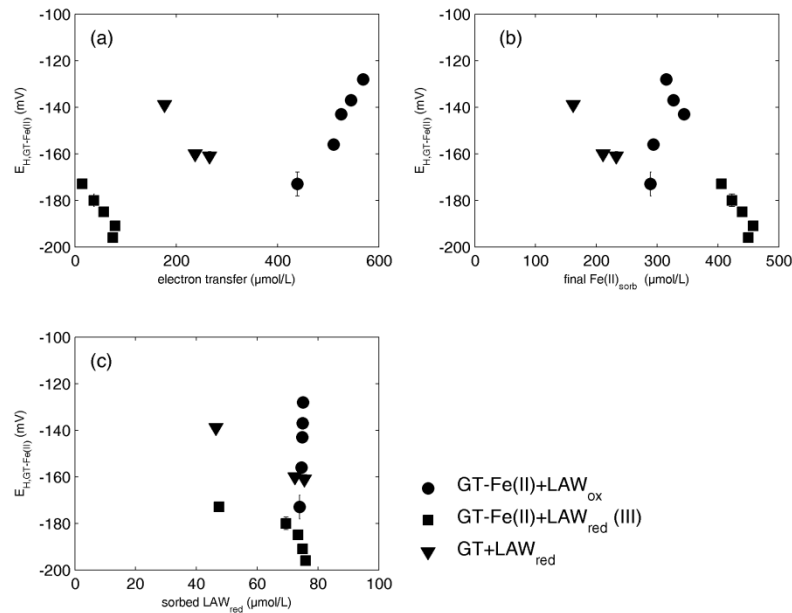


**Figure 2.6.** Correlation between $E_{H,GT-Fe(II)}$ and electron transfer (a), Fe(II)$_{sorb,final}$ (b) and $LAW_{red(sorb)}$ (c) under various experimental conditions.

It is worth mentioning that the estimated redox potentials are valid for the reported pH and Fe(II) loading of each system (i.e. they are conditional values). As sorption of Fe(II) and quinone as well as the redox potential of the quinone are pH-dependent: an increase in pH would cause higher sorption of Fe(II) and lower sorption of quinone/hydroquinone to the mineral surface.

Due to the high redox buffer intensity of goethite-Fe(II) systems, the quinone/hydroquinone redox couple can be utilized for tracing the apparent reduction potential of ferrous iron at the goethite surface. Orsetti et al. reported a reduction potential of goethite/Fe(II) ($E_{H,GT-Fe(II)}$) at pH = 7 of approximately −170 mV vs SHE based on the speciation of the non-sorbing quinone AQDS.[27] However, as listed in Table 2.4, the apparent reduction potentials of the goethite-Fe(II)-(hydro)quinone surface evaluated by measuring dissolved lawsone redox couples are close to those obtained from AQDS speciation in the presence of similar amounts of electrons transferred. By comparison with $E_H$ measurements using the non-sorbing quinone AQDS we conclude that the presence of sorbed quinone/hydroquinone does not significantly alter the redox potential of the goethite/goethite-Fe(II) surface.

**Table 2.4.** $E_H$ values determined from quinone/hydroquinone speciation of AQDS (non sorbing) and Lawsone (sorbing) at apparent equilibrium with goethite or goethite-Fe(II) systems.

| Quinone System | AQDS (without sorption) | | | Lawsone (with sorption) | | |
|---|---|---|---|---|---|---|
| | Initial added quinone ($\mu$M) | Electrons transfer ($\mu$M) | $E_{H,GT\text{-}Fe(II)}$ (mV) | Initial added hydroquinone ($\mu$M) | Electrons transfer ($\mu$M) | $E_{H,GT\text{-}Fe(II)}$ (mV) |
| GT-Fe(II)+Quinone (pH = 7.0 $\pm$0.1; Fe(II)$_{tot, initial}$ = 1.5 mM, Fe(II)$_{sorb, initial}$ = 0.5 mM) | 500 | 498 | -170 $\pm$2 | 260 | 439 | -173 $\pm$5.1 |
| GT+Hydroquinone (pH = 7.0 $\pm$0.1; no initial Fe(II) loading) | 200 | 360 | -169 $\pm$0.7 | 450 | 266 | -161 $\pm$1.9 |

## 2.4 Environmental Significance

This work aims at providing a mechanistic basis for predicting interfacial redox processes of natural and anthropogenic compounds at iron minerals in the presence of organic coatings. The naphthoquinone lawsone, a sorbing analogue for redox active natural organic matter, showed a complex sorption behavior at goethite depending on its redox state as well as the amount and distribution/speciation of Fe(II) at goethite. Sorption of the hydroquinone species (LAW$_{red}$) is consistent with surface-complex formation involving Fe(II) and Fe(II)/Fe(III) surface sites at goethite.

Our findings demonstrate that the thermodynamics of reversible electron transfer between redox active sites at the mineral-water interface and dissolved reactants appears to be unaffected by the presence of quinone coatings of the surface. The sorbing model quinone lawsone showed reversible electron transfer with both ferric and ferrous sites at Fe(II)/goethite, in line with earlier studies on non-sorbing AQDS, an effective electron transfer mediator that does not significantly accumulate at the mineral-water interface.[27]

While the present study focused on the thermodynamics in quinone/goethite/Fe(II) systems, sorption of quinones or natural organic matter may influence the pathways or kinetics of electron transfer which needs to be further studied. As in natural organic matter the abundance of redox active quinones is low compared to non-redox active ligands, ongoing work evaluates the significance of the quinone-mineral interactions described here to electron transfer across the NOM-iron mineral/water interface.

# Chapter 3

**Effects of Sorbed Natural Organic Matter (NOM) on Electron Transfer at Goethite/Fe(II) Interfaces**

# Abstract

Iron mineral, Fe(II) and dissolved organic matter are ubiquitously present in the soil and groundwater. The sorptive interactions of organic matter with iron mineral have been widely reported. However, studies with iron mineral-Fe(II) systems have been little understood yet to our knowledge. Thus, the overall goal of this study is to investigate the sorption and electron transfer process of organic matter in anoxic goethite-Fe(II) system using Aldrich humic acid (AHA) as model compound. We conducted batch experiments in suspensions containing goethite, Fe(II) and AHA under oxic and anoxic conditions. Our results indicated that the presence of associated Fe(II) at goethite surface can significantly enhance the sorption of redox-active organic matter depending on its redox state such as untreated and electrochemically reduced AHA. Also, the presence and amount of aqueous Fe(II) in the goethite-Fe(II) system may also alter the sorption of AHA. Furthermore, it was concluded by the sorption isotherms that sorption of AHA on goethite in the absence of sorbed Fe(II) was not affected by its redox state. On the other side, redox reaction between humic acid and iron mineral-Fe(II) was expected to be favourable since the redox potential ($E_H$) of goethite/Fe(II) system was negative enough to reduce the untreated humic acid with more positive $E_H$ values. Consequently, the sorption and electron transfer process may cause remodelling of the mineral-water interphase and thus may affect electron transfer process in the anoxic aquifer.

# 3.1 Introduction

In the recent years, a substantial amount of research has been devoted to demonstrate the importance of Fe(II) associated with solid phases in reductive transformation of organic and inorganic pollutants and microbial process in soils and groundwater.[2, 3, 11, 25, 27, 28, 35, 56, 74] A common conclusion of these studies is that the mineral bounded Fe(II) is much more reactive than the dissolved Fe(II), because sorption of Fe(II) on iron mineral enhances its reducing ability with a lower standard redox potential.[13] And, the conditional reducing potential of reactive ferrous iron sorbed on goethite has been reported around -170 mV vs SHE, by employing non-sorbing quinone as redox probes. [27, 56]

Humic substances, such as humic acid (HA), are redox-active natural organic matter in the environment. The redox reactivity of HA has been ascribed to quinone/hydroquinone moieties.[45, 52] Due to the potentially reactive functional groups rich in the structure, humic acid may act as an electron mediator in heterogeneous chemical and microbial processes.[2, 7, 8, 10, 12, 42] Additionally, humic substances cover a wide range of redox potentials. Recent electrochemical studies have reported the apparent reduction potential ($E_H^0$) of HA of -0.3 to 0.8 V vs SHE at neutral pH.[36, 45] Thus, it is plausible for the redox reaction between associated Fe(II) at goethite surface and HA at neutral pH condition, due to their redox potential difference.

Apart from the redox property of humic acid, it is also a major sorbent present throughout ecosystems. HA has the ability of forming complexes with metal cations, such as Pb(II), Cu(II), Fe(II)/Fe(III) and As(III),[82-87] which has been investigated to a great extent, typically through IR spectroscopy studies and modelling simulation.[86, 88-91] Furthermore, the transport of humic acid in the subsurface is influenced strongly by its interaction with solid surfaces.[18, 21, 36, 37, 46, 60, 92] Consequently, the mineral components in soil can associate to humic acid forming organic-mineral mixture compounds by various kinds of interactions: hydrophobic bonding, electrostatic interactions, hydrogen bonding, ligand exchange and so on.[17-19, 21, 46] The fractions of HA rich in carboxyl and aromatic functional groups are preferentially adsorbed through the surface complexation-ligand exchange mechanism by iron oxide surfaces at low pH conditions.[21, 46] While sorption of HA to iron oxides under oxic condition has been widely studied, the sorption capacity of iron mineral associating with reducing species such as ferrous iron has been little investigated yet. The presence of organic sorbent is likely to modulate the reactivity of surface-bound Fe(II) species in aqueous systems as chemical environments, due to the functional groups and arrangement of organic ligands which may strongly affect the redox potential of adsorbed Fe(II) at mineral surface. The formation of reactive Fe(II) surface sites as well as organic matter-iron mineral interactions are highly sensitive to the type of organic matter and environmental conditions. We studied a ternary humic acid-ferrous iron-mineral system to mimic an important aspect of geochemical complexity of natural groundwater systems.

For a comprehensive understanding of electron transfer processes in organic matter-Fe(II) iron mineral systems, a systematic investigation of organic matter interaction with bound iron minerals in the presence of Fe(II) at various environmentally relevant conditions were conducted. In this study, commercial Aldrich humic acid (AHA) is introduced as a representative for natural organic matter during the course of proposed batch experiments. The overall goals of this research are: i) to quantitatively evaluate sorption isotherms for nonreduced and electrochemically reduced NOM on Fe(II)-iron mineral interface as well as iron mineral at neutral pH condition; ii) to evaluate the electron transfer process in the heterogeneous Fe(II)/iron mineral systems by the input of organic matter; iii) to establish a possible conceptual mechanistic model for electron cycling and reaction pathways between iron minerals, Fe(II) and NOM by the comparison of sorption and electron transfer processes of Aldrich humic acid with model quinone compounds lawsone in my previous study.[93]

## 3.2 Materials and Methods

**Chemicals**. Hydrochloric acid (HCl), boric acid ($H_3BO_4$) and zinc chloride ($ZnCl_2$) were acquired from Merck. Potassium chloride (KCl), acetic acid ammonium salt ($NH_4COOCH_3$, 98%) and Ferrozine (98%) were acquired from Acros Organics. Aldrich humic acid (Humic acid, Sodium salt) was purchased form Aldrich. Diquat dibromide monohydrate (DQ) was acquired from Fluka and 2,2'-azino-bis (3-ethylbenzthiazoline-6-sulfonic acid) diammomonium salt ($> 98\%$, ABTS) was purchased from Sigma. All aqueous solutions were prepared with Millipore water. Goethite ($\alpha$-FeOOH, Bayferrox 920Z) was received from LANXESS; specific surface area ($N_2$-BET) = 9.2 $m^2$/g; pHpzc = 6.5.[35]

Fe(II) stock solution (0.5 M in 1M HCl) was prepared according to Bucholz et al.[35] Zn(II) stock solution (0.5 M) was prepared by dissolving $ZnCl_2$ powder into Millipore water.

**Preparation of GT, GT-Fe(II) and GT-Zn(II) Stock Suspensions**. Goethite suspensions with a final goethite concentration of 100 $m^2$/L were prepared in a serum glass bottle. The detailed preparation procedures of goethite (GT) and GT-Fe(II) stock suspensions were described by Orsetti et al.[27]

To prepare GT-Zn(II) samples the goethite suspension was purged with $N_2$ and then transferred into the glovebox, adjusting its pH to 7.0 $\pm$ 0.1 with NaOH or HCl. Zn(II) was added from the stock solution into this suspension under continuous stirring, achieving a final total Zn(II) of approximately 3 mM followed by pH readjustment to 7 and equilibrium for three days.

**Aldrich humic acid stock (AHA) solution.** According to their redox states, AHA solutions can be termed as untreated (AHA_untre), reduced (AHA_red) and reoxidized Aldrich humic acids (AHA_reox). AHA_untre stock solutions were prepared by dissolving AHA into Millipore water, centrifuging and filtering through 0.45 μm membrane filter (mixed cellulose ester, Whatman).

$AHA_{red}$ stock represents the solutions that were reduced by Direct Electrochemical Reduction (DER) method, detailed shown later. The reoxidized solution ($AHA_{reox}$) from previous reduced AHA was exposed to air by opening the bottle and stirring for one day to reoxidize it outside the glovebox.

**Electrochemical Reduction and Quantification.**  $AHA_{red}$ stock solution (160 ml) was prepared by the Direct Electrochemical Reduction (DER) of $AHA_{untre}$ stock in the presence of 0.1 M KCl, which was performed in the anoxic glovebox using a 200 ml bulk electrolysis cell, an Ag/AgCl reference electrode, a glassy carbon working electrode and a platinum-wire counter electrode.[36] A reduction potential of -0.8V vs SHE was applied with an Autolab PGSTAT101 instrument (Metrohm, Germany) and also pH was controlled between 5 and 7 by titrating with HCl discontinuously during the course of the reduction. The reduction was monitored by following the Electron Donator Capacities (EDC) of AHA in time and it was considered finished when no significant change was detected by Mediated Electrochemical Oxidation (MEO, details see Supporting Information).[36, 54] The final pH was readjusted to 7 with NaOH for further experiments.

**Sorption experiments.** All oxygen-susceptible procedures and experiments were carried out in the anoxic glovebox (Braun, Germany, 100% $N_2$). Eight batch experiments were conducted to survey: i) effect of Fe(II) on the sorption of untreated and electrochemically reduced AHA at goethite-Fe(II) interface; ii) possible change on sorption of AHA to goethite altered by the redox states of AHA; iii) electron transfer reaction between humic acid and Fe(II)-goethite. The detailed initial conditions and compositions are listed in the Table 3.1.

The conducted batch procedures were generalized as: aliquots of 25 ml of either GT, GT-Fe(II) or GT-Zn(II) stock suspensions were pipetted into 50 ml serum brown bottles. $AHA_{untre}$, $AHA_{red}$ or $AHA_{reox}$ were equilibrated with these suspensions in a 1:1 dilution, resulting in the required initial AHA concentrations and a goethite density of 5.43 g/L respectively. The pH was adjusted to $7.0 \pm 0.1$ with NaOH or HCl. After shaking overnight, the suspensions were filtered through 0.45 μm syringe filters and the absorbance spectra of the supernatant were recorded using hermetical quartz cuvettes and a UV-Vis spectrophotometer (photoLab 6600, WTW, Germany). The total dissolved organic carbon concentration (DOC) of the filtered samples was measured. Also, final aqueous Fe(II)/Zn(II) contents were determined. Control treatments consisted of homologous goethite suspension and Millipore water. Besides, another control system containing AHA and Millipore water was used to check whether the AHA concentration was influenced by the filtration process. All batches were prepared in duplicate.

**Table 3.1.** Terminology and compilation of experimental conditions and setups.

(goethite loading: 50 m$^2$/L; solid density: 5.43 g/L, GT = goethite; AHA = Aldrich Humic Acid)

| Experiment Label | Conditions | pH[a] | Initial Ions loading[b] | | | Objective |
|---|---|---|---|---|---|---|
| | | | Fe(II)$_{aq}$ or Zn(II)$_{aq}$ (mM) | Fe(II)$_{tot}$ (mM) | Fe(II)$_{sorb}$ (mM) | |
| GT+AHA$_{untre}$ | oxic | 7.0 ±0.1 | - | - | - | |
| GT+AHA$_{red}$ | anoxic | 7.0 ±0.1 | - | - | - | Effect of the redox state of AHA on its sorption |
| GT+AHA$_{reox}$ | oxic | 7.0 ±0.1 | - | - | - | |
| GT-Zn(II)+AHA$_{untre}$ | anoxic | 7.0 ±0.1 | 1.26 ±0.01 | 1.50 ±0.01 | 0.24 ±0.01 | Evaluation of electrostatic component in the sorption |
| GT-Fe(II)+AHA$_{untre}$ (I) | anoxic | 7.0 ±0.1 | 0.91 ±0.01 | 1.37 ±0.01 | 0.46 ±0.01 | Effect of Fe(II) loading on AHA$_{untre}$ sorption and electron transfer |
| GT-Fe(II)+AHA$_{untre}$ (II) | anoxic | 7.1±0.1 | 0.047 ±0.002 | 0.39 ±0.01 | 0.34 ±0.01 | |
| GT- AHA$_{untre}$ +Fe(II) | anoxic | 7.1±0.1 | 0.84 ±0.01 | 1.30 ±0.01 | 0.46 ±0.01 | Effect of Fe(II) addition sequence on AHA$_{untre}$ sorption and electron transfer |
| GT-Fe(II)+AHA$_{red}$ | anoxic | 7.0 ±0.1 | 1.04 ±0.01 | 1.56 ±0.01 | 0.52 ±0.01 | Effect of sorbed Fe(II) on AHA$_{red}$ sorption and electron transfer |

[a] no buffer added, pH adjusted by acid and base.
[b] initial Fe(II)$_{aq/tot}$ and Zn(II)$_{aq}$ concentration were experimental determined.

**Fe(II)$_{aq}$ and Fe(II)$_{tot}$ determination.** Fe(II) was determined photometrically at 562 nm using the ferrozine assay.[71] The samples for Fe(II)$_{aq}$ were measured in the filtrate (0.45 μm). Fe(II)$_{tot}$ was measured in unfiltered samples after 24 hrs storage in 1M HCl to desorb/extract Fe(II) from goethite. It should be noted that the presence of AHA may interfere the Fe(II)$_{aq}$ determination by photometric method (details see Supporting Information). Thus the Fe(II)$_{aq}$ quantification for the final filtered samples has been corrected considering this interference. Also, significant amount of aqueous Fe(II) was detected in the reduced AHA in the range of 0 to 75 μmol/L, depending on the AHA$_{red}$ concentration (see Table S3.2 in the Supporting Information).

Aqueous Zn(II)$_{aq}$ was measured photometrically at 620 nm after reaction with zincon (2-carboxy-2'-hydroxy-5'-sulfoformazylbenzene) as described elsewhere.[72] All analytical measurements were performed in duplicates.

**AHA$_{aq}$ Quantification.** The Dissolved Organic Carbon concentration (DOC) of all the dissolved AHA (AHA$_{aq}$) samples was measured by high TOC Analyzer (Hanau, Germany).

**Sorption Model**. A generic Langmuir model is applied to describe the sorption isotherm of AHA in goethite/Fe(II) system, shown in following eq.(3.1):

$$[AHA_i]_{sorb} = \frac{K_{L,i,j} \cdot [AHA_i]_{sorb,max,j} \cdot [AHA_i]_{aq}}{K_{L,i,j} \cdot [AHA_i]_{aq} + 1} \qquad (3.1)$$

Where, $K_{L,i,j}$ is the Langmuir constant [L/mgDOC] (i:untre/red, j:GT/GT-Fe(II)), $[AHA_i]_{sorb,max,j}$ is (apparent) uptake maximum [mgDOC/g]; $[AHA_i]_{aq}$ is the aqueous concentration of LAW [mgDOC/L] and $[AHA_i]_{sorb}$ represents the sorbed concentration of AHA [mgDOC/g]. All the parameters ($K_{L,i,j}$ as the Langmuir constant [L/mgDOC] (i:untre/red, j:GT/GT-Fe(II) and $[AHA_i]_{sorb,max,j}$ as (apparent) uptake maximum [mgDOC/g]) by fitting the Langmuir model to experimental data are listed in Table 3.2.

## 3.3 Results and Discussion

### 3.3.1 Sorption Isotherms of Aldrich Humic Acid

AHA sorption onto goethite is a complex process, depending on redox states of AHA as well as the presence and quantity of the added Fe(II). It is expected that the presence of Fe(II) may enhance the sorption of untreated and electrochemically reduced AHA onto goethite. Thus, the sorption experiments were operated under various redox condition to verify this hypothesis. The collective results are presented in Figure 3.1a.
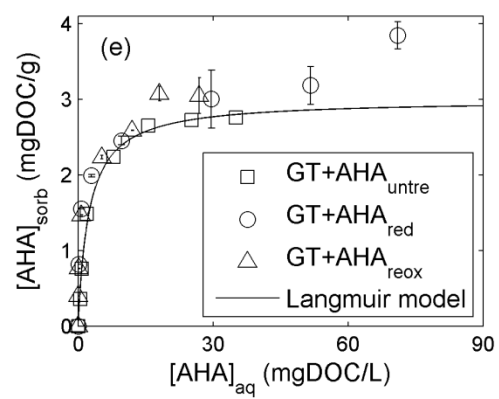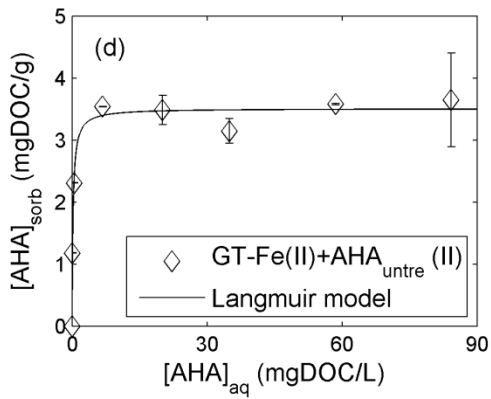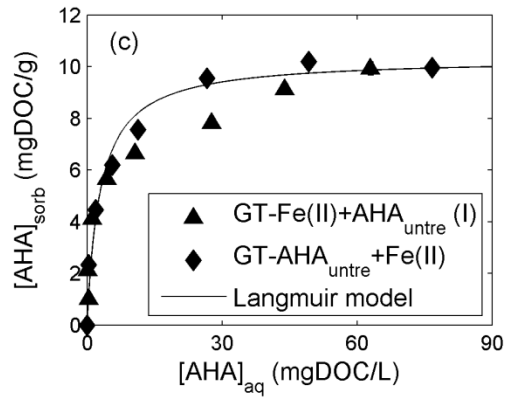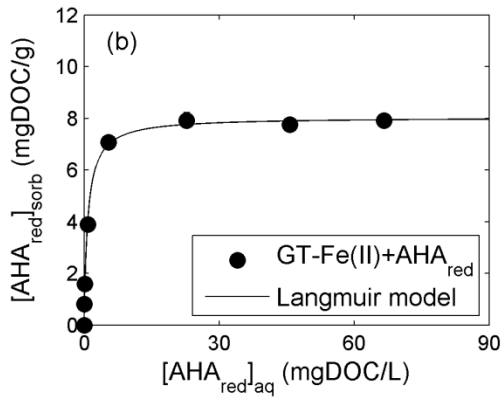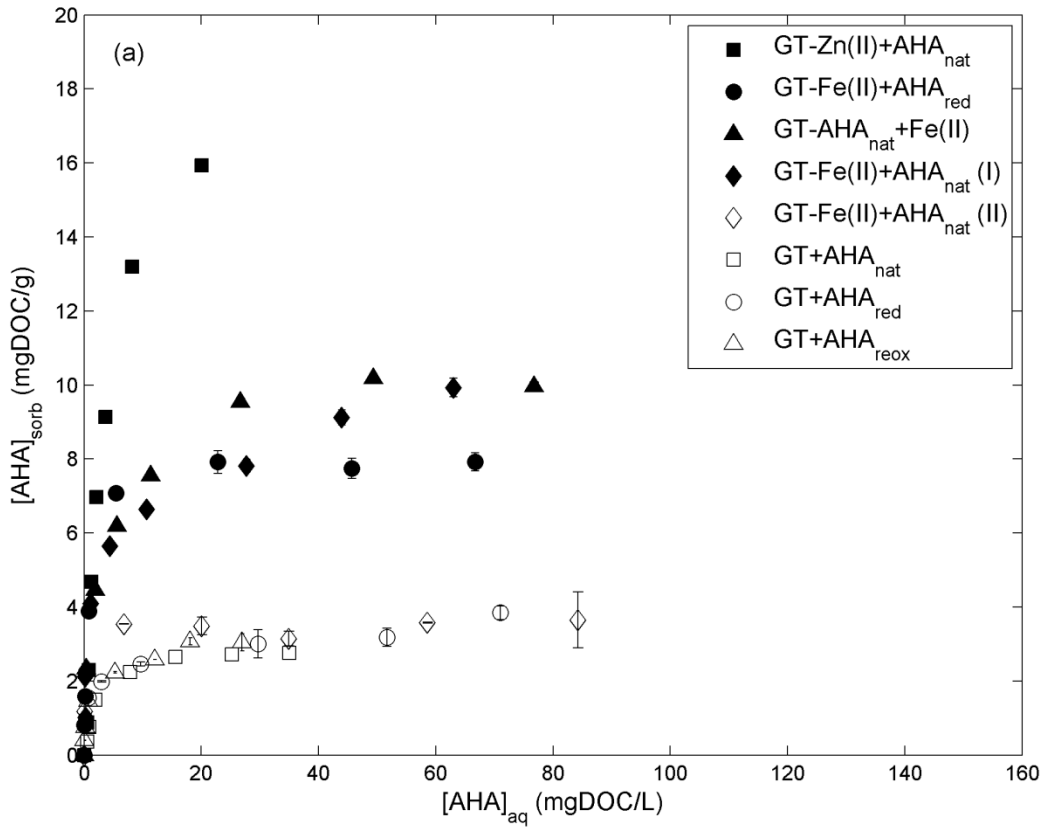
**Figure 3.1.** (a) Experimental data of Aldrich humic acid sorption to goethite/Fe(II). Data points refer to mean values of two independent experiments with error bars representing the lowest and highest values. (b) Solid circle shows the experimental data of $AHA_{red}$ sorption to GT-Fe(II). Solid Line represents fitting of $AHA_{red}$ sorption results using a Langmuir model (eq. 3.1). (c) Solid triangle shows the experimental data of $AHA_{untre}$ sorption to GT-Fe(II) (I). Solid diamonds show the experimental data of $AHA_{untre}$ sorption in the reverse order of Fe(II) addition. Solid Line represents fitting the experimental data of $AHA_{untre}$ sorption at GT-Fe(II) surface (I) using a Langmuir model. (d) Open diamond shows the experimental data of $AHA_{untre}$ sorption to GT-Fe(II) (II). Solid Line represents fitting of $AHA_{untre}$ sorption at GT-Fe(II) (II) system using a Langmuir model. (e) Open square, circle and triangle shows the shows the experimental data of $AHA_{untre}$, $AHA_{red}$ and $AHA_{reox}$ sorption to GT surface respectively. Solid Line represents fitting the experimental data of $AHA_{untre}$ sorption by using a Langmuir model. All the parameters ($K_{L,i,j}$ as the Langmuir constant [L/mgDOC] (i: untre/red, j: GT/GT-Fe(II) and $[AHA_i]_{sorb, max,j}$ as (apparent) uptake maximum [mgDOC/g]) by fitting the Langmuir model to experimental data respectively are listed in Table 3.2.

**Table 3.2.** the Langmuir constant $K_{L,i,j}$ (i:untre/red, j:GT/GT-Fe(II)) and (apparent) uptake maximum $[AHA_i]_{sorb, max,j}$

(GT = goethite; AHA = Aldrich Humic Acid)

| Experiment Label | $K_{L,i,j}$ [L/mgDOC] | $[AHA_i]_{sorb, max,j}$ [mgDOC/g] | $R^2$ |
|---|---|---|---|
| GT+AHA$_{untre}$ | $0.41 \pm 0.05$ | $2.99 \pm 0.09$ | 0.99 |
| GT+AHA$_{red}$ | $0.86 \pm 0.28$ | $3.25 \pm 0.17$ | 0.89 |
| GT+AHA$_{reox}$ | $1.30 \pm 0.28$ | $2.94 \pm 0.11$ | 0.95 |
| GT-Fe(II)+AHA$_{untre}$ (I) | $0.46 \pm 0.11$ | $9.16 \pm 0.44$ | 0.93 |
| GT- AHA$_{untre}$ +Fe(II) | $0.34 \pm 0.05$ | $10.34 \pm 0.30$ | 0.98 |
| GT-Fe(II)+AHA$_{untre}$ (II) | $4.51 \pm 1.11$ | $3.51 \pm 0.11$ | 0.94 |
| GT-Fe(II)+AHA$_{red}$ | $1.22 \pm 0.15$ | $8.04 \pm 0.16$ | 0.99 |

The adsorption isotherm of AHA$_{red}$ on the goethite-Fe(II) surface showed an initial steep slope and reached a plateau at approximately 8 mg DOC/g uptake indicating a high affinity of reduced AHA to GT-Fe(II) surface sites, illustrated by Figure 3.1b. The Langmuir model was well fitted to the sorption data. The experimental results showed that the sorbed amount of electrochemically reduced AHA onto goethite in the presence of Fe(II) (total 1.5 mM) was double as in the absence of Fe(II) (discussed later in detail). Two explanations for the strengthened sorption of reduced AHA to the goethite-Fe(II) surfaces are possible. On one hand, electrostatic attraction could be responsible for this enhancing sorption behavior. The presence of Fe(II) may lead to a less negative or even positive surface charge of GT due to sorbed Fe(II) at neutral pH, thus coating with negatively charged moieties in the reduced AHA. On the other hand, hydroquinone moieties and catechol-like phenolic groups are expected to be rich in the reduced stated of AHA so that these ligands are likely to be preferentially bound to the sorbed Fe(II) at mineral surface, forming a ternary goethite-Fe(II)-AHA$_{red}$ surface complex. Furthermore, it should be noted when Fe(II) was present with the reduced AHA in aqueous solution, no decrease in concentration of aqueous AHA$_{red}$ before and after filtration was observed (see Table S3.1 in the Supporting Information).

Furthermore, when reduced AHA was added into goethite-Fe(II) system, Fe(II)$_{aq}$ concentration remains almost constant at approximately 1 mM (Figure 3.2). This finding indicates no electron transfer between reduced AHA and GT-Fe(II), as well as reduced AHA may not compete with Fe(II) sorption on goethite surface.
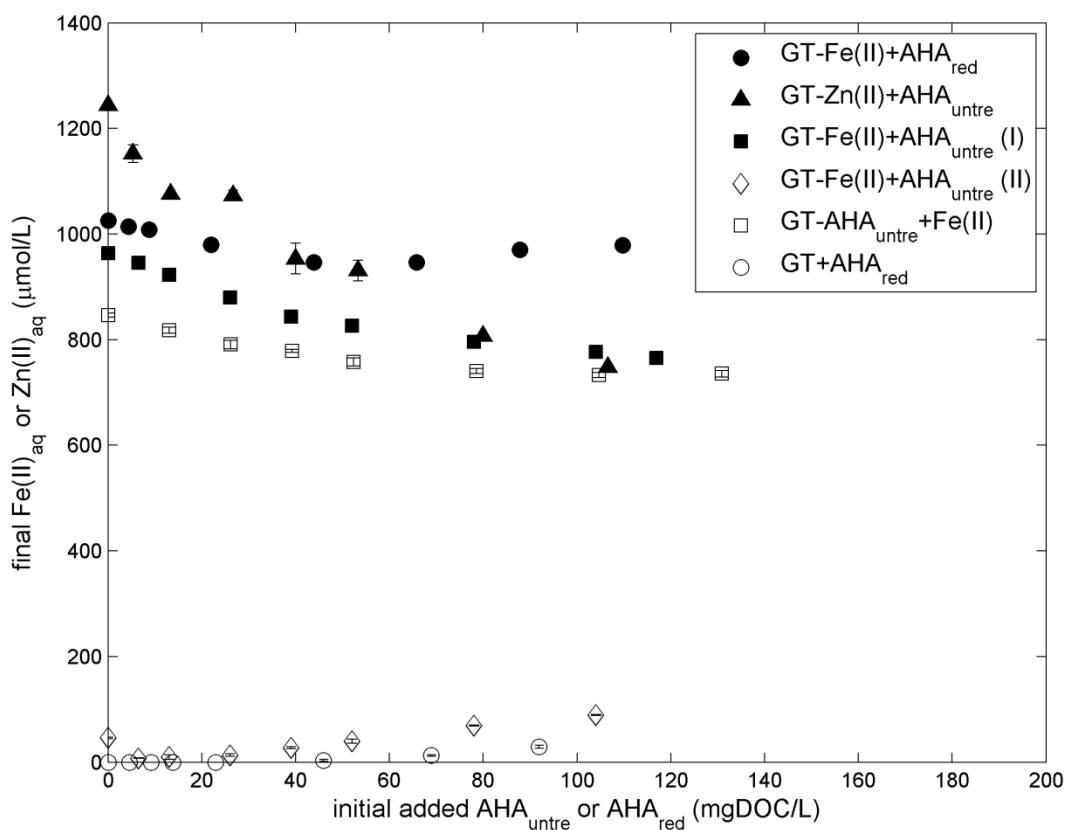
**Figure 3.2.** Equilibrium aqueous concentrations of Fe(II) or Zn(II) in goethite suspensions under different experimental conditions. Data points refer to mean values of two independent experiments with error bars representing the low and high values.

Under oxic conditions (such as 'GT+AHA$_{untre}$', no Fe(II) present), the adsorption isotherm of untreated AHA on goethite at neutral pH followed a Langmuir model (Figure 3.1e). Also, this sorption behaviour was found to be pH-dependent (Figure S3.7 in Supporting Information). This is consistent with the electrostatic interaction and ligand exchange mechanism as observed by Gu et al.[21, 46] The surface of goethite becomes slightly negatively charged at pH 7 (pH$_{pzc}$ = 6.5), whereas there remains a small number of local positive-charged surface sites which are able to attract the deprotonated carboxyl or phenolic molecules rich in the humic acid structure.

Due to the possible redox reaction between AHA$_{untre}$ and bound Fe(II)-goethite interfaces, the sorption of AHA$_{untre}$ to goethite-Fe(II) cannot be evaluated without redox reaction (i.e reduction of AHA$_{untre}$ to AHA$_{red}$). To avoid this limitation, we studied sorption of AHA$_{untre}$ at GT-Zn(II). Zn(II) was not redox active and mimicked the surface charge of goethite-Fe(II) system to investigate the possible electrostatic effect in the course of sorption process of untreated AHA. No redox reaction between

53

untreated AHA and goethite-Zn(II) was expected. The obtained sorption isotherm of $AHA_{untre}$ in goethite-Zn(II) system showed a Langmuir shape (Figure 3.1a), but not achieving saturation in the concentration range of $AHA_{untre}$ used here. The sorbed amount of humic acid was dramatically higher in the presence of sorbed Zn(II) than in its absence. Two possible effects can be considered to explain this significant increasing sorption, with regard to the electrostatic interactions and surface complex formation of surface associated Zn(II). Firstly, the presence of sorbed Zn(II) reduces the negative surface charge of goethite, thus enhancing the electrostatic interaction with untreated AHA. Secondly, since $Zn(II)_{aq}$ concentration decreased from 1.2 to 0.8 mM in the filtered fractions (see Figure 3.2), $AHA_{untre}$ is supposed to be attracted to bound Zn(II) at surface sites forming a ternary goethite-Zn(II)-$AHA_{untre}$ complex. In addition, Zn(II)-$AHA_{untre}$ complex can be formed as a black precipitation when only Zn(II) and $AHA_{untre}$ are present in aqueous phase. This binary complex was evidenced by our control samples and was in agreement with previous studies.[89, 94, 95] The Zn(II)-$AHA_{untre}$ complex could bring about the concentration loss of both $AHA_{untre}$ (5 mg DOC/L) and $Zn(II)_{aq}$ (60 μM) in the control samples (Table S3.1). Thus, the presence of Zn(II)-$AHA_{untre}$ complex formation can overestimate the sorption of $AHA_{untre}$ onto goethite-Zn(II) system up to 6% in the high added $AHA_{untre}$ concentration (100 mgDOC/L) and 40% in the low one (10 mgDOC/L). As uptake of Zn(II) by goethite was much lower than uptake of Fe(II) (0.3 instead of 0.5 mM), $AHA_{untre}$ sorption to GT-Fe(II) is expected to be stronger than GT-Zn(II). However, the change of surface charge due to metal sorption is likely different.

When untreated AHA was added into the goethite-Fe(II) system namely GT-Fe(II)+$AHA_{untre}$ (I), the amount of total sorbed AHA was almost three times higher than $AHA_{untre}$ sorbed in the goethite system (see Figure 3.1c). In this case, both specific and non-specific mineral-AHA interactions may be responsible for the high adsorption. Firstly, the sorption of ferrous iron makes the goethite surface less negative, leading to higher electrostatic attraction with negatively charged moieties in the $AHA_{untre}$. Secondly, untreated AHA is expected to be reduced to some extent by the associated reactive Fe(II) at goethite surface sites (discussed later), leading to goethite-Fe(II)-$AHA_{red}$ complexes described by goethite-Fe(II)+$AHA_{red}$ sorption isotherm. Thirdly, compared to the isotherm of GT-Fe(II)+$AHA_{red}$ (Figure 3.1b), the amount of total sorbed AHA was slightly higher especially when the remaining aqueous concentration of AHA was above 40 mgDOC/L. It is likely that the nonreduced moiety of untreated AHA ($AHA_{nonred}$) may form surface complexes with goethite-Fe(II) (goethite-Fe(II)-$AHA_{nonred}$). Thus, these findings suggest that the presence of sorbed Fe(II) could reinforce the sorption of $AHA_{untre}$ to goethite.

However, sequence of Fe(II) addition is supposed to influence the sorption of $AHA_{untre}$ to goethite, since AHA can be bounded to the mineral, resulting in the decline of Fe(II) sorption to goethite surface. To prove this, $AHA_{untre}$ was firstly spiked onto goethite by shaking the suspension overnight followed by the addition of Fe(II) into this

GT-AHA$_{untre}$ system which was allowed to equilibrate for two days. In this case, the obtained isotherm matched almost with the condition of GT-Fe(II)+AHA$_{untre}$ (I), shown in Figure 3.1c. Thus, the experimental evidence hints that the sequence of Fe(II) addition does not alter the sorbed amount of AHA$_{untre}$ to goethite-Fe(II) system.

Furthermore, amount of Fe(II) loading is also considered as another impact factor to alter the sorption of untreated AHA on goethite-Fe(II) surfaces. In this setup (GT-Fe(II)+AHA$_{untre}$ (II)), the initial total added Fe(II) concentration was only 0.4 mM instead of 1.5 mM and most of them were adsorbed at goethite surface (see Table 3.1). Consequently, the total sorbed amount of untreated AHA in the goethite-Fe(II) system with this relatively low Fe(II) loading was only halved compared to it in the reference goethite-Fe(II) (I) system, but still 17% higher than it in the goethite system with the absence of initial Fe(II) loading, shown in Figure 3.1d. This observation suggests that the sorption of untreated AHA on the goethite surface can be significantly altered by the amount of reactive Fe(II). The most possible explanation is that in the case of high Fe(II) loading (1.4 mM), the amounts of electrons transfer from AHA$_{untre}$ to AHA$_{red}$ are expected to be higher than low Fe(II) loading (0.4 mM) due to the regeneration of Fe(II)-sites at goethite after oxidation by re-adsorption of Fe(II) from solution. This Fe(II) re-adsorption process may increase the binding sites at goethite surfaces for AHA sorption. In conjunction with the previous results, we provided first evidence to support that the sorption of untreated AHA to goethite seems to present positive correlation with the initial ferrous iron loading to the iron mineral system at neutral pH condition, within a certain range of initial Fe(II) addition in our study (0-1.4 mM).

Besides of the added Fe(II) into goethite system, sorption of humic acid on goethite may also be influenced by the redox states of humic acid. Therefore, the experiment was designed by spiking electrochemically reduced AHA into goethite system without any initial Fe(II). The obtained sorption isotherm of AHA$_{red}$ on goethite surface was almost identical to AHA$_{untre}$ (Figure 3.1e). This finding is consistent with the conclusion of Bauer and Kappler that reduced and untreated AHA does not present significant changes in the sorption behavior on iron mineral with respect to the redox state of humic acid.[60] It further suggests that the changes in the chemistry and spatial structure of AHA under reduced states (such as more phenolic or hydroquinone moieties produced) may not remarkably alter the sorption interaction between AHA and the iron mineral surfaces. In addition to AHA, an enhanced reductive dissolution of Fe(III) minerals by organic solutes such as humic substances may promote the formation of Fe(II) since it has been reported that goethite can be reduced by AHA$_{red}$ with a maximum of 55-60 μeq/(g HA).[60] This little amount of Fe(II) can be adsorbed on the goethite, resulting in the formation of reactive Fe(II) species at surface sites or mineral surface remodeling. However, the presence of Fe(II) in minor quantity is not expected to affect specific interaction of AHA moieties with iron mineral interfaces.

Finally, reoxidized AHA interaction with goethite was operated to determine its sorption ability to goethite, the observed sorption isotherm was the same as AHA$_{untre}$ (Figure 3.1e). It is predictable that reoxidized and untreated AHA reveal similar sorption ability to goethite although their fractions of redox-active functional groups may vary, as previous studies have been shown that the reducing and oxidation cycling of humic substance is not reversible since O$_2$ was not able to fully reoxidize chemically (H$_2$/Pd) and electrochemically reduced humic substance.[36, 60] Therefore, our sorption dataset indicates that untreated, electrochemically reduced and reoxidized humic acid may not affect its sorption onto the goethite.

## 3.3.2 Sorption Comparison of Model Quinone and Humic Acid on Goethite/Fe(II) Interfaces

Within humic substances, quinone/hydroquinone structures are considered as the major redox active moieties,[10, 52] but also complexes iron metals and are responsible for their sorption ability to the iron mineral as it affects the abundance and type of phenolic functional groups (OH).[57, 96, 97] Catechol-like quinone such as 2-hydroxy-1,4-naphthoquinone (lawsone) has been proved to participate in the electron transfer at the goethite-Fe(II) interfaces, as well as to be adsorbed onto goethite-Fe(II) surfaces.[93] Here, the sorption dataset of AHA was compared with the obtained sorption isotherm of this specific naphthoquinone lawsone under same conditions,[93] to reveal the relative sorption ability contribution of quinone/hydroquinone moiety by electrostatic and specific interactions to Fe(III)/Fe(II) system within humic acid structure.

Comparison of these sorption dataset revealed that surprisingly the sorption behaviour of lawsone on the goethite/Fe(II) surfaces is quite similar to that of AHA (Figure 3.3), despite of the strong discrepancy in the sorption ability between lawsone and AHA. On one hand, the presence of reactive Fe(II) significantly enhancing the sorption of oxidized and reduced lawsone (LAW$_{ox}$/LAW$_{red}$) at goethite surface is analogous to AHA. Non-specific and specific goethite-Fe(II)-lawsone/AHA interactions are responsible for it.[93] On the other hand, the amount of sorbed AHA to goethite/Fe(II) surfaces is three times higher than lawsone compound, since a large number of reactive functional groups such as phenol and carboxylic acid are rich in humic acid structure besides of quinone/hydroquinone moiety. These reactive moieties could be attracted by the adsorption sites at Fe(II)/Fe(III) surfaces.[57, 78, 98] Also, electron transfer reactions between organic matter (e.g. lawsone/humic acid) and goethite-Fe(II) interfaces are expected to be favourable (discuss later), even though quinone/humic acid are adsorbed to goethite. Thus, we suggest that sorption of the organic matter such as quinone and humic substances is in agreement with surface-complex

formation involving Fe(II) surface sites as it is affected by the abundance and type of reactive Fe(II)-sites at goethite as well as the re-formation of such sites after oxidation by continuous adsorption of aqueous Fe(II).[93]
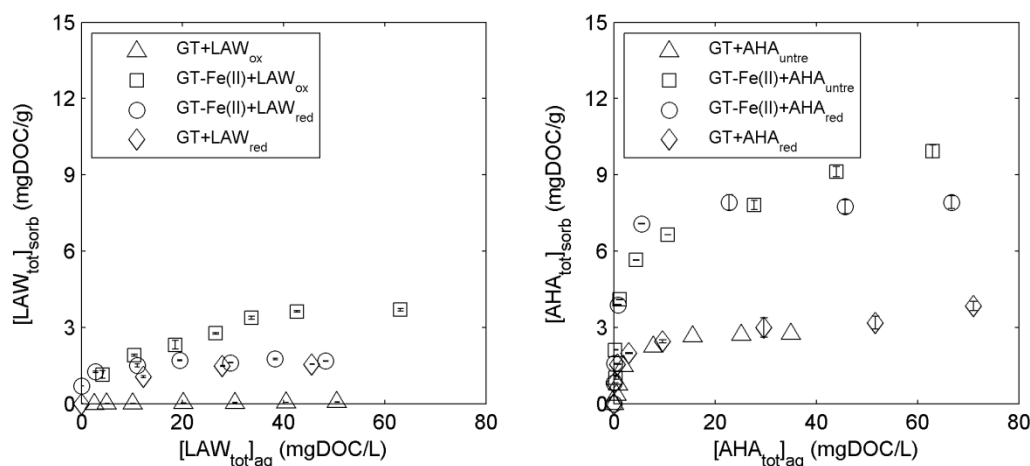


**Figure 3.3.** Comparison of Sorption behaviors of Aldrich humic acid with model quinone lawsone on goethite-Fe(II) interfaces under different redox conditions at neutral pH. Lawsone sorption dataset is sourced from Xue et al.[93]

## 3.3.3 Electron Transfer Reaction between Goethite/Fe(II) System and Aldrich Humic Acid

The electron transfer process in heterogeneous goethite-Fe(II) interfaces may be influenced by the reactivity of sorbed Fe(II) and the redox species of sorbing organic matter in the system. Unfortunately, it should be noted that the redox speciation of AHA in final filtered samples as well as at surface sites could not be experimentally determined, since the aqueous speciation of AHA was not possible to be distinguished between untreated and reduced states by UV-Vis and Fluorescence spectroscopic study (details see Figure S3.1 and S3.2 in the Supporting Information), consistent with the findings of Maurer et al.[99]   Also, the redox speciation of AHA in our final filtered samples could not be determined by electrochemical technique due to the presence of aqueous Fe(II). Thus, the electron transfer across the goethite-Fe(II) surface was investigated in the angle of the difference of redox potential between Fe(II) associated with goethite and dissolved humic substance, as well as detectable $Fe(II)_{aq}$ concentration in the filtered fractions.

GT-Fe(II)+AHA$_{untre}$ (I). Untreated AHA was expected to serve as electron acceptor during the interaction with goethite-Fe(II) reference system (initial Fe(II) loading 1.5 mM). The extension of electron transfer from bound Fe(II) to untreated AHA depends

mainly on the delta value of the redox potential ($E_H$) between the electron donator and acceptor. As previously reported by Orsetti et al,[27] the apparent reduction potential of goethite-Fe(II) system at neutral pH was estimated around -170 mV vs SHE (standard hydrogen electrode) on the basis of the equilibrium aqueous speciation of non-sorbing quinone AQDS.[27] Similarly in our previous study using the sorbing quinone lawsone speciation as redox probe, the reduction potential $E_H$ of goethite/goethite-Fe(II) interfaces in the range of -127 to -173 mV vs SHE,[93] is not significantly influenced by sorption of quinone/hydroquinone. Meanwhile, a number of redox potential values of humic substances (HS) have been experimentally determined and reported ranging from -300 mV to +800 mV (chemically, Pd/H$_2$)[61, 62] or -300 to +150 mV (electrochemical method).[45] Therefore, $E_H$ of goethite/Fe(II) system might be negative enough to reduce AHA$_{untre}$ with more positive $E_H$ values.

Furthermore, an electron balance between the reducing adsorbed Fe(II) and untreated AHA can be roughly estimated, on the basis of the Electron Accepting Capacity (EAC) of AHA$_{untre}$ and the Fe(II)$_{aq}$ loss in the filtered fractions. The EAC values of untreated AHA were electrochemically detected by Mediated Electrochemical Reduction (MER, details see Supporting Information) and are listed in Table S3.2 in the Supporting Information. The EAC values of untreated AHA in our study was $3.19 \pm 0.3$ µmol e$^-$/mgDOC, which was slightly higher than the ones reported in literature: 1.9 to 2.5 µmol e$^-$/mgDOC.[36, 100] The electron accepting properties of HA has been ascribed to quinone moieties.[36, 101] To estimate their contribution to the EAC of our AHA$_{untre}$, using data from Aeschbacher et al, the content of quinones in untreated AHA was counted within the range of 8 to 200 µmol e$^-$/L, assuming that all reversible sites of electrons transferred within AHA$_{untre}$ were derived from redox-active quinone.[36, 100] This value could explain the maximum accepted electrons for AHA$_{untre}$ across the goethite-Fe(II) interface. Linking to the measured Fe(II)$_{aq}$ concentration of filtered samples declining 0.2 mM with the amount of the untreated AHA addition increasing (Figure 3.2), it act as an indirect indicator to verify the oxidation of sorbed Fe(II) to Fe(III) by untreated AHA in the occurrence resulting in the re-adsorption process of aqueous Fe(II). It is worthwhile mentioning that the concentration of sorbed Fe(II) could not be directly measured since a large quantity of humic acid are bound to GT-Fe(II) surfaces, enhancing the difficulty of desorbing Fe(II) completely at surface. Furthermore, the decline trend of Fe(II)$_{aq}$ of filtered fraction in goethite-Fe(II)+AHA$_{untre}$ (I) system, is also consistent with the case in goethite-Fe(II)+LAW$_{ox}$ system (Fe(II)$_{tot}$ = 1.5 mM), shown in Figure 3.4. It provided the evidence that quinone moiety within HA can play an important role in the redox active interaction with bulk reductant such as associated Fe(II) at iron mineral surface.
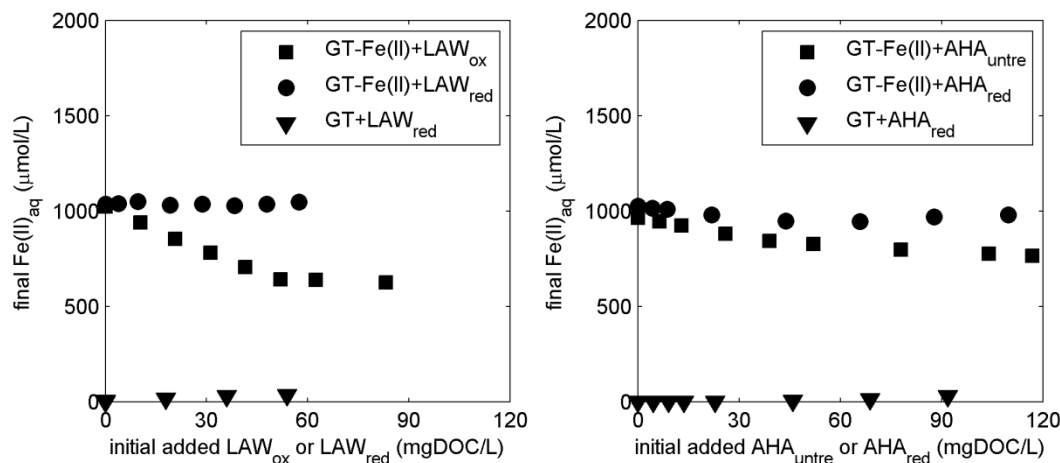
**Figure 3.4.** Comparison of final Fe(II)$_{aq}$ dataset of filtered samples after Aldrich humic acids and quinone lawsone interaction with on goethite/goethite-Fe(II) system at neutral pH. Fe(II)$_{aq}$ dataset of Lawsone sorption experiment comes sourced from Xue et al. [93]

GT-AHA$_{untre}$+Fe(II). In the case of reversing the order of Fe(II) addition, reduction of AHA$_{untre}$ by associated Fe(II) at goethite surface is foreseeable. However, the amount of electron transfer in this setup is expected to be lower than the reference goethite-Fe(II) system, since Fe(II) sorption to goethite surface may become weaker due to the first step of AHA$_{untre}$ binding to goethite. It was also indirectly evidenced by the results of Fe(II) concentration in the filtered samples declining from 850 to 750 μM with the increase of untreated AHA addition. The declining values 100 μM were observed smaller than 200 μM in the reference system (shown in Figure 3.2). Thus, it demonstrates that the initially AHA sorption to goethite may lead to a relatively lower reducing capacity of goethite-Fe(II) surfaces.

GT-Fe(II)+AHA$_{untre}$ (II). When initial Fe(II) loading to goethite system was one quarter as the reference goethite-Fe(II) system (initial total 0.4 mM), small amount of Fe(II) (50 μM) remained in aqueous phase before untreated AHA was added. We expected the reduction of untreated AHA by sorbed Fe(II), however, to a limited extent compared to the reference goethite-Fe(II) system. The results of Fe(II) quantified in the filtered samples showed that Fe(II) concentration initially declined from 50 μM to 7 μM, then climbing to 114 μM with the increase of untreated AHA addition (see Figure 3.2). This observation may be explained by two-stage reactions: initially oxidation of sorbed Fe(II) by untreated AHA, leading to a newly aqueous Fe(II) re-adsorption process; Then either untreated AHA or partially reduced AHA binds to associated Fe(II) on goethite surfaces, carrying it into the aqueous phase.

<u>GT+AHA$_{red}$</u>. The oxidation of AHA$_{red}$ by Fe(III) associated to goethite (i.e. 'backward' reaction) was investigated by adding electrochemically reduced AHA into goethite suspension without initial added Fe(II). Bauer et al has reported that chemically reduced AHA by Pd/H$_2$ has the ability to reduce Fe(III) associated with goethite to Fe(II) since the redox potential of reduced AHA was negative enough to reduced Fe(III) mineral with very positive E$_H$ values.[60] Also it has been reported that the reduction of goethite mineral occurs with a maximum amount of electron to 0.3 μmol e$^-$/mgDOC.[60] Using this data for our calculation in this experiment, freshly produced Fe(II) by reduction of Fe(III) was estimated within a range of 1.5 to 30 μmol/L corresponded to our reduced AHA added. Combining the results of measured aqueous Fe(II) concentration of filtered samples climbing from 0 to 30 μmol/L, it fully matches with the amount of the electrons transfer from reduced AHA to Fe(III). Additionally, compared to the data of Fe(II) concentration in the filtered samples when reduced lawsone compound interacted with goethite (see Figure 3.4), similar rising trend was observed after both AHA$_{red}$ and reduced lawsone addition into goethite system. It suggested that hydroquinone moiety within reduced AHA can be mainly responsible for the electrons transfer during the interaction with iron mineral.

## 3.4 Environmental Significance

The interaction between organic matter and heterogeneous Fe(III)/Fe(II) systems is predominantly composed of sorption and electron transfer processes. Our results indicated that electrochemically reduced humic acid may not alter the sorption behavior on the iron mineral compared to the untreated and reoxidized one. However, the presence of associated Fe(II) at goethite surface can strongly enhance the sorption behavior of redox-active organic matter dependent on its redox state such as untreated and reduced humic acids. Also, the amount of aqueous Fe(II) in the goethite-Fe(II) may significantly alter the sorption behaviour of untreated humic acid. Additionally, redox reaction between humic acid and iron mineral/Fe(II) was favourable relying on the big gap between the redox potential of Fe(III) mineral-Fe(II) surfaces and dissolved humic acid. Consequently, the sorption and electron transfer process may cause remodelling of the mineral-water interphase and thus may affect electron transfer process in the anoxic aquifer, illustrated by Figure 3.5.
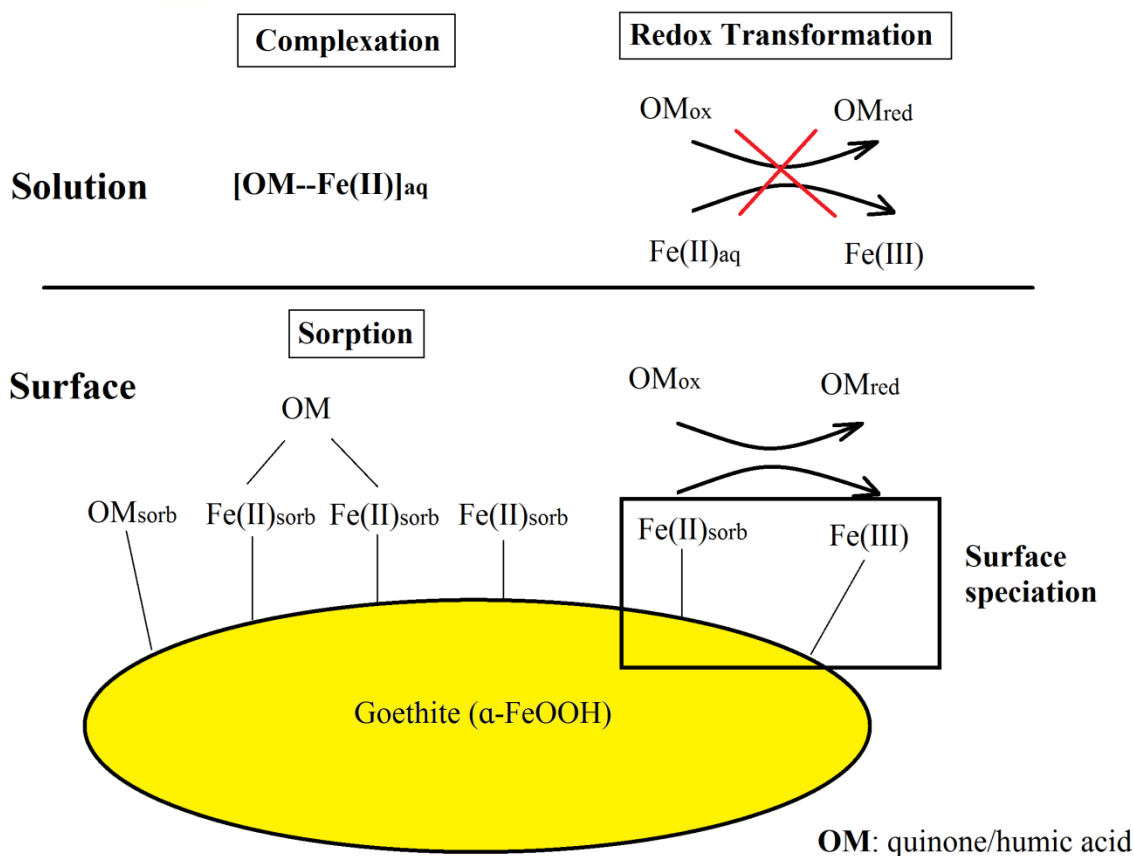
**Figure 3.5.** Scheme of possible interactions between NOM and iron mineral (goethite) in the presence of Fe(II).

Furthermore, it is highlighted that quinone/hydroquinone compound representing important structural and functional properties of natural organic matter macromolecules, shows similar trend in sorption and electron transfer process at the associated Fe(II)-mineral interfaces as humic substance. Our results also provide the evidences to explain the findings that quinone/humic substance especially at high concentrations can inhibit the reduction of organic pollutant such as nitrobenzene and carbon tetrachloride in the associated Fe(II) mineral systems,[2, 12] as electron transfer and sorption process of organic matter may consume the redox reactivity of mineral-Fe(II) interfaces.

# Chapter 4

**Surface Complexation of Quinone/Humic Acid at the Goethite/Fe(II) Interface: An UV-Vis/ATR-FTIR Study**

# Abstract

Insights regarding the adsorption mechanisms of quinone interactions with iron minerals can improve our understanding of the fate and transport of such molecules in the environment. However, an identification of the bonding mechanism at molecular level is still missing in the literature and will be addressed in this study for the adsorption process of quinone/humic acid at the goethite/aqueous interface. UV-Vis analysis in conjunction with in situ flow cell measurements of Attenuated Total Reflectance Fourier-Transform Infrared (ATR-FTIR) spectroscopy were used to explore the adsorption mechanisms. 2-Hydroxy-2, 4-naphthoquinone (lawsone) was chosen as model quinone as well as 1,2-dihydroxybenzene (catechol) for comparison and validation for the ATR-FTIR flow through setup. Our UV-Vis spectroscopic results have shown that the spectra of aqueous lawsone were identical to the one of dissolved Fe(II)-lawsone mixtures, suggesting Fe(II)-lawsone complexes are not formed to a significant extent in the aqueous phase. Also, the ATR-FTIR results proved negligible sorption of oxidized lawsone on goethite/water interfaces in the absence of Fe(II). On the other hand, the ATR-FTIR experimental setup was validated using catechol that forms bidentate surface complex at goethite as studying the characteristics, proved in the literature. Furthermore, the ATR-FTIR technique was applied for surface interactions between goethite and humic substances to the sorption mechanism. Comparison of ATR-FTIR spectra obtained for adsorbed and dissolved Aldrich Humic Acid (AHA) indicated that carboxyl and phenol functional groups in AHA were responsible for sorption to goethite. Overall, our results suggest that sorption of quinones and humic substances were to goethite is due to both electrostatic attraction and surface complexation.

# 4.1 Introduction

Interactions between iron and quinone moiety have been reported in several important biochemical systems and environmental phenomena, including electron-transport chains involved in photosynthesis and respiration, nutrient acquisition, as well as mineral weathering, and pollutant reduction.[68-70, 73, 96, 102] In view of the importance of quinone-iron complex, apparently a large number of research has been done to characterize iron complexes with quinone, semiquinone or hydroquinone ligands.[69, 70, 96, 97, 102] Catechol and its structure-like molecules are an important class of hydroquinones/quinones in the environment. These hydroxyaromatic compounds are highly reactive with aqueous iron and readily associated with iron oxides mineral.

In aqueous phase, catechol can form complex with both Fe(II) and Fe(III). Several types of complexes have been described which can be classified as binary complexes and ternary complexes. On one hand, since early 1980s, it was noted that catechol reacts with Fe(II)/Fe(III) to form the binary complex (metal:ligand = 1:1)[75, 77] and it has been reported that the stability constants of Fe(III)-catechol complexes can be examined by potentiometric and spectroscopic methods.[76, 103] On the other hand, Cox et al described ternary complexes between a protein (enzyme), Fe(III) and catechol, reporting binding constants and spectral properties.[104] They also investigated the effects of different polydentate model ligands (mimicking binding sites of Fe(III) at the protein) on the properties of the ternary complexes with catechol (protein-Fe(III)-catechol).

Furthermore, surface complex formation between catechol and iron mineral has been widely investigated. The hydroxyaromatic compound has been reported to be readily adsorbed onto the iron oxides.[46, 105] Fourier transform infrared (FTIR) spectroscopic measurements have suggested that catechol binds predominantly as inner-sphere complex on $Fe_2O_3$ in a mononuclear monodentate configuration at pH < 5 and a mononuclear bidentate at pH > 5.[58] Additionally Yang et al[57] has indicated that catechol adsorbed on goethite in mononuclear monodentate and binuclear bidentate chelates at pH 5 to 9.

Another nathoquinone to our interest is 2-hydroxy-2,4-naphthoquinone lawsone, representing naturally occurring catechol-like molecule. It is worthwhile to note that it can provoke many biological activities through the chelating of metals.[65-70] Similar to catechol-iron aqueous complexes, Lawsone (LAW)-metal complexes seem also to be separated as binary complexes and ternary complexes. Concerning binary complex, it has been investigated that Fe(II)-lawsone complex [$Fe^{II}$(Lawsone)$_2$(H$_2$O)$_2$] can be chelated by the mixture of lawsone and FeSO$_4$·7H$_2$O in methanol and Mössbauer and EPR spectroscopic data was also reported.[66] It has also been described that ferrous/ferric complexes of hydroxynathoquinone (lawsone and juglone) are highly cytotoxic to rat hepatocytes.[65, 106] In addition, it has been published about ternary complexes of lawsone, reporting the electrochemical properties for a series of lawsone and pyridine (Py) complexes with different metallic ions - Ni(II); Co(II), Zn(II)-symbolized as [Metal(II)(lawsone)(Py)$_2$] by cyclic voltammetry and spectroelectrochemical-Electron Spin

Resonance experiments.[107] However, little is known about the aqueous complex formation of lawsone and iron (LAW-iron) in water solution especially the reduced state of lawsone ($LAW_{red}$) with iron, since it is consisted of catechol-like-OH functional groups.

Previously, we reported that oxidized and reduced state of lawsone ($LAW_{ox/red}$) can be adsorbed onto the goethite-Fe(II) interfaces.[93] However, no clear bonding mechanism of adsorbed $LAW_{ox/red}$ has been recognized. It seems plausible that ternary complexes may form in our goethite systems. Similar to the protein-Fe(III)-catechol complex, here the mineral ́s surface would take on the role of the protein in the ternary complex and reduced lawsone the role of the catechol ligand (mineral-Fe(II)-$LAW_{red}$). To fill this knowledge gap, it is necessary to further explore the sorption mechanism of lawsone at goethite-Fe(II) interface for a better understanding of quinone interaction with iron(oxide). This study has utilized UV-Vis analysis in conjunction with in situ flow cell measurements of Attenuated Total Reflectance Fourier-Transform Infrared (ATR-FTIR) spectroscopy to probe the bonding mechanism. The UV-Vis spectra were taken to assess whether the aqueous iron-LAW complexes are present under environmental pH conditions. ATR-FTIR spectroscopy of particle films immersed in solution is a useful tool to investigate the details of surface reaction at solid-solution interfaces.[80, 108] Iron oxide films deposited on ATR crystals can allow the adsorbate at the interface to be directly monitored due to the high surface area.[57, 58, 109] In this work, ATR-FTIR setup was firstly validated by the aqueous catechol and sorbed one at iron mineral surface, and then was utilized to evaluate the adsorption mode of our target compound (lawsone) at iron mineral/Fe(II) surface.

The adsorption studies of well-defined quinones are useful to explain the sorption behavior of Natural Organic Matter (NOM). NOM sorption is inevitably more complicated than quinone molecules due to their inherent complexities with various functional groups. Until now, NOM sorption mechanisms on goethite still remain unclear. Therefore, the ATR-FTIR technique was extended to explore the adsorptive fractionation of organic matter such as humic acid as another important objective.

## 4.2 Materials and Methods

**Chemicals**. Potassium chloride (KCl), acetic acid ammonium salt ($NH_4COOCH_3$, 98%) and Ferrozine (98%) were from Acros Organics. 2-hydroxy-2,4-naphthoquinone (Lawsone, 97%), Aldrich humic acid solids (Humic acid, Sodium salt) and sodium hydroxide were purchased from Sigma-Aldrich. 1,2-dihydroxybenzene (catechol, 99%) was provided by Alfa Aesar. Hydrochloric acid (HCl) was from Merck. All aqueous solutions were prepared with Millipore water. Goethite ($\alpha$-FeOOH, Bayferrox 920Z) was received from LANXESS; specific surface area ($N_2$-BET) = 9.2 $m^2$/g; pHpzc = 6.5.[35]

Fe(II) stock solution (0.5 M in 1M HCl) was prepared according to Bucholz et al.[35] Fe(III) stock solution was purchased from Merck. The preparation of dissolved lawsone ($LAW_{ox/red}$)[93] and untreated Aldrich humic acid (AHA)[110] solutions were based on my previous protocol.[93, 110]

**UV-Vis Measurements.** The oxygen-susceptible procedures were carried out inside a Unilab anoxic glovebox (M. Braun, Germany, $O_2 < 1ppm$, 100% $N_2$). UV-Vis spectra were measured to investigate the possibility of the aqueous iron-LAW complexes in the pH range of 2 to 7.

The general procedure was that firstly, four reference solution spectra including ferrous iron (Fe(II)), ferric iron (Fe(III)), oxidized lawsone ($LAW_{ox}$) and reduced lawsone ($LAW_{red}$) in the pH range 2 to 7 were obtained in the anoxic quartz cuvettes by UV-analysis. Secondly, aliquots of 25 ml of either Fe(II) or Fe(III) solution were pipetted into 50 ml brown serum bottles. $LAW_{ox}$ or $LAW_{red}$ were equilibrated with these iron solutions in a 1:1 dilution for about one hour, resulting in initial lawsone concentration of 30 μM and iron content of 10 μM. The pH was adjusted in the pH range 2 to 7 with NaOH or HCl. And the spectra recorded in the wavelength range of 200-800 cm at each pH in the anoxic quartz cuvettes by UV-analysis.

**ATR-FTIR Spectroscopy Analysis**. ATR-FTIR measurements were performed with a Bruker VERTEX 80V spectrometer equipped with a LN-MCT detector and a horizontal BioATR II accessory (8 reflections, Bruker, Germany). The water bath was connected to the ATR accessory to control the temperature at 25°C. The flow-through cell was fitted with a ZnSe crystal. All of the spectra were taken at 400 scans and with a resolution of 4 cm$^{-1}$. The spectra were recorded in the range of 800-4000 cm$^{-1}$ and only shown for the region of 1000-1800 cm$^{-1}$. Data collection and spectral analysis such as manipulation of the atmosphere signal ($CO_2$ and $H_2O$) were carried out using OPCS 7 software (Bruker, Germany).

The reference spectra of quinones (catechol/lawsone) solution were obtained in flow through system and static state for validation (setup shown in Figure S4.5). No background electrolyte was introduced in the whole experiment.

The spectra of quinones interaction with the goethite film at neutral pH were measured on the ZnSe crystal by flow through system. Goethite film with high surface area was prepared by placing 30 μL of goethite suspension (108.6g/L, pH 7) directly on the ZnSe crystal and evaporating to dryness at room temperature. Prior to use, the film with rinsed with Millipore water to remove the loosely deposited particles. A background spectra was obtained that consisted of the deposited goethite and Millipore water. A sample (1 ml) of quinone/AHA solution was then passed through the flow cell by an air-tight glass syringe and spectra measurements were acquired as a function of time for one hour.

## 4.3 Results and Discussion

### 4.3.1 UV-Vis Measurements

As revealed in my previous study,[93] sorption behaviors of $LAW_{ox}$ and $LAW_{red}$ happened on goethite-Fe(II) system. One possible scenario for the adsorption process was iron-lawsone complex formation. Thus, aqueous-phase iron-lawsone experiment setup was to investigate the possible complex. Figure 4.1 shows the UV spectra analysis of aqueous Fe(II)/Fe(III), $LAW_{ox/red}$, and their mixture at neutral pH. It was observed (Figure 4.1a) that the measured spectra of the mixture with Fe(II) and $LAW_{ox}$ was the same as only $LAW_{ox}$, as well as identical to the calculated composite of Fe(II) and $LAW_{ox}$ individually. No evidence was provided to support Fe(II)-$LAW_{ox}$ complex formation in the aqueous phase. Similar to Fe(II)+$LAW_{ox}$, the spectra of the measured mixture with Fe(II)+$LAW_{ox}$, Fe(III)+ $LAW_{red}$ and Fe(III)+$LAW_{red}$ was the same as the calculated composite ones (Figure 4.1b, c and d), suggesting the lack of aqueous complex formation between iron and lawsone ($[Iron\text{-}LAW]_{aq}$). Also, this phenomenon was observed in a wide pH range from 2 to 7, evidenced by the UV-Vis spectra shown in Figure S4.1, S4.2, S4.3 and S4.4 in the supporting information. Furthermore, it is worthy to mention that Fe(II) and Fe(III) species stayed in the aqueous phase since the concentrations in this study (10 μM) were below their individual solubility. And electron transfer reaction was not found including reduction of $LAW_{ox}$ to $LAW_{red}$ by $Fe(II)_{aq}$ and oxidation of $LAW_{red}$ to $LAW_{ox}$ by $Fe(III)_{aq}$, since no new absorption bands were detected.
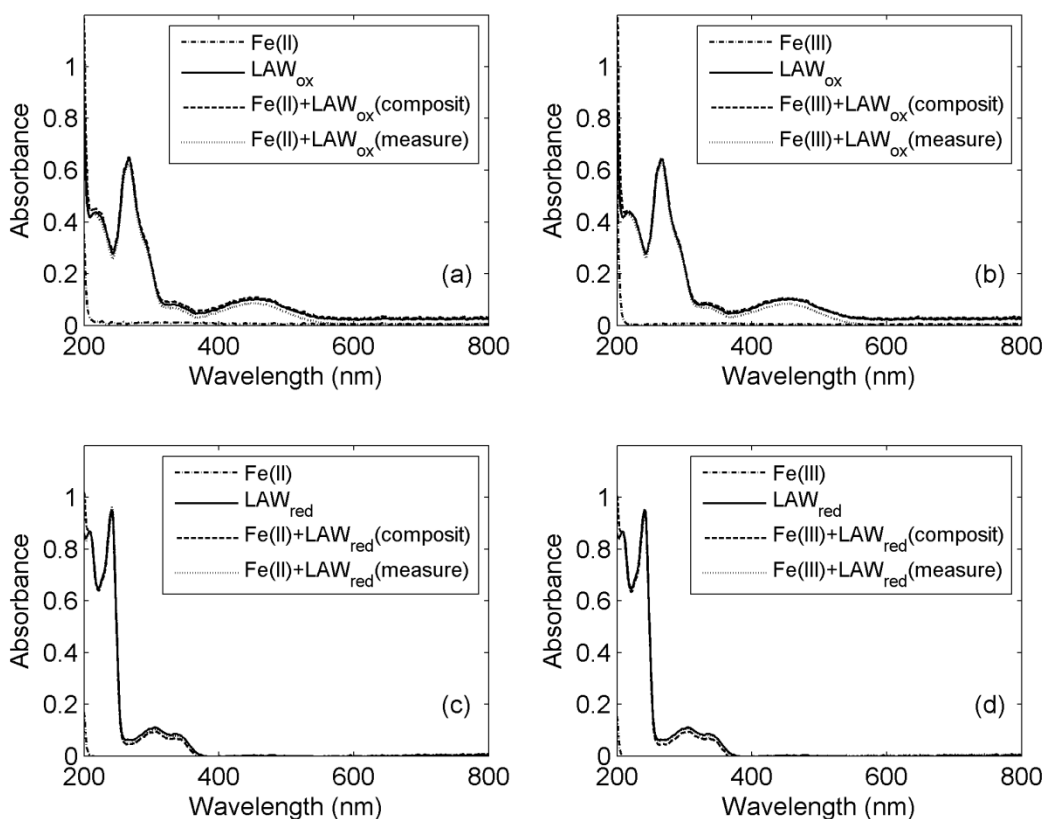
**Figure 4.1.** UV-Vis spectra diagrams of aqueous iron (10 μM), LAW(30 μM), Iron+LAW (composite) and Iron+LAW (measure) at pH 7. a) Fe(II)+LAW$_{ox}$; b) Fe(III)+LAW$_{ox}$; c) Fe(II)+LAW$_{red}$; d) Fe(III)+LAW$_{red}$. Composite: calculated sum of the individual spectra of iron and LAW; Measure: measured spectra of mixture species with iron and LAW.

## 4.3.2 ATR-FTIR Analysis

Sorption behavior of quinone can be investigated by the bulk adsorption measurement, but only indirect estimates about the type of surface complexes on the iron mineral can be made. ATR-FTIR spectroscopy analysis provides more valuable evidence in a direct angle to survey how quinone molecules interact with mineral surface.

Dissolved catechol. Figure 4.2 shows the spectra of aqueous catechol at the neutral pH with static state and flow through system at the scan number of 400 and 1500. The shape of spectra and peak positions at the flow through system were validated identical to the static state (see Figure 4.2a and 4.2c). Also, the spectral quality with 400 scan was proved as good as with 1500 scan (see Figure 4.2a and 4.2b). Thus, the ATR-FTIR flow through setup with 400 scan numbers was applied for the further study.

The observed peak position and assignments are listed in Table 4.1. At neutral pH, dissolved catechol is in the protonated form (p$K_{a1}$ = 9.4; p$K_{a2}$ = 12.8). The peak centered at 1203 cm$^{-1}$ for $\delta$(OH) represented the protonated species. The bands at 1258 and 1278 cm$^{-1}$ were assigned to $\nu$(CO) mode. The peak centered at 1375 cm$^{-1}$ was corresponding to the couple $\delta$(OH) and $\nu$(CC). In addition, the bands at 1470 and 1516 cm$^{-1}$ were attributed to $\nu$(CC) and $\delta$(CH). These peak positions of aqueous catechol were generally in agreement with the literature.[57, 58]
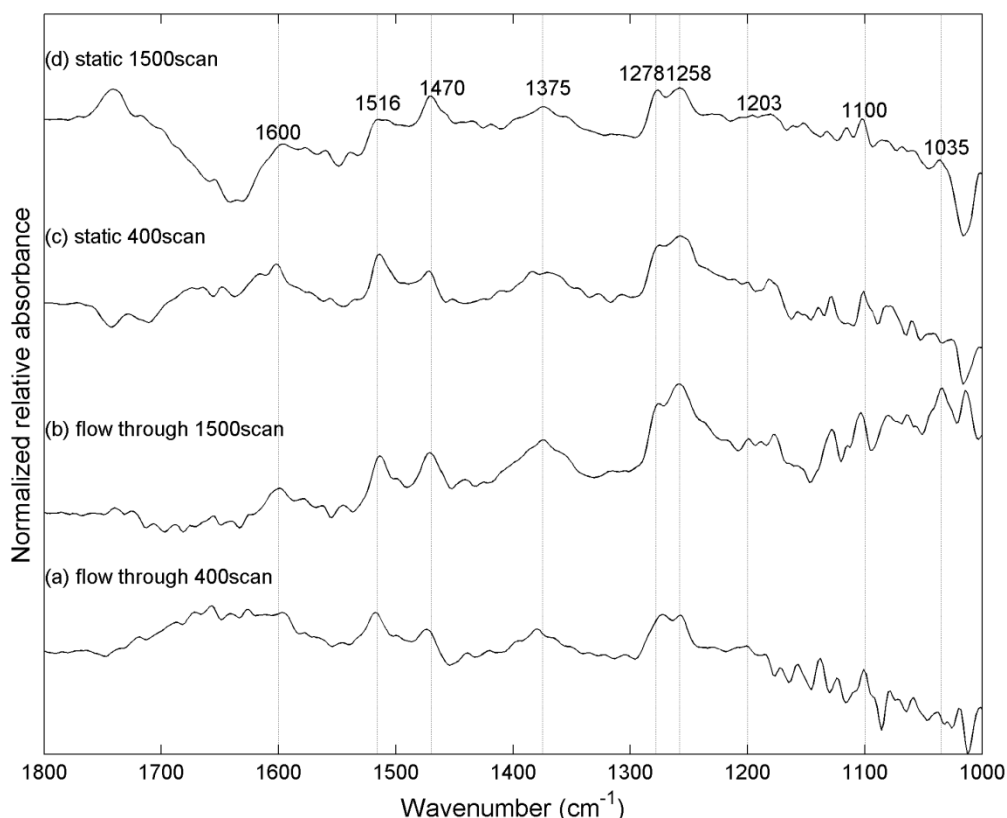


**Figure 4.2.** ATR-FTIR spectra comparison of catechol (10 mM, pH 7) with a) flow through with 400 scan; b) flow through with 1500 scan; c) static state with 400 scan and d) static state with 1500 scan. Spectra were normalized to the peak with the strongest intensity.

Adsorbed Catechol at Goethite Interface. Figure 4.3 shows the time-dependent spectra of surface interfacial species from 5 min to one hour at pH 7 with 10 mM catechol. Compared to the spectra of dissolved catechol, the shape and position of the peaks of adsorbed catechol changed significantly, suggesting the formation of a covalent bond.[57, 58] The observed frequencies and peak assignments are listed in Table 4.1.

Adsorption behavior is a dynamic process, illustrated by the change of peak area as a function of time (shown in Figure 4.3b to 4.3e). Neither new peaks nor peak position shifting was found from the time-dependent IR spectra. Shoulder peaks were significantly climbing at 1263, 1276 and 1477 cm$^{-1}$, along with the reaction time from 5 min to one hour. Variation in the shape of the overlapped peaks in 1103, 1200, 1383, 1440 and 1515 cm$^{-1}$ suggested an uneven enhancement in peak intensity as a function of time.

Additionally, the spectra shape and the peak position of the catechol interaction with goethite were generally consistent with the published data.[57, 58] The bands in 1477,1439, 1276, 1263, 1203 and 1103 cm$^{-1}$ were similar to the reported peaks of dianionic catecholate in 1M NaOH (1473,1428, 1284, 1256, 1207 and 1099 cm$^{-1}$), indicating a bidentate structure configuration.[57, 58] Although the surface properties of goethite in our study, such as surface area and point of zero charge, were different with the synthesized one used in the literature, the agreement of spectra shape and peak position with literature has validated our ATR-FTIR setup and can be further broaden to other quinone and even organic matter.
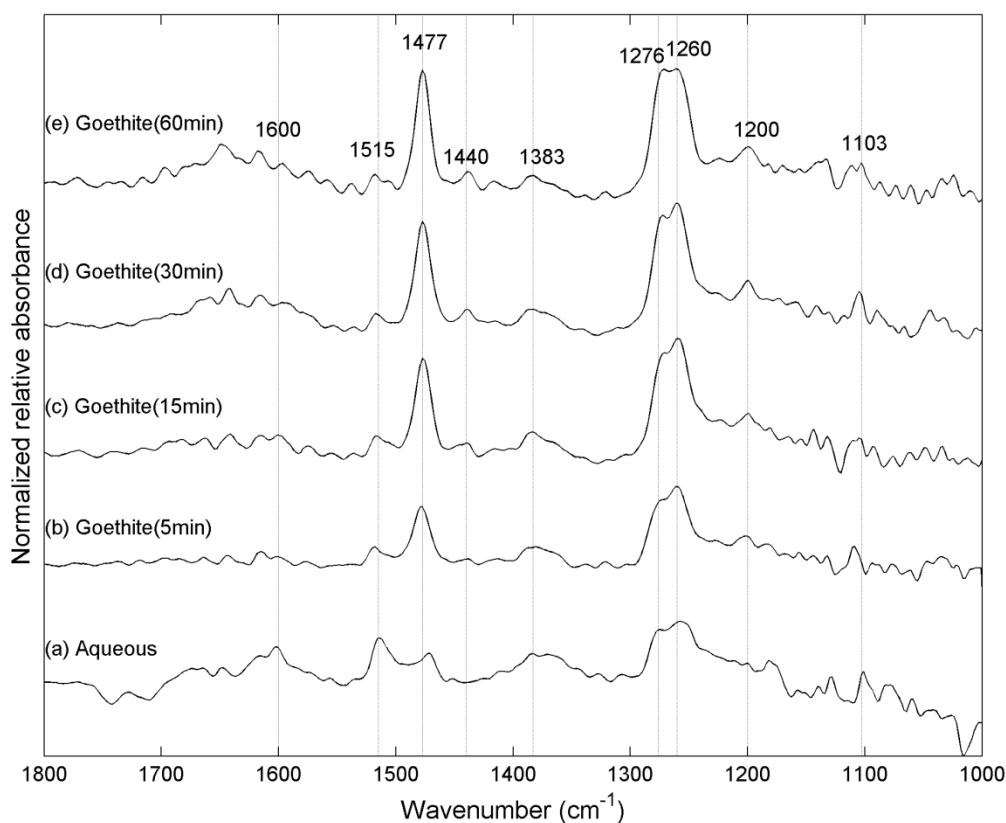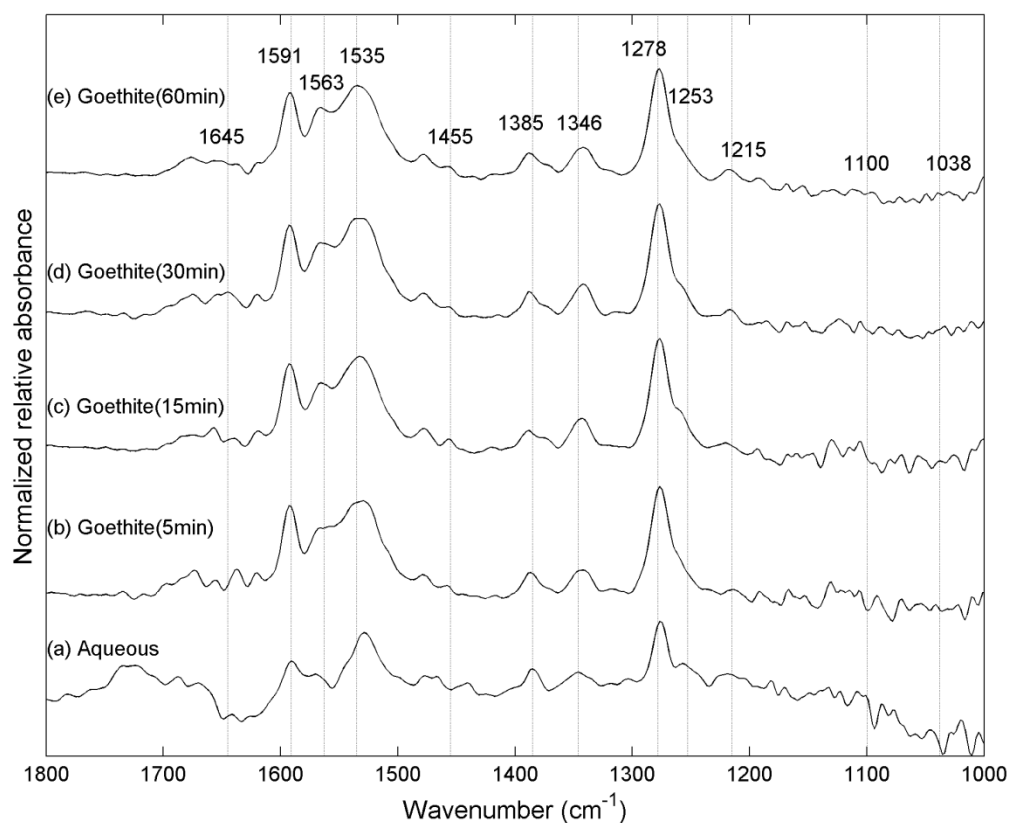


**Figure 4.3.** ATR-FTIR spectra of (a) aqueous catechol (10 mM, pH 7) and its interaction with goethite film acquired at (b) 5 min, (c) 15 min, (d) 30 min, and (e) 60 min.

**Table 4.1.** Peak position and assignment of aqueous catechol and its interaction with goethite. ($\nu$ means stretching vibration; $\delta$ is bending vibration.)

| Wavenumber (cm$^{-1}$) | | | |
|---|---|---|---|
| aqueous 10 mM, pH 7 | on Goethite | assignment | refs |
| 1103 | 1100 | $\delta$(CH) | [57, 58] |
| 1203 | 1200 | $\delta$(OH) | [57, 58] |
| 1258<br>1278 | 1260<br>1276 | $\nu$(CO) | [57, 58] |
| 1375 | 1383 | $\delta$(OH) + $\nu$(CC) | [57, 58] |
| 1470 | 1440<br>1477 | $\nu$ (CC) | [57, 58] |
| 1516 | 1515 | $\nu$(CC) + $\delta$(CH) | [57, 58] |
| 1600 | 1600 | $\nu$(CC) + $\delta$(CO) | [57, 58] |

Dissolved LAW$_{ox}$. The spectra of dissolved oxidized lawsone species from pH 2 to 7 are present in Figure 4.4. The frequency and peak assignment are listed in Table 4.2. A reference spectrum of aqueous LAW$_{ox}$ was acquired from 8.3 mM solution at pH 7 (Figure 4.4a). This solution ensured a sufficient high concentration for ATR-FTIR measurements. Otherwise, the peak intensity of IR spectra was much lower given its low solubility (Figure 4.4b to d), even though the shape of spectra and the peak position of LAW$_{ox}$ at low concentration (0.83 mM) were the same as the one with ten times higher concentration (8.3 mM).

In agreement with the species distribution, significant difference in the spectra were observed between the neutral LAW$_{ox}$ and the acid one at pH 2 (see Figure 4.4b and 4.4d). Deprotonation of the OH group dramatically changed the peak number and position of the IR bands (pK$_a$ = 3.9). At pH 7, the fully deprotonated species was predominant in the dissolved LAW$_{ox}$. Consequently, two bands were resolved at 1278 and 1535 cm$^{-1}$ due to $\nu$(CO) and $\nu$(C=C) aromatic ring respectively. These two bands were also detected at pH 4, where about 50% of LAW$_{ox}$ remains deprotonated form. However, the peak for the $\delta$(OH) vibration at 1257 cm$^{-1}$ was growing significantly in intensity at pH 2 since the protonated species were dominant at acid condition. This pH-dependent change was also observed by other quinone compound such as catechol with similar molecular structure.[57, 58] The bands centered at 1346, 1385 and 1593 cm$^{-1}$ were attributed to $\nu$(CO) coupled with the $\nu$(CC) mode. The peaks centered at 1660 cm$^{-1}$ may be corresponding to C=O double band with a relatively small intensity for protonated and deprotonated species.
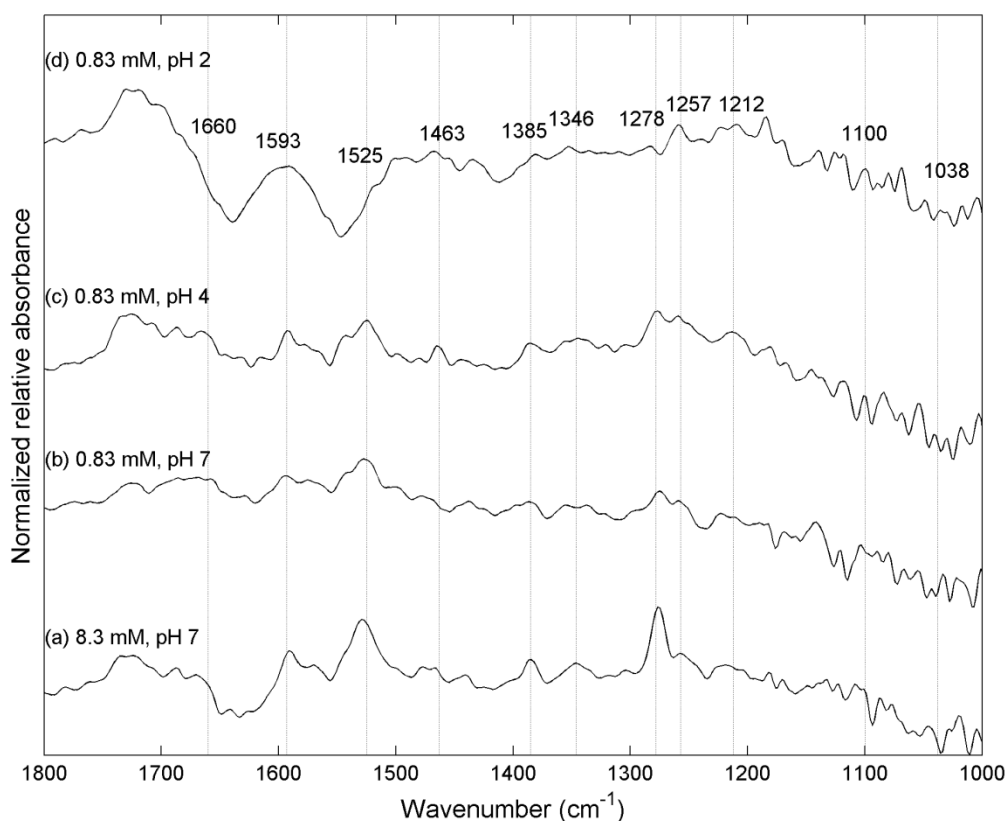
**Figure 4.4.** ATR-FTIR analysis of LAW$_{ox}$ (8.3 mM at pH 7 and 0.83 mM at pH 2, 4, 7) with flow through system by 400 scan.

<u>Adsorbed LAW$_{ox}$ at Goethite/Aqueous Interface.</u> The spectra of surface interfacial species as a function of time at pH 7 with 8.3 mM LAW$_{ox}$ is illustrated by Figure 4.5. Neither new peaks nor peak position shifting was found from the time-dependent IR spectra. The shape of the spectra and the peak position of LAW$_{ox}$ interaction with goethite was generally the same as the aqueous one except for the peak at 1563 cm$^{-1}$. Combing with the bulk adsorption dataset in my previous study,[93] it is a direct evidence for negligible sorption of oxidized lawsone on goethite surface.

**Figure 4.5.** ATR-FTIR spectra of (a) aqueous LAW$_{ox}$ (8.3 mM, pH 7) and its interaction with goethite film acquired at (b) 5 min, (c) 15 min, (d) 30 min, and (e) 60 min.

**Table 4.2.** Peak position and assignment of aqueous $LAW_{ox}$ and its interaction with goethite. ($\nu$ means stretching vibration; $\delta$ is bending vibration.)

| Lawsone | Wavenumber (cm$^{-1}$) | | assignment | refs |
|---|---|---|---|---|
| | aqueous | on Goethite | | |
| 8.3 mM, pH 7 | 1038 | 1038 | | |
| 0.83 mM, pH 7 | 1038 | | $\delta$(CH) | [57, 58, 80] |
| 0.83 mM, pH 4 | 1038 | | | |
| 0.83 mM, pH 2 | 1038 | | | |
| 8.3 mM, pH 7 | 1212 | 1212 | | |
| 0.83 mM, pH 7 | 1212 | | $\delta$(OH) | [57, 58, 80] |
| 0.83 mM, pH 4 | 1212 | | | |
| 0.83 mM, pH 2 | 1212 | | | |
| 8.3 mM, pH 7 | 1257 | 1253 | | |
| 0.83 mM, pH 7 | 1257 | | $\delta$(OH) | [57, 58, 80] |
| 0.83 mM, pH 4 | 1257 | | | |
| 0.83 mM, pH 2 | 1257 | | | |
| 8.3 mM, pH 7 | 1278 | 1278 | | |
| 0.83 mM, pH 7 | 1278 | | $\nu$(CO) | [57, 58, 80] |
| 0.83 mM, pH 4 | 1278 | | | |
| 0.83 mM, pH 2 | | | | |
| 8.3 mM, pH 7 | 1346 | 1346 | | |
| 0.83 mM, pH 7 | 1346 | | $\nu$(CO) + $\nu$(CC) | [57, 58, 80] |
| 0.83 mM, pH 4 | 1346 | | | |
| 0.83 mM, pH 2 | | | | |
| 8.3 mM, pH 7 | 1385 | 1385 | | |
| 0.83 mM, pH 7 | 1385 | | $\nu$(CO) + $\nu$(CC) | [111] |
| 0.83 mM, pH 4 | 1385 | | | |
| 0.83 mM, pH 2 | 1385 | | | |
| 8.3 mM, pH 7 | 1463 | 1455 | | |
| 0.83 mM, pH 7 | 1463 | | $\nu$(C=C) | [57, 58, 80] |
| 0.83 mM, pH 4 | 1463 | | | |
| 0.83 mM, pH 2 | 1463 | | | |
| 8.3 mM, pH 7 | 1525 | 1535 | | |
| 0.83 mM, pH 7 | 1525 | | $\nu$(C=C) + $\delta$(CH) | [57, 58, 80] |
| 0.83 mM, pH 4 | 1525 | | | |
| 0.83 mM, pH 2 | | | | |
| 8.3 mM, pH 7 | 1593 | 1591 | | |
| 0.83 mM, pH 7 | 1593 | | $\nu$(CC) + $\delta$(CO) | [57, 58, 80] |
| 0.83 mM, pH 4 | 1593 | | | |
| 0.83 mM, pH 2 | 1593 | | | |

| 8.3 mM, pH 7 | 1660 | 1645 | | |
|---|---|---|---|---|
| 0.83 mM, pH 7 | 1660 | | | |
| 0.83 mM, pH 4 | 1660 | | $\nu(C=O)$ | [112, 113] |
| 0.83 mM, pH 2 | 1660 | | | |

Dissolved Untreated Aldrich Humic Acid (AHA$_{untre}$). Quinone is abundant in the natural organic matter such as humic acid (~10%).[114, 115] The strong adsorption behavior of Aldrich humic acid on goethite has been investigated by batch experiments.[110] Here, The ATR-FTIR technique is introduced to identify its sorption mechanism and surface species directly in details.

Figure 4.6a shows ATR-FTIR spectra of the untreated AHA dissolved in water with a Dissolved Organic Carbon (DOC) concentration of 1000 mgDOC/L at pH 7. A reference spectrum of dissolved AHA$_{untre}$ was obtained in the wavenumber region of 800 - 4000 cm$^{-1}$ (Figure S4.7). However, the spectra were shown for the fingerprint region 900 – 1800 cm$^{-1}$ only (Figure 4.6a), since large water noises appeared in the region of 3000 – 3500 cm$^{-1}$ and also no apparent peak was observed between 2000 and 3000 cm$^{-1}$ wavenumber.

The ATR-FTIR spectra emphasize speciation and functional groups of AHA at neutral pH. The band features of the spectra are 1020, 1103, 1365, 1570 cm$^{-1}$ and peak assignments are listed in Table 4.3. A fairly broad band at 1570 cm$^{-1}$ was assigned to the coupled aromatic ring $\nu(CC)$ and an asymmetric carbonyl stretch in carboxylic acid bonds. The band at 1365 cm$^{-1}$ indicated C-O stretching of phenolic OH and the presence of symmetric carbonyl stretch.[116] The absorption band centered at 1020 and 1103 were corresponding to the $\delta(CH)$ and $\nu(CO)$ respectively.[117, 118]

Adsorbed AHA$_{untre}$ on Goethite Surface. The time-dependent spectra of surface interfacial AHA$_{untre}$ species from 5 min to 60 min at neutral pH condition are present in Figure 4.6b to 4.6e and S4.7. The equilibrium of AHA adsorption onto goethite interface was established in around 30 min, as the spectral shape and peak intensity of adsorbed AHA at 30 min was almost equal to one at 60 min, shown in Figure 4.6d and 4.6e.

The ATR-FTIR spectra displayed for AHA$_{untre}$ interaction with goethite by flow through cell measurement in Figure 4.6b to 4.6e, bear some similarities to those for aqueous AHA$_{untre}$. For instance, the spectra shown in Figure 4.6 all possess a strong peak at 1570 cm$^{-1}$, and a broad feature in the spectral region of around 1300 – 1500 cm$^{-1}$. On the other hand, the spectra in Figure 4.6 are most notable for the presence of additional peaks observed in the adsorbed AHA$_{untre}$. By comparison with aqueous AHA$_{untre}$, the stretching band of carboxylate COO$^-$ of the adsorbed AHA fractions onto goethite was shifted from 1570 cm$^{-1}$ to 1620 and 1640 cm$^{-1}$ respectively, indicating that COO$^-$ functional groups rich in humic acid may be complexes with goethite surfaces.[80, 111, 119, 120] Similarly, many FTIR spectroscopy studies have reported that the organic molecules consisted of carboxylic acid groups, for examples, phthalic acid, gentistic acid, and naphthoic acid, can be strongly bounded to iron oxides by out-sphere and inner-sphere complexation.[108, 109, 121, 122]  Therefore, it is hinted both electrostatic out-sphere

and inner-sphere complexation may occur between the carboxylic acid functional group of the humic acid and the iron mineral surface.

Another important observation is that a shoulder band at 1210 cm$^{-1}$ appeared due to the phenolic OH functional groups, which confirms that phenolic moieties such as catechol-like quinone, may be an important component to adsorb on goethite.[46, 57, 58, 105] Also, the clear peak at 1620 and 1640 cm-1 representing the C=C of aromatic moieties, which suggested that goethite may strongly coated with the aromatic moieties. Furthermore, the spectra of adsorbed AHA$_{untre}$ showed a band shifting from 1020 to 1010 cm$^{-1}$, compared with the aqueous one. This intensity reduction reveals the complexation between carbohydrates or polysaccharide-like substance of AHA and goethite mineral, in line with many previous reports.[18, 21, 22, 120]  To sum up, it is suggested that carboxyl acid and phenol functional groups in humic acid structure are responsible for the adsorption mechanism by electrostatic attraction and surface complexation. However, further identification of surface complex structure using ATR-FTIR technique may be ambiguous.
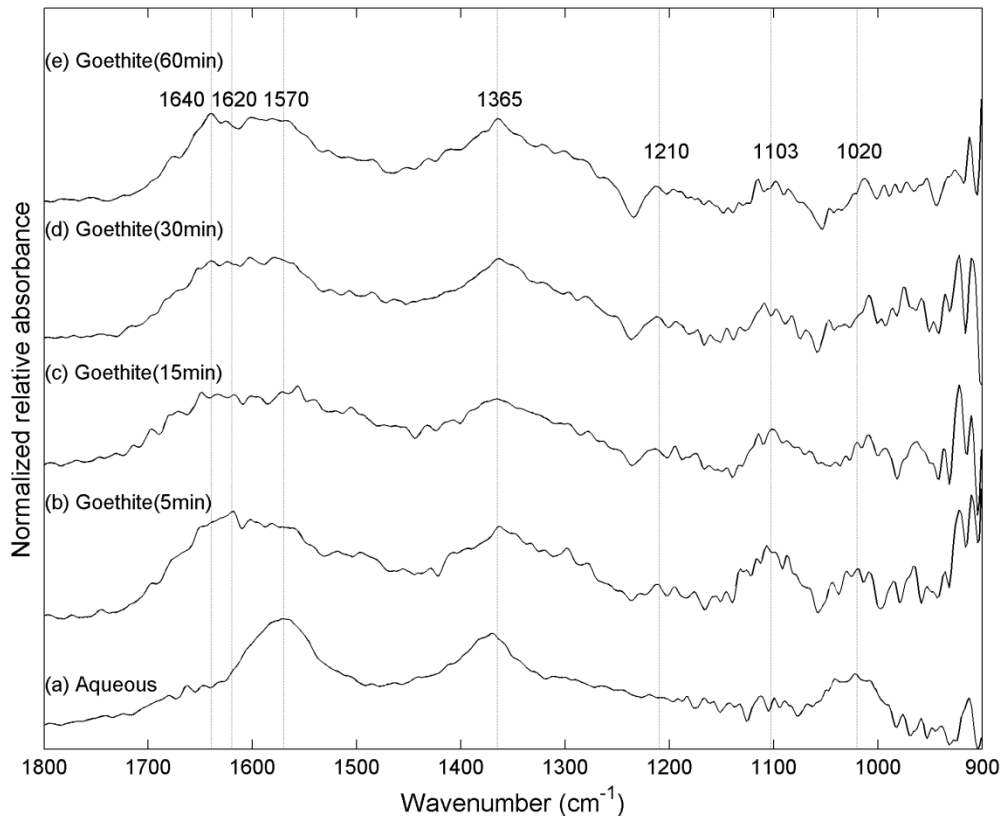


**Figure 4.6.** ATR-FTIR spectra of (a) aqueous AHA$_{untre}$ (1000 mgDOC/L, pH 7) and its interaction with goethite film acquired at (b) 5 min, (c) 15 min, (d) 30 min, and (e) 60 min.

**Table 4.3.** Peak position and assignment of aqueous AHA$_{untre}$ and its interaction with goethite. ($\nu$ means stretching vibration; $\delta$ is bending vibration; asy and sy represent asymmetric and symmetric stretching respectively.)

| Wavenumber (cm$^{-1}$) | | | |
|---|---|---|---|
| aqueous 1000 ngDOC/L, pH 7 | on Goethite | assignment | refs |
| 1020 | 1020 | $\delta$(CH) carbohydrate (-OH); polysacchride | [116, 118-120] |
| 1103 | 1103 | $\nu$(CO) | [116, 118, 119] |
| | 1210 | $\delta$(OH) | [116, 118, 119] |
| 1365 | 1365 | $\delta$(CH); $\nu$(CO) + $\nu$(COO)$_{sy}$ | [116, 118, 119] |
| 1570 | 1570 | $\nu$(CC) + $\nu$(COO)$_{asy}$ | [116, 118, 119] |
| | 1620 1640 | $\nu$(CC) + $\nu$(COOH)$_{asy}$ | [116, 118, 119] |

## 4.4 Environmental Significance

In this study, sorption mechanism of quinone/humic acid at goethite/Fe(II) interface has been investigated with multiple complementary techniques. Our results demonstrated that the naphthoquinone lawsone did not form binary complex with iron in both aqueous and solid phase. On one hand, UV-Vis spectroscopic results indicated that aqueous iron-lawsone complex could not be detected in the pH range of 2 to 7. On the other hand, it is the first time to illustrate by the ATR-FTIR experiments that the spectra shape and peak position of free oxidized lawsone was in accordance with its interaction with goethite, providing strong evidence for negligible sorption of lawsone on goethite/water interfaces. Also it is important to note that the ATR-FTIR flow through setup has been validated by the fact that catechol binds predominantly as a bidentate surface complex on goethite, in agreement with the published paper. Furthermore, the findings of this study provide insights into quinone surface complexes on the molecular scale that can be applied to describe and predict the adsorption behaviour of organic matter with complex structure in the environment. The humic acid sorption mechanisms on goethite surface were examined employing flow cell measurements of ATR-FTIR spectroscopy. The spectroscopic data of adsorbed and dissolved AHA indicated that goethite provides sorption sites predominantly for the carboxyl and phenol functional groups at neutral pH.

However, due to the limitation of time framework, only ATR-FTIR experiments under oxic condition including quinone/humic acid-goethite interaction has been conducted. However, the FTIR flow through setup under the oxygen free condition for reduced lawsone and goethite-Fe(II) system is currently operated. It is worthwhile to mentioning that both $LAW_{red}$ and Fe(II) are very sensitive to $O_2$, and thus the whole flow through setup should avoid oxygen contamination. Identification of surface species and sorption mechanisms on Fe(II)-bearing goethite system (e.g. goethite-Fe(II)-$LAW_{red}$) using ATR-FTIR spectrometer should be studied in future experiments.

# Chapter 5

## Conclusions and Outlook

# 5.1 Conclusions

Within the available time frame of the Ph.D. thesis, the results from my experiments significantly advanced the state of the knowledge about the electron transfer processes in the aqueous Fe(II)-iron mineral system. The main purpose of the present work was to monitor and characterize the adsorption behavior and electron transfer reactions of organic matter across the Fe(II)-iron mineral interfaces. Various laboratory experiments have been conducted within the thesis, including batch experiments to quantify redox species of the model quinone, as well as humic acid sorption ability onto the iron mineral-Fe(II) surface, and spectroscopic investigations to explore the sorption mechanisms. Summarized, the key conclusions of each study are:

(i)     The naphthoquinone lawsone showed a complex sorptive interaction with goethite surface. Its sorption behaviour can be affected by the redox state of the quinone, as well as the amount and distribution of Fe(II) associated with goethite. It is an important point that the sorbing quinone showed reversible electron transfer at goethite/Fe(II) interfaces, i.e., its oxidized species can accept the electron from ferrous iron bound to goethite and backwards the reduced one is able to donate the electron to the ferric iron at goethite surface. This is in agreement with studies on non-sorbing quinone anthraquinone-2,6-disulfonate (AQDS).[27] Furthermore, the apparent reduction potential of the goethite-Fe(II) surface was estimated by the dissolved redox couple of quinone/hydroquinone and the obtained value is in a range of -150 ± 23 mV vs SHE. As compared to similar redox potential measurements by using the non-sorbing quinone AQDS, we conclude that the accumulated quinone/hydroquinone has no significant effect on the redox potential of the goethite/goethite-Fe(II) surface.

(ii)    The interactions between natural organic matter (e.g. humic acid) and iron mineral/Fe(II) surfaces are mainly involved in sorption and electron transfer reaction processes. On one hand, the batch sorption experiments indicated that untreated humic acid showed the same sorption behavior on goethite surface as the electrochemically reduced and reoxidized one. Also, it was observed that the amount and species of Fe(II) sorbed to goethite can significantly enhance the sorption behavior of redox-active organic matter. On the other hand, it is worthwhile to note that electron transfer is to occur based on the difference between the redox potential of goethite/Fe(II) surface and dissolved humic acid. Therefore, it is foreseeable that the sorption and electron transfer reaction of organic matter might consume the redox activity of the reductant associated Fe(II) with iron mineral and further to inhibit the reduction or degradation of organic pollutants in the iron mineral-Fe(II) systems.

(iii)    The results of the spectroscopic experiments allows us to better understand the adsorption mechanism of organic matter such as quinone and humic acid at mineral-water interface. The naphthoquinone lawsone was shown to not chelate with dissolved iron and also the mineral phase by UV-Vis analysis and ATR-FTIR spectroscopic study. For comparison, previous research has demonstrated that catechol can form binary complex with both free iron and the mineral phase.[76, 78] Furthermore, ATR-FTIR spectroscopy was applied to further investigate natural organic matter with more complicated structure and the results indicated that carboxylic acid and phenol functional groups rich in the humic acid structure are preferably adsorbed on goethite/aqueous interfaces. Thus, the results suggest that sorption of organic matter such as quinone and humic substance to goethite/water interface is driven by both electrostatic attraction and surface complexation. However, the flow cell ATR-FTIR setup for oxygen free conditions such as goethite-Fe(II)-LAW$_{red}$ system, needs to be further evaluated and optimized.

## 5.2 Outlook

The combined approaches and data enable us to set up a framework for speciation and surface reaction of ferrous iron and reactive organic matter at mineral phases. This study may be a first step to predict effects of changing environmental conditions on redox processes and their effects on pollutant fate in heterogeneous systems. Future work will need to address the application to various geochemical settings, summarized as the following:

(i)    In this work, the selected quinone is Lawsone as representative. Due to its redox potential ($E_{H(pH7)} = 152$ mV), the model quinone can serve as indicator for the redox properties of the iron mineral surface. However, the investigation of sorption and electron transfer reaction of other naphthoquinone (such as 5-hydroxy-1,4-naphthalenedion juglone) onto iron (hydr)oxides could be extended. At pH 7, lawsone is deprotonated (pK$_a$ = 3.9) and hence anionic, while juglone remains in its protonated form (pK$_a$ = 8.0, shown in Figure 1.3). Therefore, significantly different sorption behavior of these two quinones to goethite and goethite/Fe(II) mineral surfaces are expected.

(ii)    The sorptive interaction between natural organic matter and iron mineral/Fe(II) interfaces have been investigated. However, the presence of competing inorganic anions, such as phosphate, has a strong effect of NOM sorption on minerals.[17, 24] Other reactive electrolytes such as $Ca^{2+}$, $Al^{3+}$, may compete with the organic matter for the sorbing sites at the mineral surfaces.[51, 123] Furthermore, these metal ions forming complexes with NOM,[124-126] might also

influence NOM sorption behavior onto the iron minerals. Hence, the potential effect of reactive solutes on NOM sorption at the iron mineral surfaces can be further studied. It will help us to comprehensively understand the multiple interactions between natural organic matter and iron minerals at various geochemical conditions.

(iii)   Fe(II)/mineral phases as well as reduced organic matter can catalyze the reductive transformation of chlorinated hydrocarbons.[12, 30] It remains however unclear how the presence of organic matter affects the surface reactivity of Fe(II)/mineral phases towards reductive dechlorination. To this goal, kinetic batch experiments can be set-up with a defined goethite-Fe(II) suspension at constant pH (pH 7) and various amounts of selected organic matter (quinones or humic acids). The batches can be spiked with carbon tetrachloride ($CCl_4$) as a model for chlorinated hydrocarbons and the degradation rates of $CCl_4$ as well as product formation (e.g. $CHCl_3$) will be monitored with time by GC-MS analysis, following the protocol of Buchholz et al.[35]

# Supporting Information for Chapter 2

# Effects of Sorbed Quinone/Hydroquinone on Electron Transfer and Apparent Redox Potential of Goethite

<u>Supplemental Information Summary</u>

Number of pages: 17

Number of tables: 3

Number of figures: 13

# 1.Reference Spectra of LAW$_{ox}$ and LAW$_{red}$ by UV-Vis Analysis.

Figures S2.1 and S2.2 show the reference spectra of the two states of lawsone.

*Oxidized State (LAW$_{ox}$)*
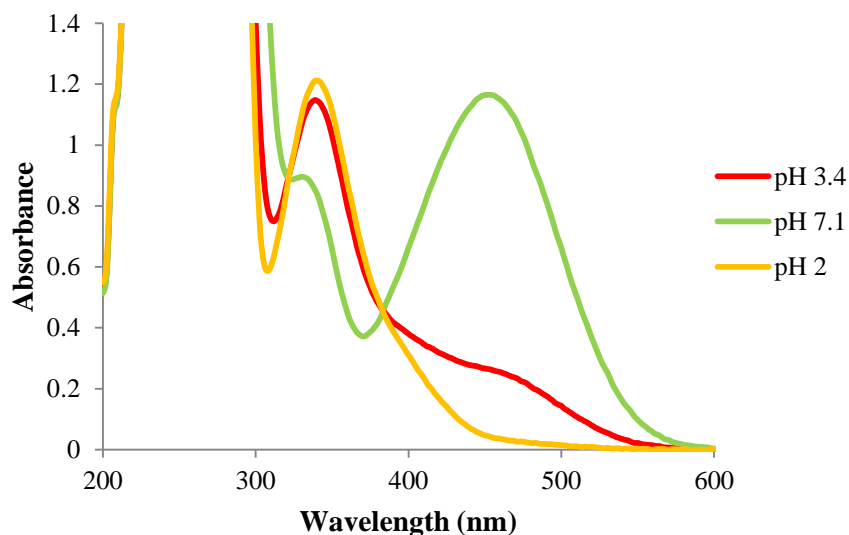


**Figure S2.1.** UV-Vis spectrum of 0.46 mM (= 54.8 mgDOC/L) lawsone at pH 2.0, 3.4, and 7.1 respectively.

*Reduced State (LAW$_{red}$)*
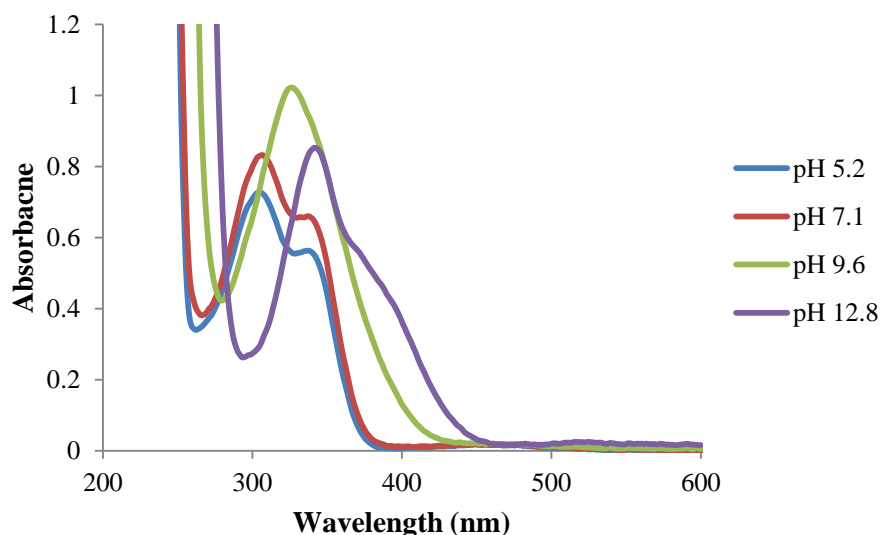


**Figure S2.2.** UV-Vis spectrum of 0.23 mM (= 27.4 mgDOC/L) reduced lawsone at pH 5.2, 7.1, 9.6, and 12.8 respectively measured in 0.1 M KCl and 0.1 M phosphate buffer (pH 7) .

The reduced lawsone can be re-oxidized to **LAW$_{ox}$** when purging with $O_2$ for several minutes. The UV spectra (Figure S2.3) provide evidence of reversible reduction and re-oxidation of lawsone.
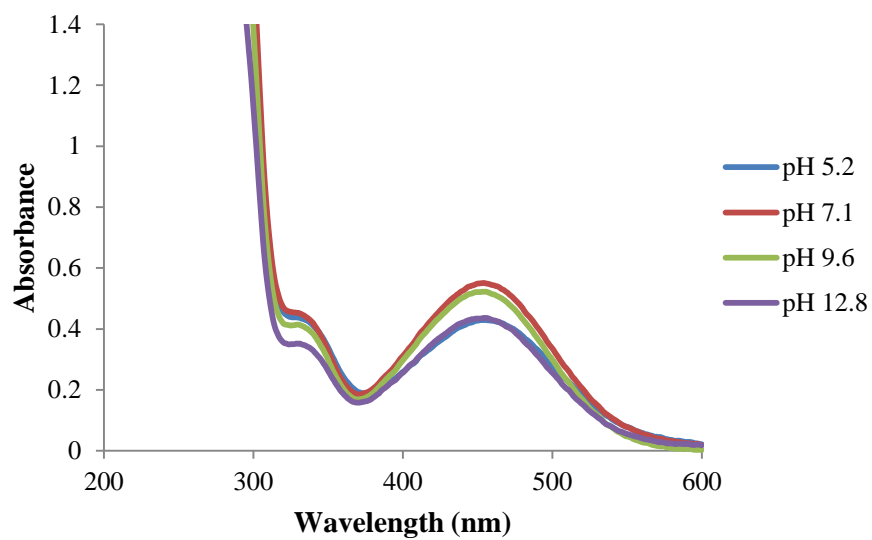
**Figure S2.3.** UV-Vis spectrum of 0.23 mM (= 27.4 mgDOC/L) re-oxidized lawsone at pH 5.2, 7.1, 9.6, and 12.8 respectively measured in 0.1 M KCl and 0.1 M phosphate buffer (pH 7) .

## 2.'Buffer + EDTA' Method for Re-oxidation of Reduced Lawsone in the presence of Fe(II).

As tested before, bare buffer solutions (either pH 7 or pH 4.76), could not be used in the re-oxidation process of reduced lawsone when the Fe(II) content was high involving the UV method. Consequently, a 'MOPS + EDTA' method was introduced so that Fe(II) or Fe(III) would form complexes with EDTA (EDTA-Fe(II) and EDTA-Fe(III)) and keep Fe(III) stable in solution, thus avoiding Fe(III) precipitation.

As shown in Figure S2.4, for only EDTA, in the UV spectra, there is no absorbance above 250 nm. In the presence of Fe(II) at pH 7, absorbance peak appeared in the spectra in the range of 240 - 320 nm, but no absorbance beyond 320 nm was obtained. This suggested that EDTA-Fe(II) complex formation occurred to some extent. In the presence of Fe(III), the UV spectra were different. The absorbance was largely decreasing below 430 nm and remained close to zero above 430 nm. This might indicate the appearance of some EDTA-Fe(III) complex in the aerobic condition. Based on the results, quantification of the oxidized lawsone can be done at 453 nm in the presence of sufficient amounts of Fe(III) at pH 7 by the 'MOPS + EDTA' method.
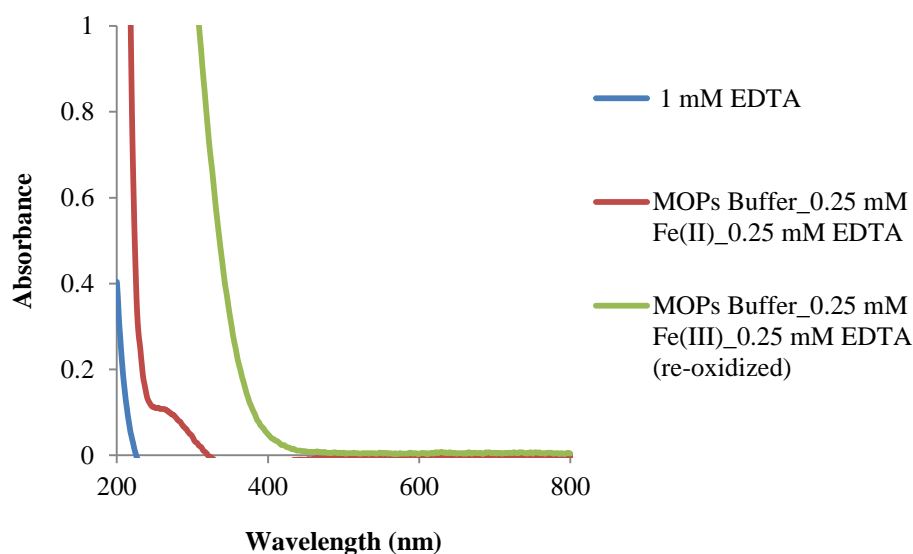


**Figure S2.4.** UV spectra of EDTA, EDTA-Fe(II) with MOPS buffer and EDTA-Fe(III) with MOPS buffer.

The second issue was to investigate whether the 'Buffer + EDTA' method could be used for the re-oxidation process of lawsone in the presence of high amounts of Fe(II) and Fe(III). As illustrated in Figure S2.5, due to EDTA-Fe(II) and EDTA-Fe(III) complex formation, the UV spectra of oxidized lawsone was different. At wavelengths above 430 nm, three UV spectra (oxidized lawsone, oxidized lawsone with EDTA-Fe(II) and oxidized lawsone with EDTA-Fe(III)) seemed to overlap.
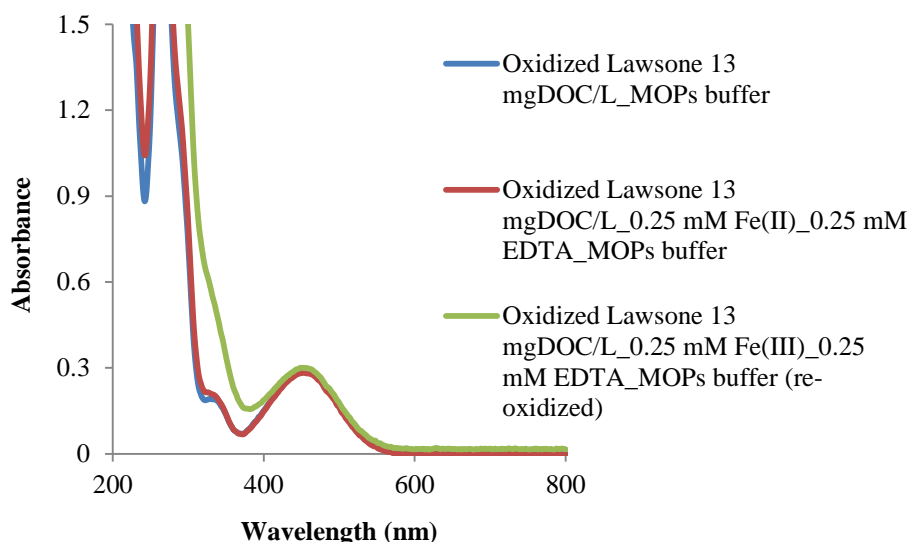
**Figure S2.5. UV spectra of oxidized lawsone with MOPS buffer, oxidized lawsone with EDTA-Fe(II) and MOPS buffer, and oxidized lawsone with EDTA-Fe(III) and MOPS buffer.**

The UV spectra of reduced lawsone in the presence of EDTA-Fe(II) and after its re-oxidation in the presence of EDTA-Fe(III) at pH 7 were also measured. Results are shown in Figures S2.6a and b. In Figure S2.6a, the UV spectra of reduced lawsone in the presence of EDTA-Fe(II) was different compared to the spectra the absence of EDTA-Fe(II) below 330 nm, but both were almost the same above 330 nm. This was caused by EDTA-Fe(II) complex formation. In Figure S2.6b, the UV spectra of re-oxidized lawsone in the presence of EDTA-Fe(III) was different compared to the spectra in the absence of EDTA-Fe(III) below 430 nm, yet both were almost the same above 430 nm again due to interference of EDTA-Fe(II) complex formation. Hence, for the re-oxidation process of lawsone in the presence of high amounts of Fe(II), the 'Buffer + EDTA' method can be used for oxidized lawsone quantification, but not to the reduced lawsone.
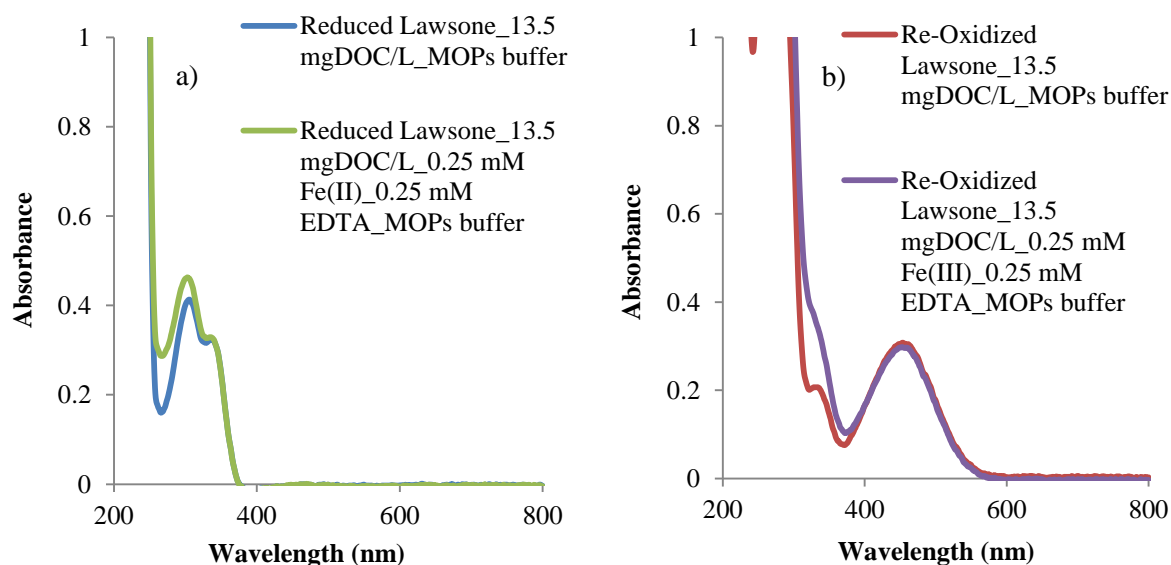
**Figure S2.6.** UV spectra of reduced lawsone with MOPS buffer, reduced lawsone with EDTA-Fe(II) and MOPS buffer (a); UV spectra of re-oxidized lawsone with MOPS buffer, re-oxidized lawsone with EDTA-Fe(II) and MOPS buffer (b).

In this 'Buffer + EDTA' method at pH 7, MOPS buffer was used instead of phosphate buffer since $PO_4^{3-}$ may react with Fe(III).

## 3. Goethite-Fe(II) + LAW$_{red}$ (I) system.

Figures S2.7 show the UV spectra of the filtered samples in the presence of MOPS buffer.
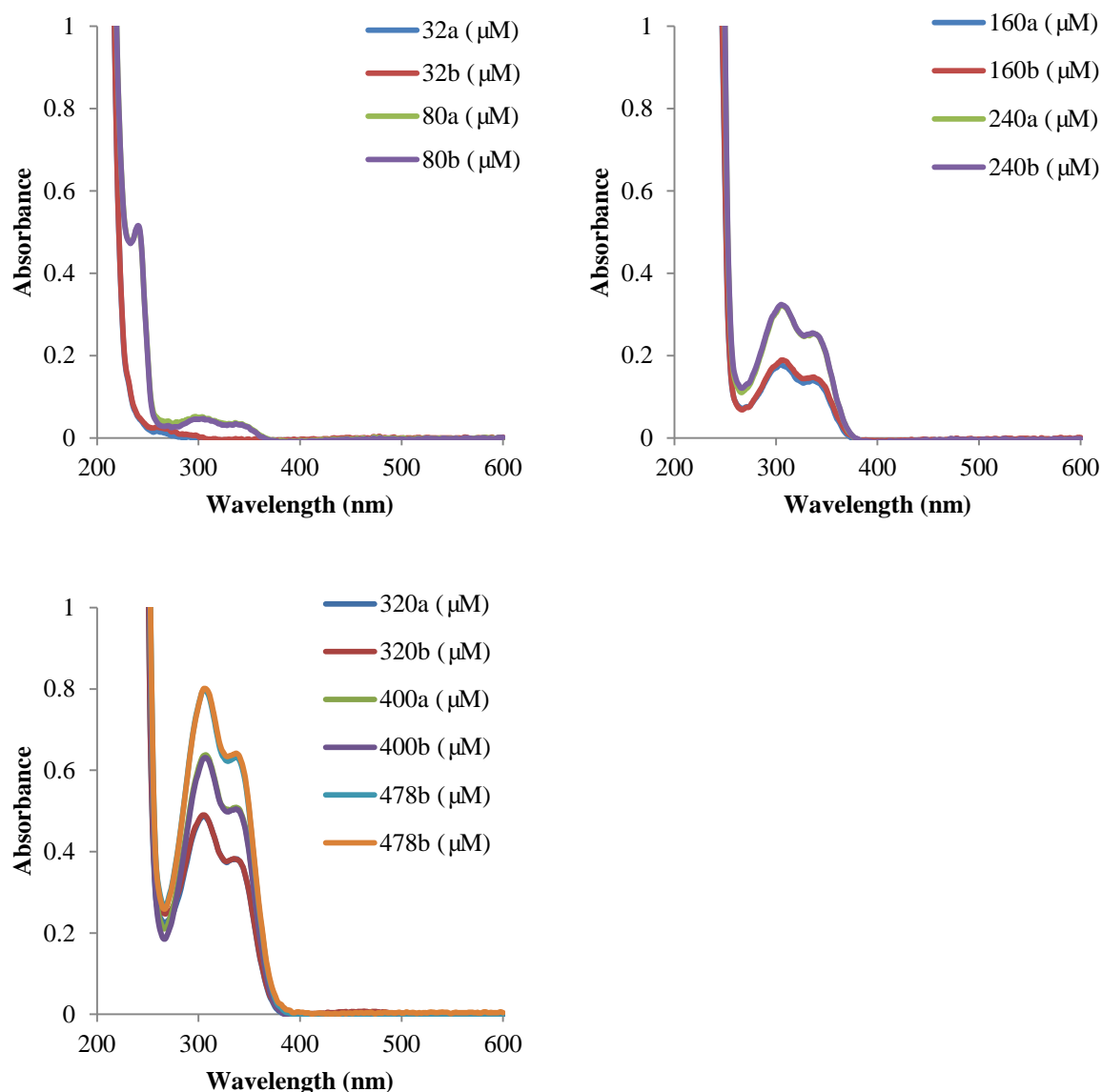


**Figure S2.7.** UV spectrum of fully reduced lawsone samples with different initial concentration after filtration in the presence of MOPS buffer.

The absorbance spectra of final, filtered samples of LAW$_{red}$ in the GT-Fe(II) (I) system were similar to the    GT-Fe(II) and GT-Fe(II)/Fe(III) systems, all showing only reduced species in the aqueous phase.

## 4.    Goethite-Fe(II)+ LAW$_{ox}$ system

Figure S2.8 shows UV spectra of final filtered samples with different initial LAWox concentration (0, 87, 173, 260, 346, 433, 520, and 693 µmol/L).
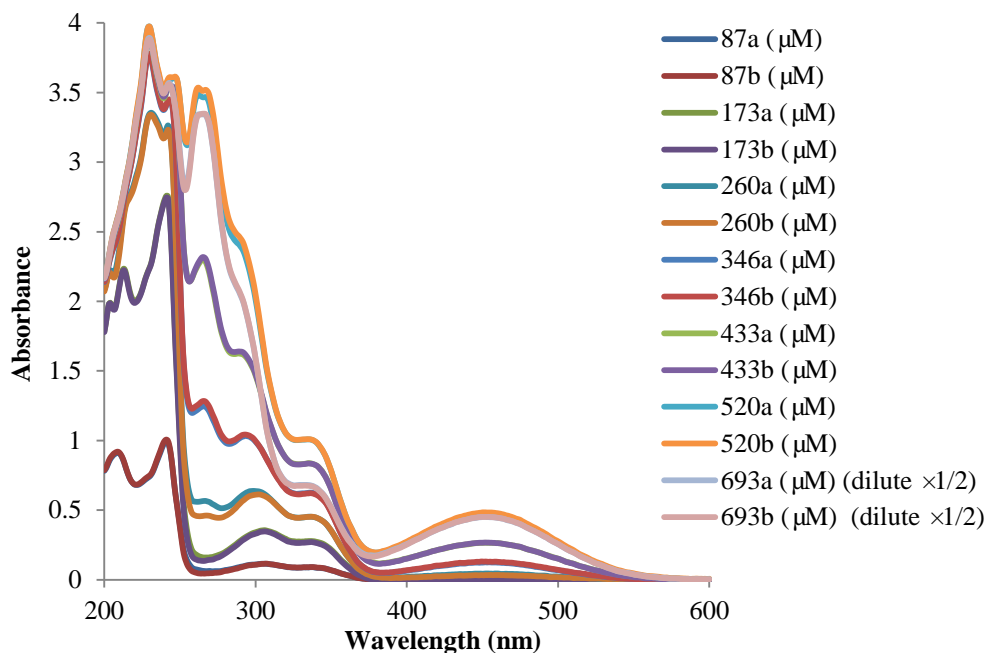


**Figure S2.8.** UV spectra of the supernatant samples after filtration with different initial LAW$_{ox}$ concentration (0, 87, 173, 260, 346, 433, 520, and 693 µmol/L).

The UV spectra of the filtered samples and their re-oxidized solution in the presence of MOPS buffer and EDTA solution are shown in the following Figure S2.9.
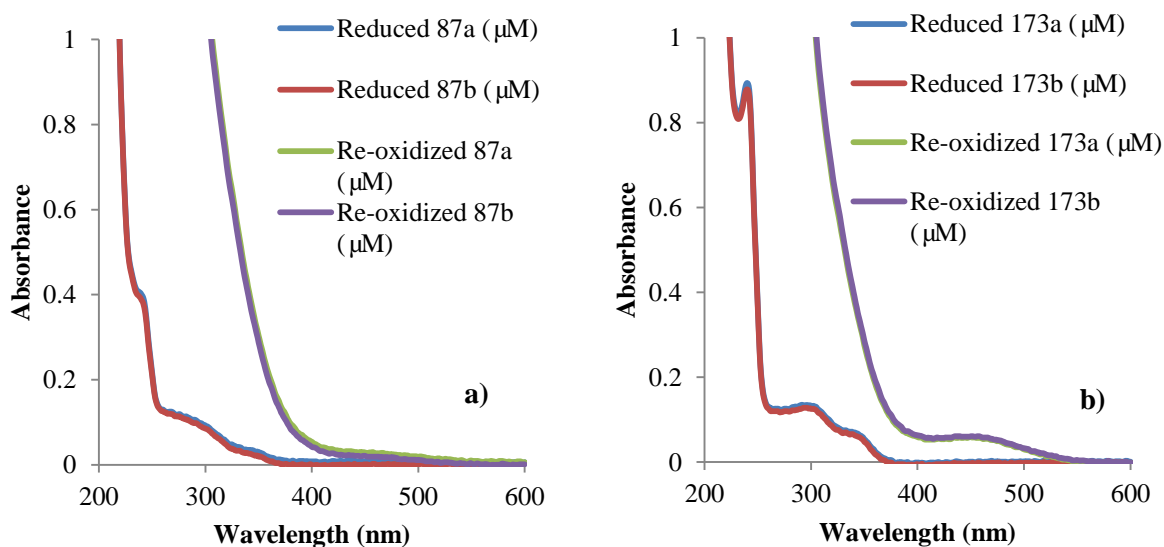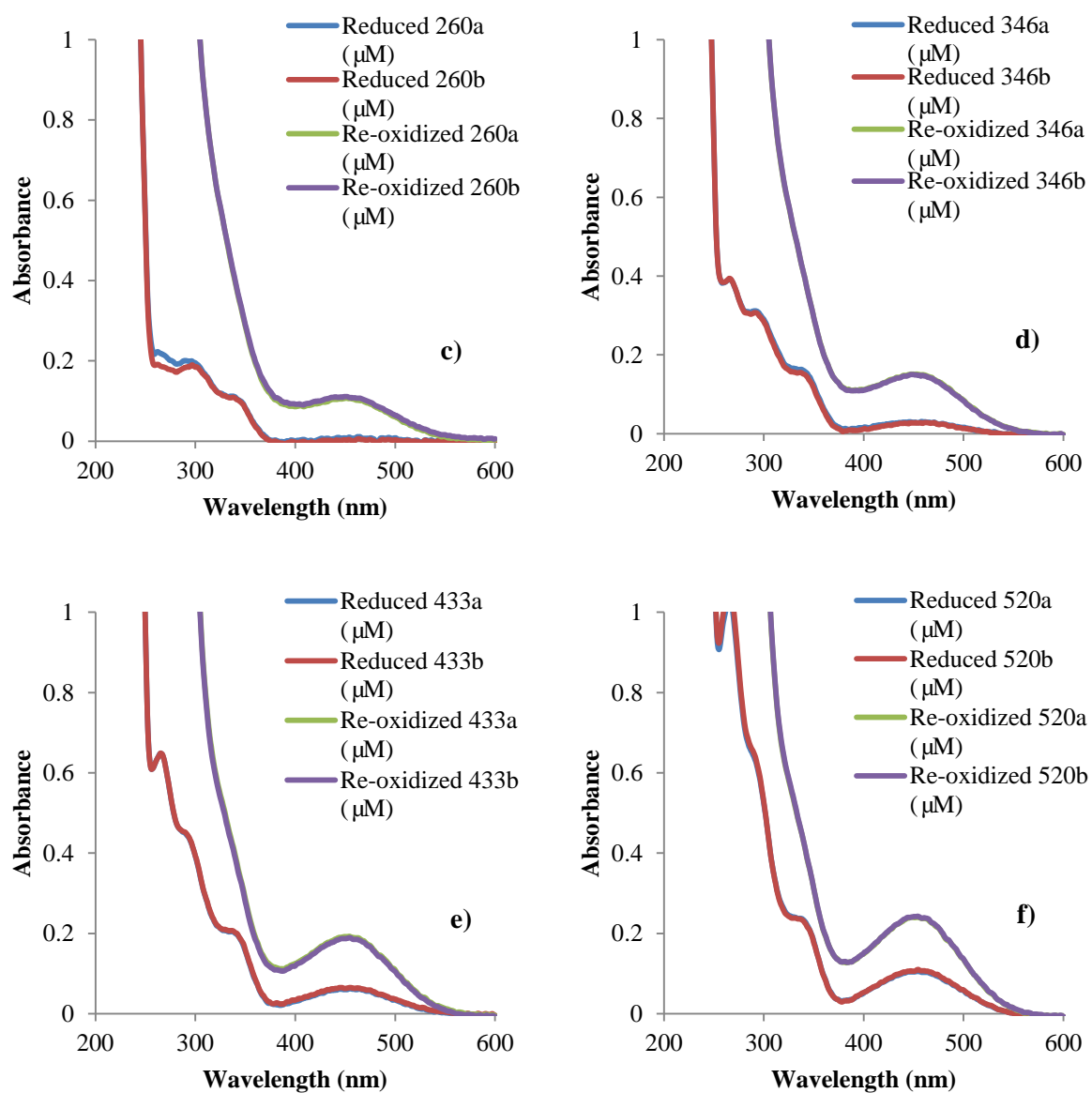
**Figure S2.9.** UV spectra of the filtered samples and their re-oxidized lawsone samples with different amounts of initially oxidized lawsone in the presence of MOPS buffer and EDTA. a) 87 μmol/L; b) 173 μmol/L; c) 260 μmol/L; d) 346 μmol/L; e) 433 μmol/L; f) 520 μmol/L;

## 5. GT+LAW<sub>red</sub> system
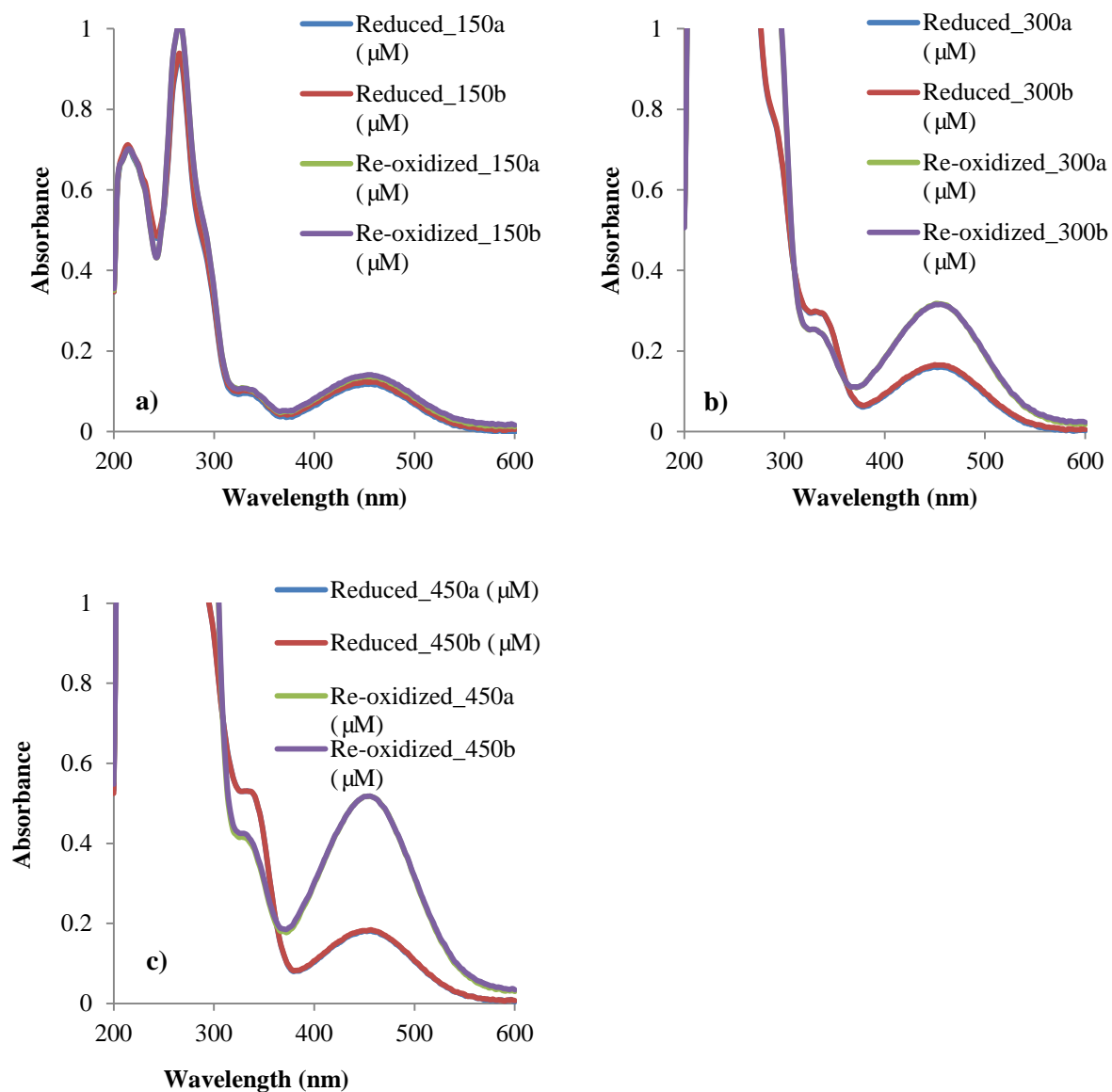


**Figure S2.10.** UV spectrum of the partially oxidized lawsone after filtration and the re-oxidation lawsone samples with different amounts of initially reduced lawsone in the presence of phosphate buffer. a) 150 μmol/L; b) 300 μmol/L; c) 450 μmol/L.

## 6. GT-Fe(II)+LAW$_{red}$ (III) system
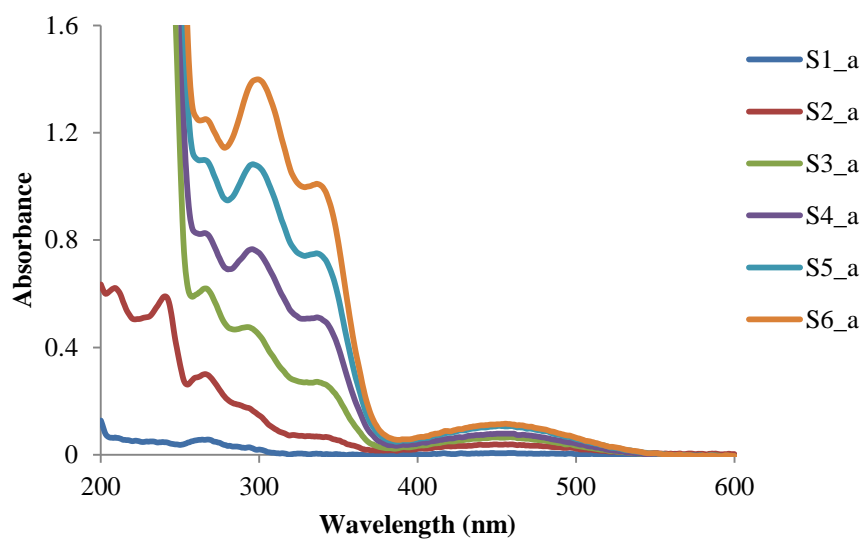


**Figure S2.11.** UV spectrum of the partially oxidized lawsone after filtration.

## 7. Sorption isotherm of Zn(II) at goethite surface

Figures S2.12 show the sorption isotherm of zinc to goethite with equilibrium 3 days, the same as equilibrium 4 days.
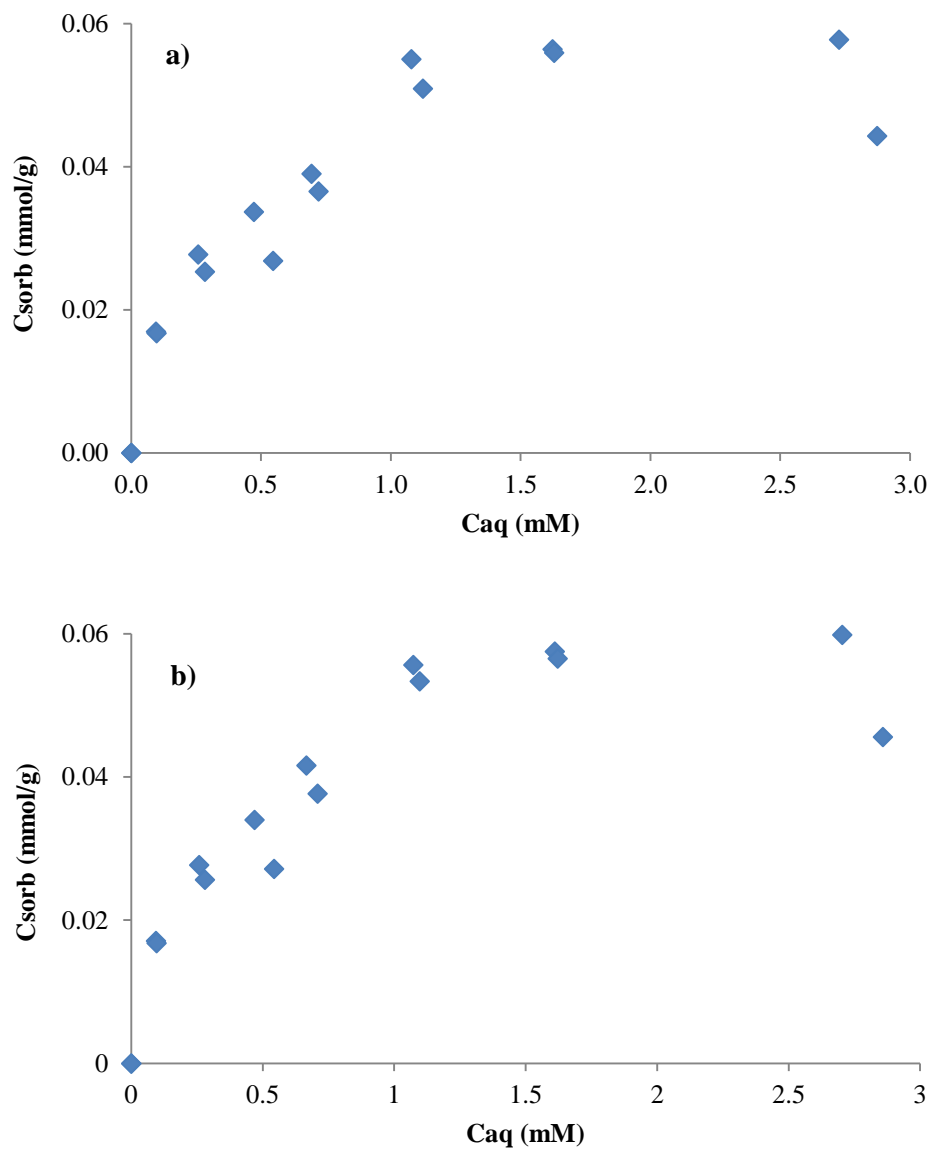


**Figure S2.12.** Sorption isotherm of Zn(II) on the goethite surface (100 $m^2$/L) at pH 7. a) Equilibration for 3 days; b) Equilibration for 4 days

## 8. Sorption isotherms by DOC analysis
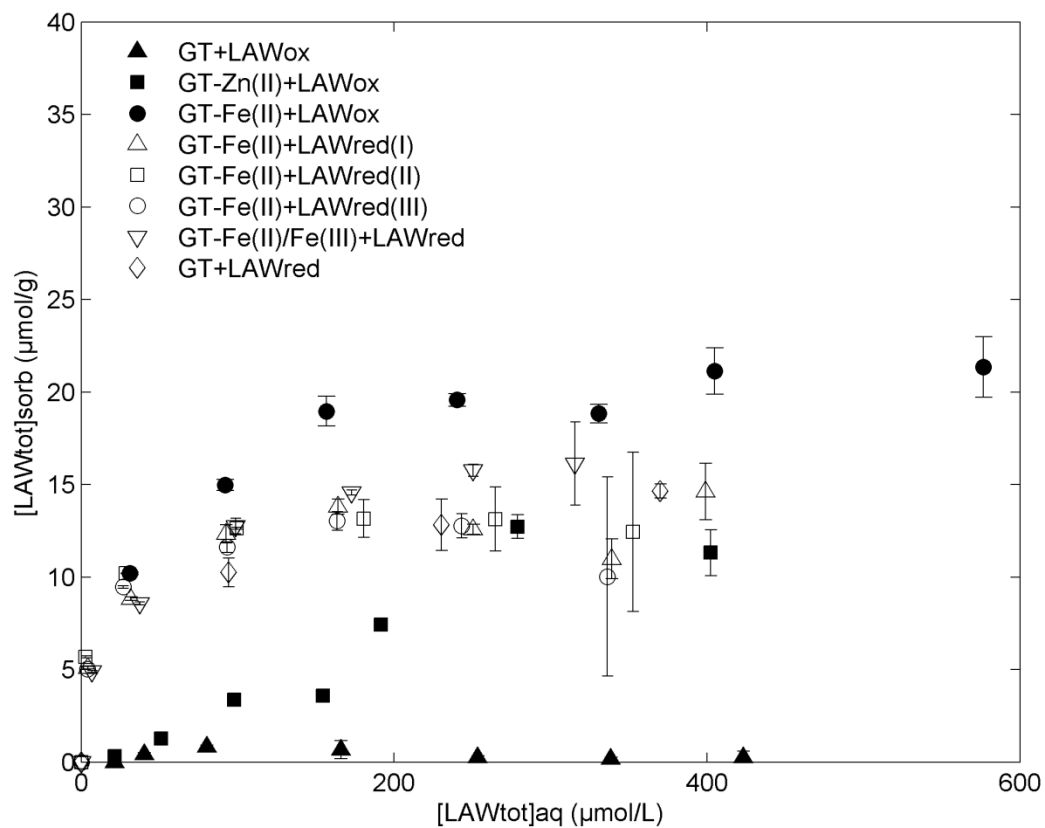


**Figure S2.13.** Uptake behavior of lawsone by DOC analysis under different redox conditions.

## 9. Equation for calculating the redox potential at goethite surfaces in the presence of Fe(II)

In order to correctly calculate the reduction potential of quinone, the redox species of quinone need to be defined individually. The oxidized form of lawsone ($Z_T$) contained protonated and deprotonated forms ($Z^o$ and $Z^-$). On the other hand, three protonation levels of reduced species ($X_T$) exist ($XH_2{}^o$, $XH^-$, and $X^{2-}$). The corresponding Nernst equation is written as the following Equation (S2.1):[127]

$$E_{h,lawsone} = E_{h,lawsone}{}^0 + \frac{RT}{zF}\ln\left(\frac{[Z^o][H^+]^2}{[XH_2{}^o]}\right)$$

$$= E_{h,lawsone}{}^0 + \frac{RT}{zF}\ln\left(\frac{Z_T \cdot [H^+] \cdot ([H^+]^2 + [H^+] \cdot K_{a_{R1}} + K_{a_{R1}} \cdot K_{a_{R2}})}{([H^+]+K_a) \cdot X_T}\right)$$

$$= E_{h,lawsone}{}^0 + \frac{RT}{zF}\ln\left(\frac{Z_T}{X_T}\right) + \frac{RT}{zF}\ln\left(\frac{[H^+]^3 + [H^+]^2 \cdot K_{a_{R1}} + [H^+] \cdot K_{a_{R1}} \cdot K_{a_{R2}}}{[H^+]+K_a}\right) \qquad \text{(S2.1)}$$

where $E^0$ is the standard redox potential of quinone at 0.351 V, R is the gas constant, T is the absolute temperature (K), F is the Faraday constant and z is the number of electrons transferred (z = 2). The acid-base equilibrium constants for the oxidized and reduced forms of quinone lawsone are reported in Clark's work (oxidized form: $K_a = 1.04 \times 10^{-4}$; reduced form: $K_{a_{R1}} = 2.09 \times 10^{-9}$, $K_{a_{R2}} = 1.95 \times 10^{-11}$).[38]

To estimate the pH effects on the redox potential of lawsone, Eq. (S2.1) can be rewritten as follows:

$$E_{h,lawsone} = E_{h,lawsone}{}^0 + \frac{2.303RT}{zF}log_{10}\left(\frac{Z_T}{X_T}\right) + \frac{2.303RT}{zF}log_{10}\left(\frac{[H^+]}{[H^+]+K_a}\right) + \frac{2.303RT}{zF}$$

$$\times log_{10}([H^+]^2 + [H^+] \cdot K_{a_{R1}} + K_{a_{R1}} \cdot K_{a_{R2}}) \qquad \text{(S2.2)}$$

Using the relationships $pH = -log_{10}[H^+]$ and $pK_a = -log_{10}K_a$, the expression for the redox potential of lawsone at $pH = 7$ can be simplified by Eq. (S2.3), since $pH \gg pK_a$ and $pH \ll pK_{a_{R1}}$: $[H^+]^2 \gg [H^+] \cdot K_{a_{R1}} + K_{a_{R1}} \cdot K_{a_{R2}}$

$$E_{h,lawsone} \cong E_{h,lawsone}{}^0 + \frac{2.303RT}{zF}\left(log_{10}\left(\frac{Z_T}{X_T}\right) + log_{10}\left(\frac{[H^+]}{K_a}\right) - 2pH\right) \qquad \text{(S2.3)}$$

**Table S2.1.** $E^0_H$ (pH = 7) values calculated from Lawsone redox speciation in solution (directly measured; subscript aq) or sorbed at goethite/Fe(II) (calculated form electron balance, subscript surf)

| GT-Fe(II)+LAW$_{ox}$ system | | | |
|---|---|---|---|
| LAW$_{ox}$ added (μM) | pH | $E^0_{H(pH7),LAW(aq)}$ (mV) | $E^0_{H(pH7),LAW(surf)}$ (mV) |
| 86.6 | 6.95 | -152 | - |
| 173.2 | 6.95 | -152 | - |
| 259.8 | 6.81 | -152 | $-156 \pm 1.6$ |
| 346.4 | 6.80 | -152 | $-144 \pm 2.9$ |
| 433.0 | 6.76 | -152 | $-136 \pm 1.6$ |
| 519.6 | 6.77 | -152 | $-132 \pm 1.8$ |
| 692.8 | 6.74 | -152 | $-122 \pm 2.3$ |

**Table S2.2.** Comparison of Langmuir model parameters in various systems

| System | $K_L$ [L/μmol] | LAW$_{sorb, max}$ [μmol/g] |
|---|---|---|
| GT-Fe(II)+LAW$_{red}$ | 0.11 | 14.5 |
| GT-Fe(II)+LAW$_{ox}$ | 0.033 | 18.8 |

Two types of Langmuir Fitting to data ($LAW_{red(aq)}$ vs $LAW_{tot(sorb)}$) in Figure 2.3 have been conducted: one is fitting individual listed experimental data with a Langmuir model, which can provide several groups of K and $S_{max}$ values, and also the average values and standard deviations; the other one is fitting together with all the dataset of listed experiments, only one group of K and $S_{max}$ value, thus no standard deviations. Both fitting procedures show the same parameters for Langmuir model. The details are listed in the following Table S2.3.

**Table S2.3.** Two types of Langmuir Fitting to data ($LAW_{red(aq)}$ vs $LAW_{tot(sorb)}$) in Figure 2.3.

| Name | Individual Fitting | | | Fitting together | | |
|---|---|---|---|---|---|---|
| | K | $S_{max}$ | $R^2$ | K | $S_{max}$ | $R^2$ |
| GT-Fe(II)+$LAW_{red}$ (I) | 0.106 ±0.025 | 14.456 ±0.355 | 0.885 | | | |
| GT-Fe(II)+$LAW_{red}$ (II) | 0.098 ±0.016 | 15.318 ±0.300 | 0.953 | | | |
| GT-Fe(II)+$LAW_{red}$ (III) | 0.184 ±0.070 | 13.924 ±0.553 | 0.786 | 0.115 ±0.043 | 14.457 ±0.624 | 0.834 |
| GT-Fe(II)+O2+$LAW_{red}$ (I) | 0.139 ±0.043 | 13.939 ±0.398 | 0.837 | | | |
| GT-Fe(II)+O2+$LAW_{red}$ (II) | 0.154 ±0.015 | 15.787 ±0.659 | 0.892 | | | |
| GT+$LAW_{red}$ | 0.147 ±0.001 | 13.188 ±0.013 | 0.999 | | | |

# Supporting Information for Chapter 3

# Effects of Sorbed Natural Organic Matter (NOM) on Electron Transfer at Goethite/Fe(II) Interfaces

Supplemental Information Summary

Number of pages: 9

Number of tables: 2

Number of figures: 7

## 1. UV and Fluoessence Spectropy of Aldrich Humic acid
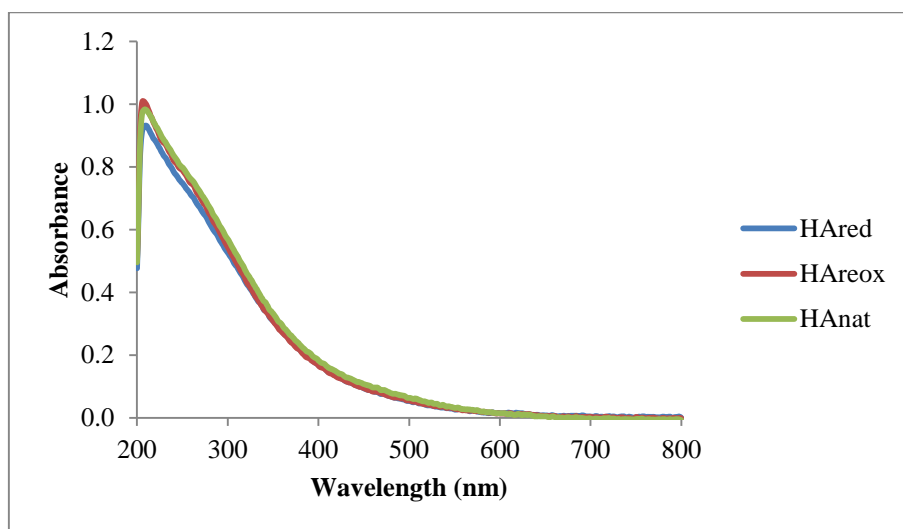


**Figure S3.1.** UV spectra of Aldrich Humic acid (9 mgDOC/L) under untreated, reduced and reoxidized states at pH 7**.**
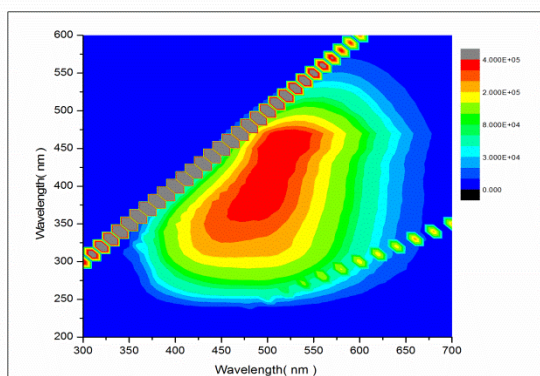
a) AHA$_{untre}$                                                    b) AHA$_{red}$
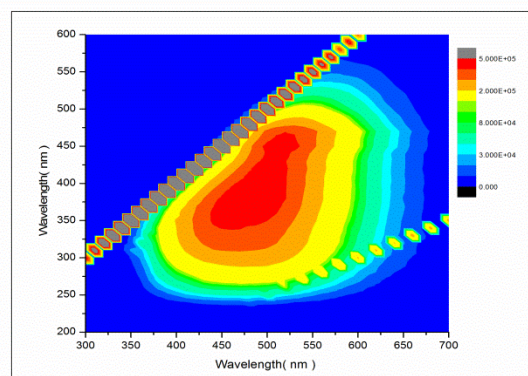


c) AHA$_{reox}$
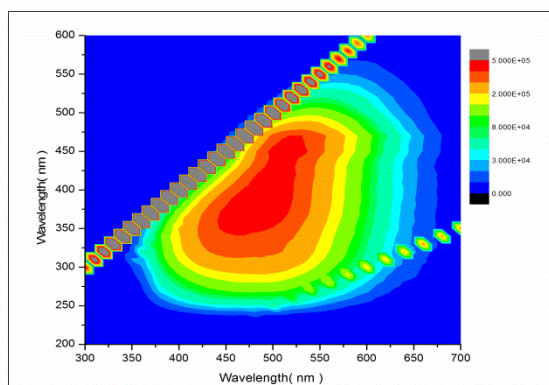
**Figure S3.2**. EEM Fluoessence spectra of Aldrich Humic acid (9 mgDOC/L) under untreated, reduced and reoxidized states at pH 7.

## 2. Validation of Aldrich HA effect on ferrozine method
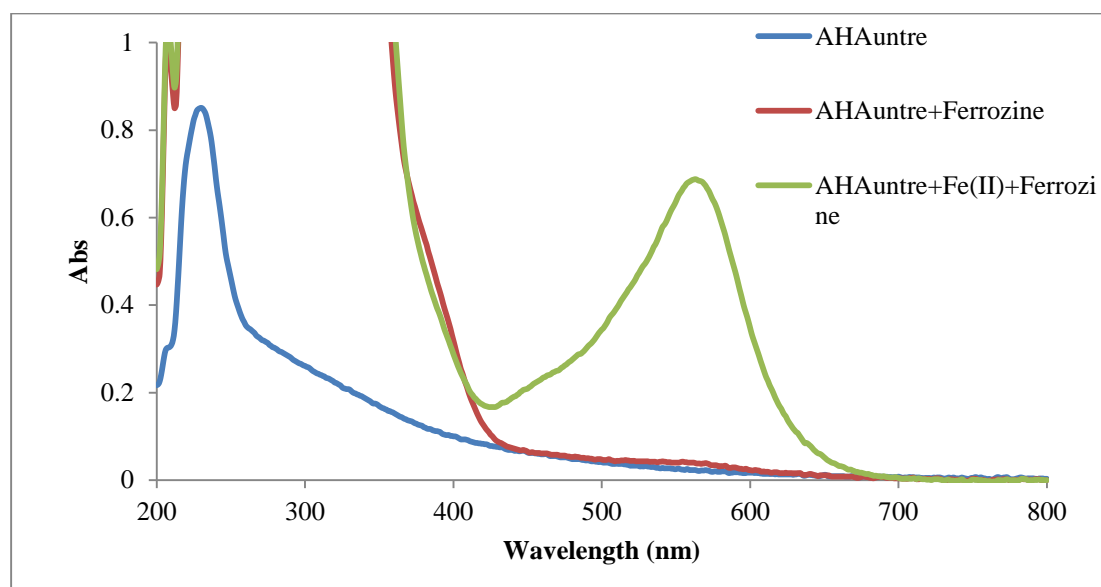


**Figure S3.3.** The spectra of ferrozine method for $Fe(II)_{aq}$ detection in the presence of 100 mgDOC/L $AHA_{untre}$.
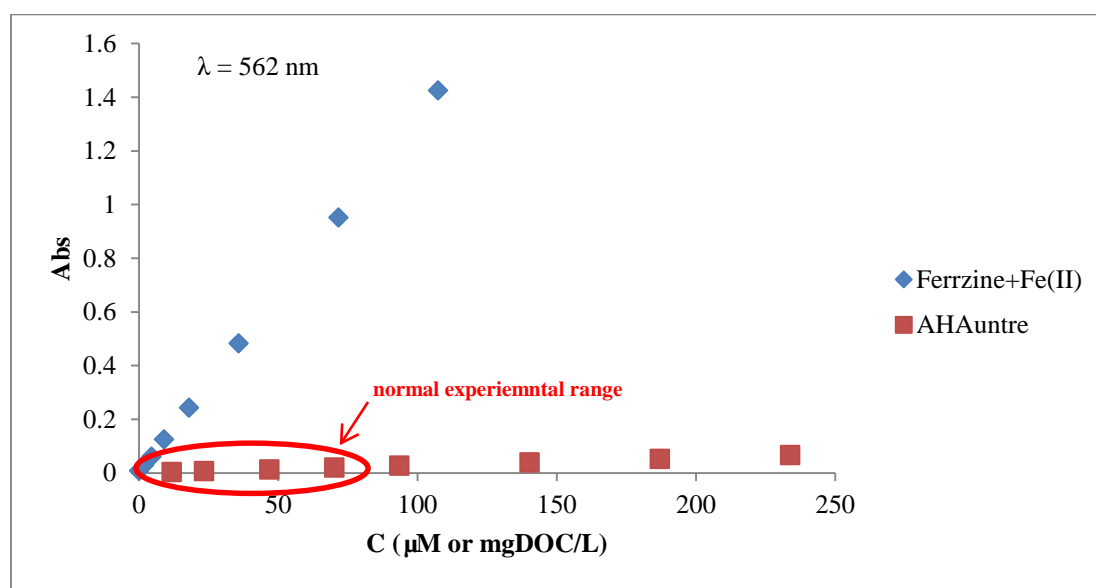


**Figure S3.4.** The interference of $AHA_{untre}$ to the Fe(II) calibration.

a)

b)
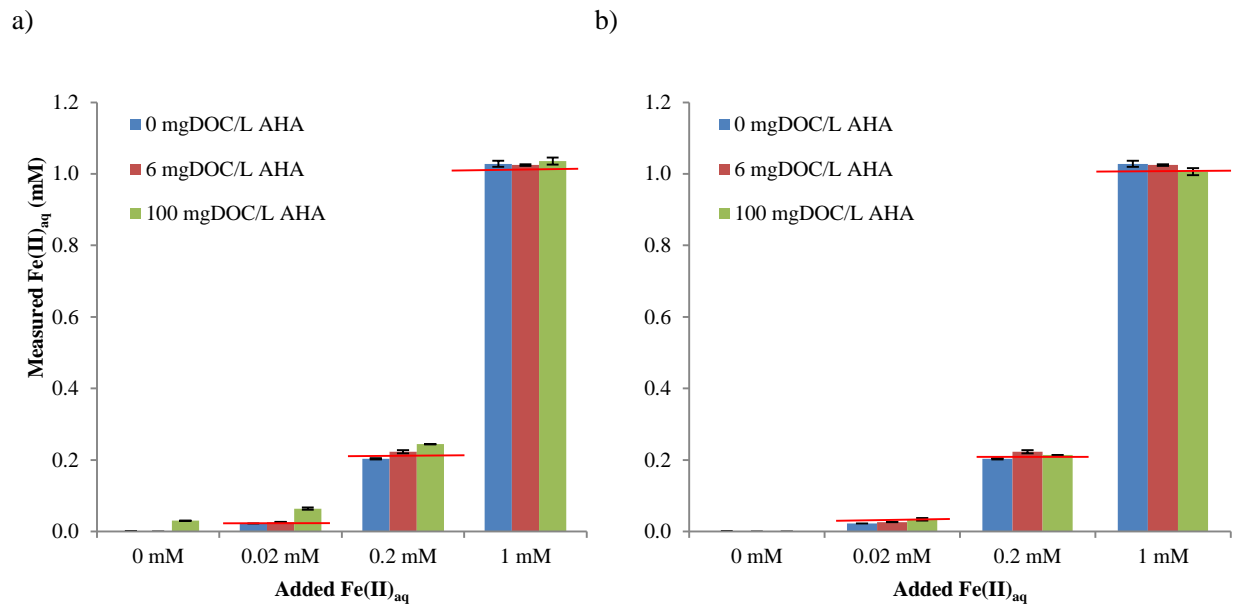


**Figure S3.5.** The interface of $AHA_{untre}$ to Fe(II) measurement by ferrozine method; a).normal measured Fe(II); b) subtraction of Fe(II) in the presence of high DOC $AHA_{untre}$.

## 3. Sorption Isotherm by UV-Vis
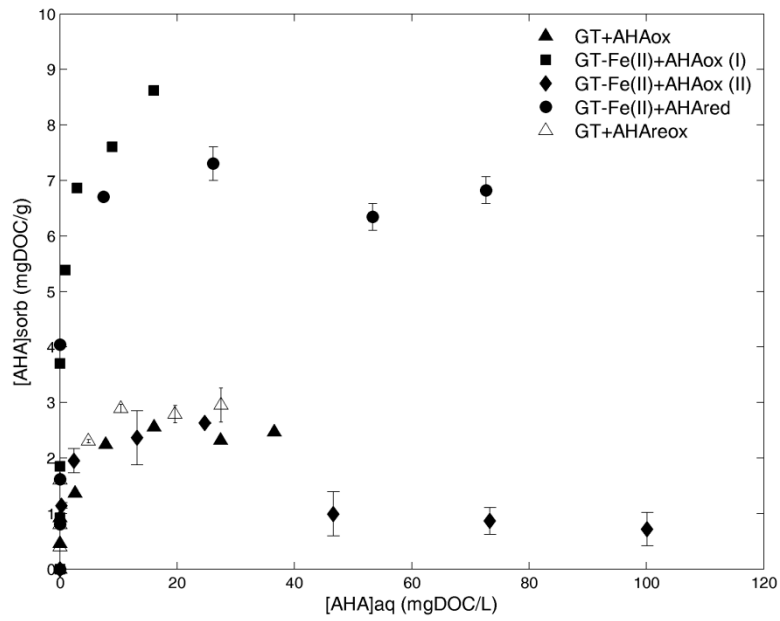


**Figure S3.6.** Sorption behaviors of AHA under different redox conditions by UV-Vis (n = 2 $\pm$ 1 SD).

## 4. Sorption Isotherm of untreated AHA to goethite at pH 6-8
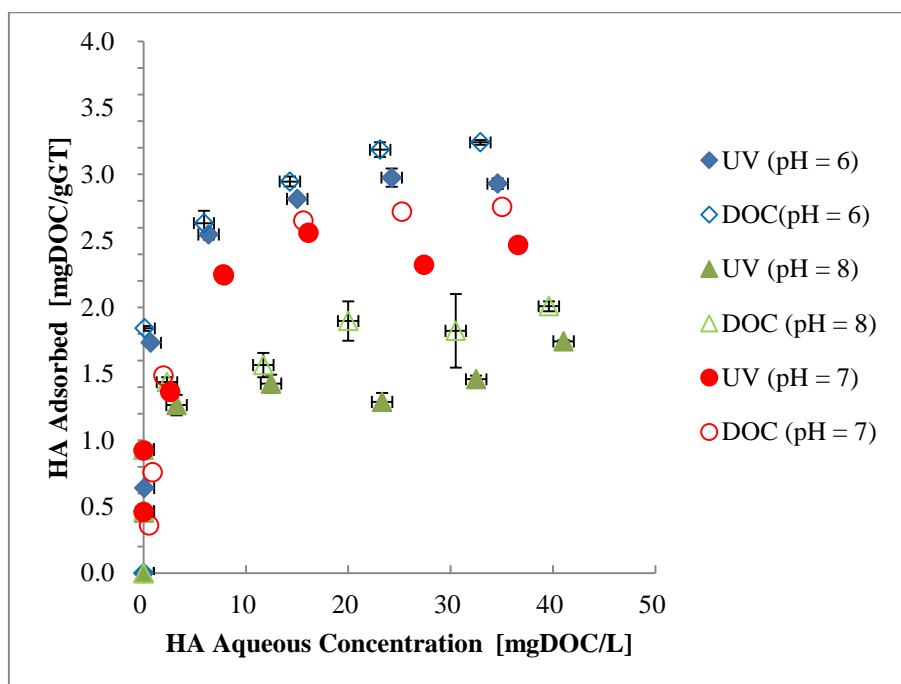


**Figure S3.**7. Sorption of untreated AHA in the absence of Fe(II) on Goethite by UV and DOC methods at pH 6 and 8 (n = 2 ± 1 SD) and at pH 7 (n = 1). Goethite surface = 50 m$^2$/L.

## 5. Mediated electrochemical oxidation (MEO) and reduction (MER)

Mediated electrochemical oxidation (MEO) and reduction (MER) quantitatively detected the electrons of either $AHA_{untre}$ or $AHA_{red}$ samples pre-reduced by DER method, which has been previously published.[36, 54] A nine mL glassy carbon cylinder (Sigradur G, HTW, Germany) was used both as the working electrode (WE) and reaction vessel to favour electron transfer through the mediators. The counter electrode was a coiled platinum wire separated by a porous glass tube. The applied redox potentials ($E_H$) were measured against Ag/AgCl reference electrode (Bioanalytical Systems Inc., USA), but exported to standard hydrogen potentials as reference. The working cell was filled with 6 ml of phosphate buffer (0.1 M KCl, 0.1 M phosphate, pH 7) and the electrode was equilibrated to the desired potentials (Eh = -0.7 V in MER and +0.4 V in MEO). Afterwards, 180 μl of mediator stock solutions (5 mM) DQ for MER and ABTS for MEO were spiked into the cell, leading to reductive and oxidative peak currents respectively. After acquisition of stable background currents, small volumes (10-100 μl) of AHA samples were added to the cells. The amounts of transferred electrons were measured by chronocoulometry and the resulting current peaking for MER and MEO were integrated by Origin software to calculate the electrons accepting (EAC) and donating capacities (EDC) (μmol e⁻/g DOC) of added samples.

$$EAC = \frac{\int I_{red} dt}{F \times V_{add} \times C_{sample}} \tag{S3.1}$$

$$EDC = \frac{\int I_{ox} dt}{F \times V_{add} \times C_{sample}} \tag{S3.2}$$

Whereas $I_{red}$ and $I_{ox}$ ([A]) are the baseline-corrected reductive and oxidative currents in MER and MEO respectively, F is faraday constant (96485 s A/mol), $V_{add}$ (μl) is the added volumes of AHA samples and $C_{sample}$ (mgDOC/L) is the DOC concentration of added samples. All samples were conducted in triplicates. And the electrochemical properties of Aldrich HA were listed in Table S3.2.

**Table S3.1.** Control Samples of Fe(II)$_{aq}$/Zn(II)$_{aq}$ with untreated and electrochemically reduced AHA in the aqueous phase at pH 7.

**Experimental Condition**

| Initial addition | | | | Equilibrium one day and filtered (measured) | | | |
|---|---|---|---|---|---|---|---|
| Fe(II)$_{aq}$ (mM) | Zn(II)$_{aq}$ (mM) | AHA$_{untre}$ (mgDOC/L) | AHA$_{red}$ (mgDOC/L) | Fe(II)$_{aq}$ (mM) | Zn(II)$_{aq}$ (mM) | AHA$_{untre}$ (mgDOC/L) | AHA$_{red}$ (mgDOC/L) |
| 1.0 | | 13.0 | | 1.00 ±0.01 | | 12.6 ±0.5 | |
| 1.0 | | 52.0 | | 0.99 ±0.01 | | 50.6 ±0.1 | |
| 1.0 | | | 9.0 | 1.02 ±0.00 | | | 9.2 ±0.2 |
| 1.0 | | | 46.0 | 1.06 ±0.01 | | | 44.1 ±0.3 |
| | 1.0 | 13.0 | | | 0.94 ±0.01 | 8.6 ±0.2 | |
| | 1.0 | 52.0 | | | 0.95 ±0.01 | 47.7 ±0.1 | |

**Table S3.2.** Electrochemical　Property and Fe(II) Content of Aldrich HA

| Electrochemical Properties | | | | |
|---|---|---|---|---|
| **Name** | **EAC$_{(MER)}$** ( μmol e$^-$/mgDOC) | **EDC$_{(MEO)}$** ( μmol e$^-$/mgDOC) | **EAC$_{(literature)}$** ( μmol e$^-$/mgDOC) | **EDC$_{(literature)}$** ( μmol e$^-$/mgDOC) |
| AHA$_{untre}$ | 3.19 ±0.3 | 3.78 ±0.2 | 1.7-2.5[36, 100] | 3.8[36] |
| AHA$_{red}$ | n.a | 6.66 ±0.4 | n.a | n.a |

| Ferrous Iron Content | | | | | |
|---|---|---|---|---|---|
| | **DOC content** (mgDOC/L) | **EDC$_{(MEO)}$** ( μmol e$^-$/L) | **Fe(II)$_{aq (ferrozine)}$** ( μmol /L) | **Fe(II)$_{aq (literature)}$** ( μmol /L) [36, 100] | **Fe(II)$_{aq}$/EDC** (%) | **Fe mass** (%) |
| AHA$_{red}$ | 92 | 634.8 | 75 ±0.8 | 54.5 | 11.8 | 1.8 |

*Aldrich HA contains significant amount of iron (1.33%);　n.a = not available.

# Supporting Information for Chapter 4

# Surface Complexation of Quinone at the Goethite/Fe(II) Interface: An UV-Vis/ATR-FTIR Study

Supplemental Information Summary

Number of pages: 9

Number of tables: 0

Number of figures: 9

## UV-Vis Spectroscopy

Figure S4.1, S4.2, S4.3 and S4.4 show that the UV spectra analysis of aqueous iron, LAW, and their mixture in the pH range from 2.1 to 7.
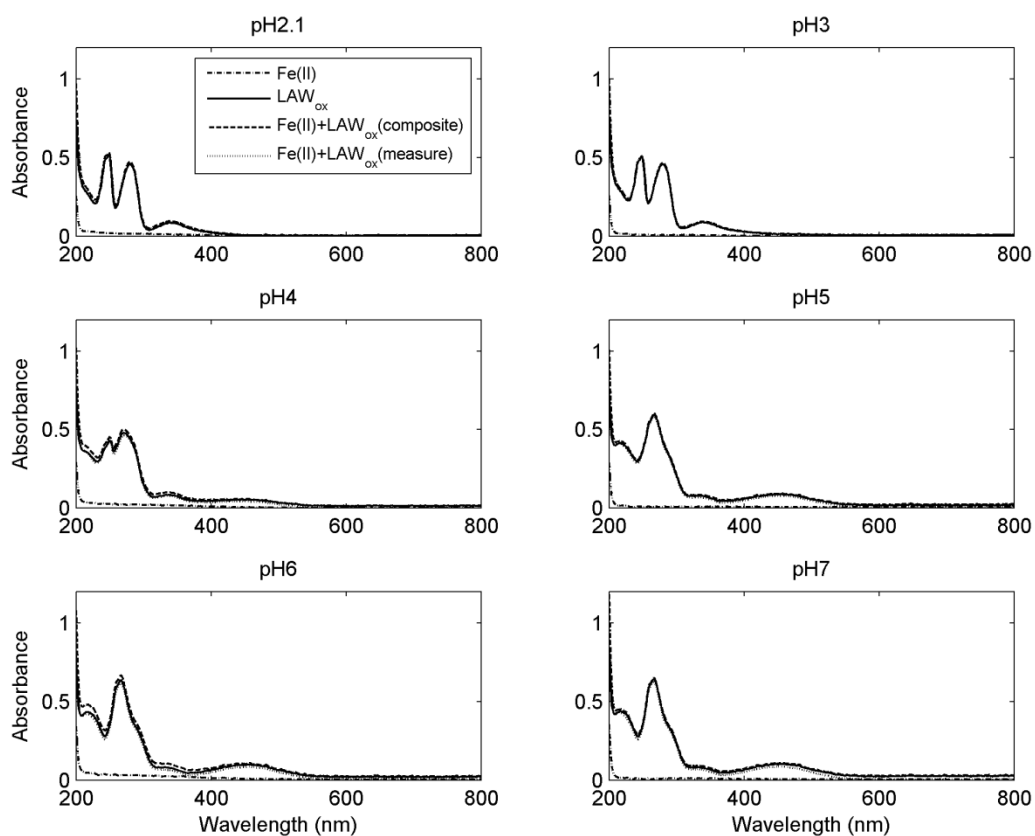


**Figure S4.1**. UV-Vis spectra diagrams of Fe(II) (10 μM), $LAW_{ox}$ (30 μM), Fe(II)+$LAW_{ox}$(composite) and Fe(II)+$LAW_{ox}$(measure) at pH 2.1 to 7. Composite: calculated sum of the individual spectra of iron and LAW; Measure: measured spectra of Iron+LAW.
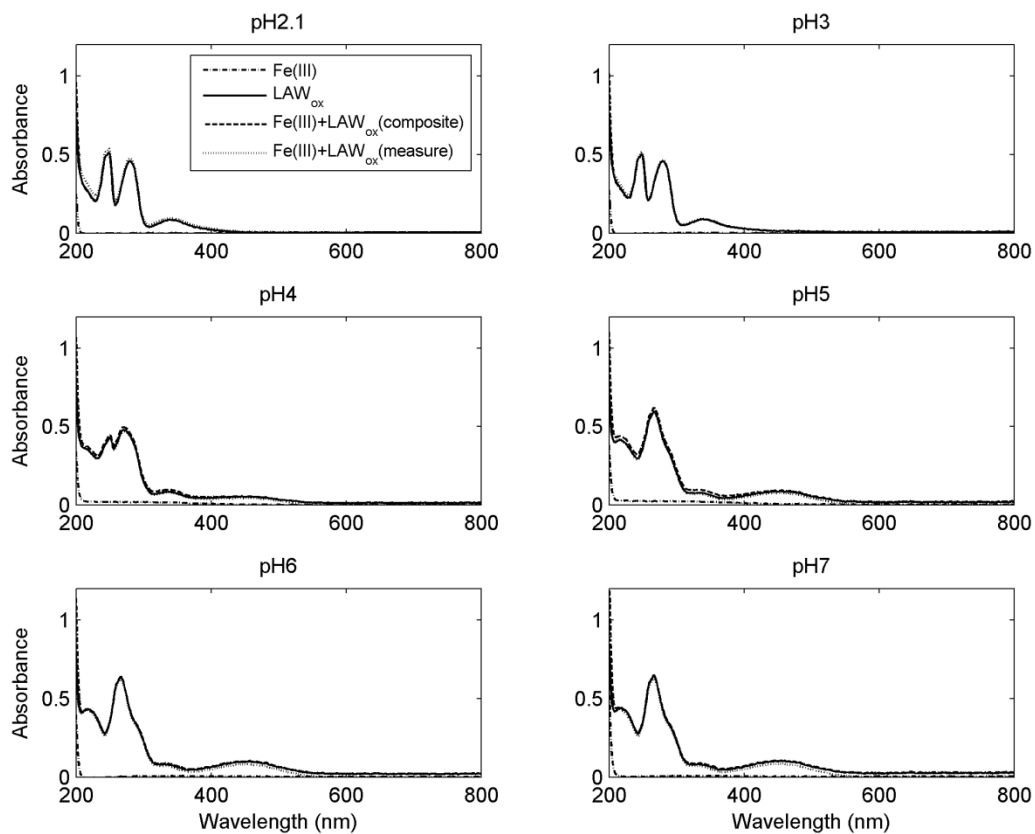
**Figure S4.2**. UV-Vis spectra diagrams of Fe(III) (10 μM), LAW$_{ox}$ (30 μM), Fe(III)+LAW$_{ox}$(composite) and Fe(III)+LAW$_{ox}$(measure) at pH 2.1 to 7.
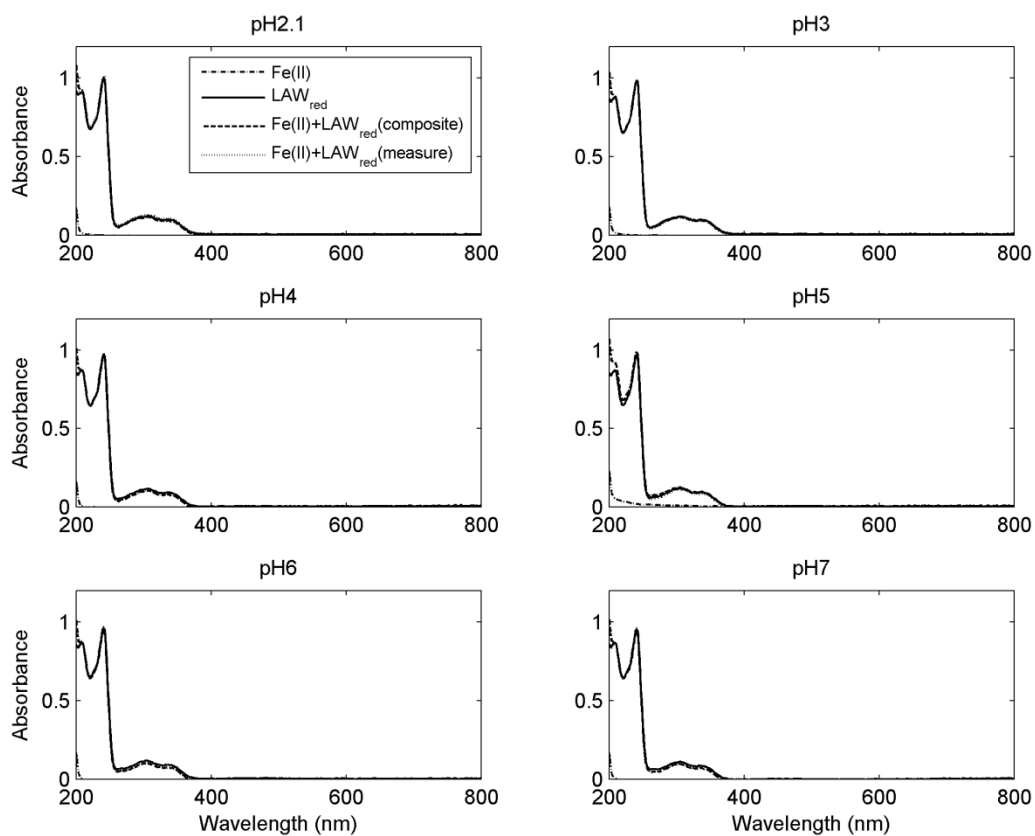
**Figure S4.3**. UV-Vis spectra diagrams of Fe(II) (10 μM), LAW$_{red}$ (30 μM), Fe(II)+LAW$_{red}$(composite) and Fe(II)+LAW$_{red}$(measure) at pH 2.1 to 7.
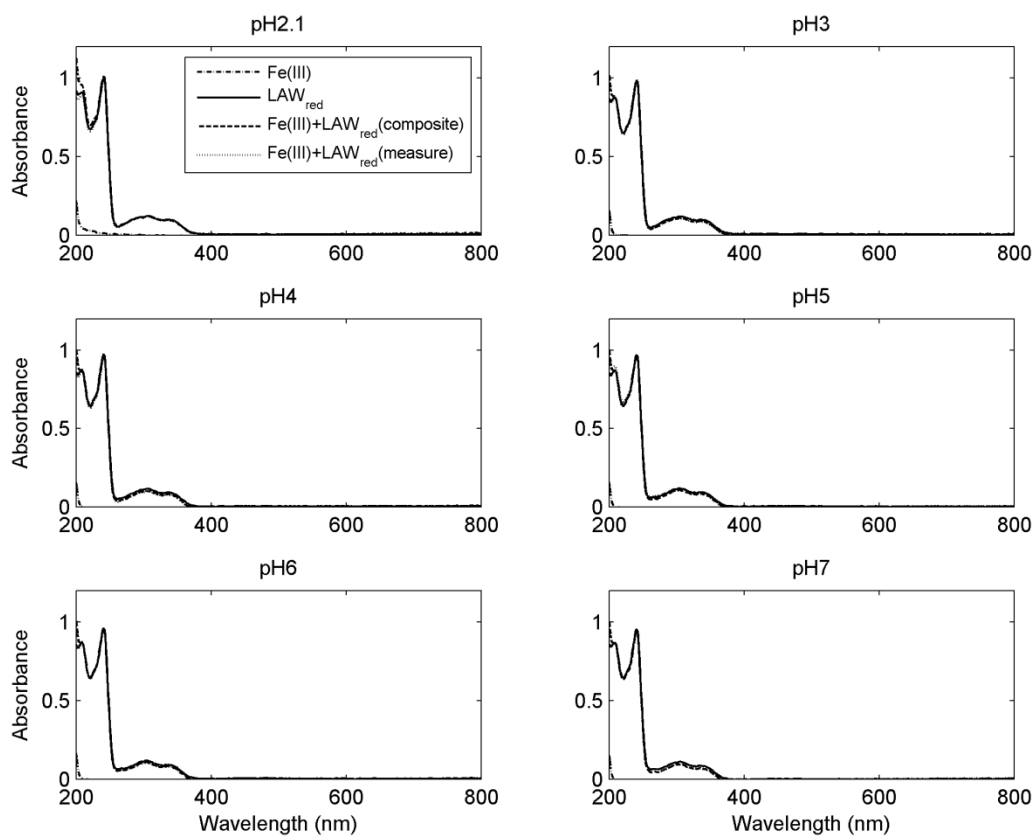
**Figure S4.4**. UV-Vis spectra diagrams of Fe(III) (10 μM), LAW$_{red}$ (30 μM), Fe(III)+LAW$_{red}$(composite) and Fe(III)+LAW$_{red}$(measure) at pH 2.1 to 7.

## ATR-FTIR Spectroscopy Analysis

Attenuated total reflectance-Fourier transform infrared (ATR-FTIR) measurements were performed with a Bruker VERTEX 80V spectrometer equipped with a LN-MCT detector and a horizontal ATR diamond accessory (BioATR II, 8 reflections, Bruker, Germany) with a ZnSe Crystal. The setup was shown in the following Figure S4.5.
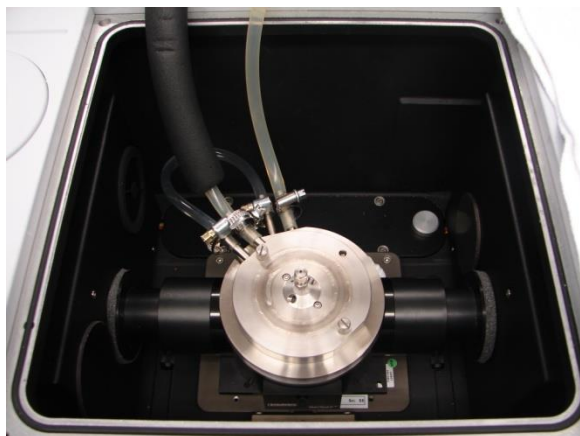
a)                                                                           b)
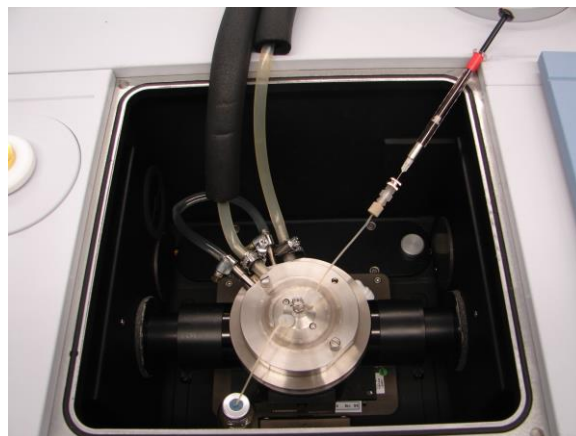


**Figure S4.5.** experiment setup for ATR-FTIR measurement with the static state (a) and flow through system (b).

Figure S4.6 shows the spectra of free oxidized lawsone species from pH 2 to 7 at static state. Its spectra shape and peak position was consistent with the flow through
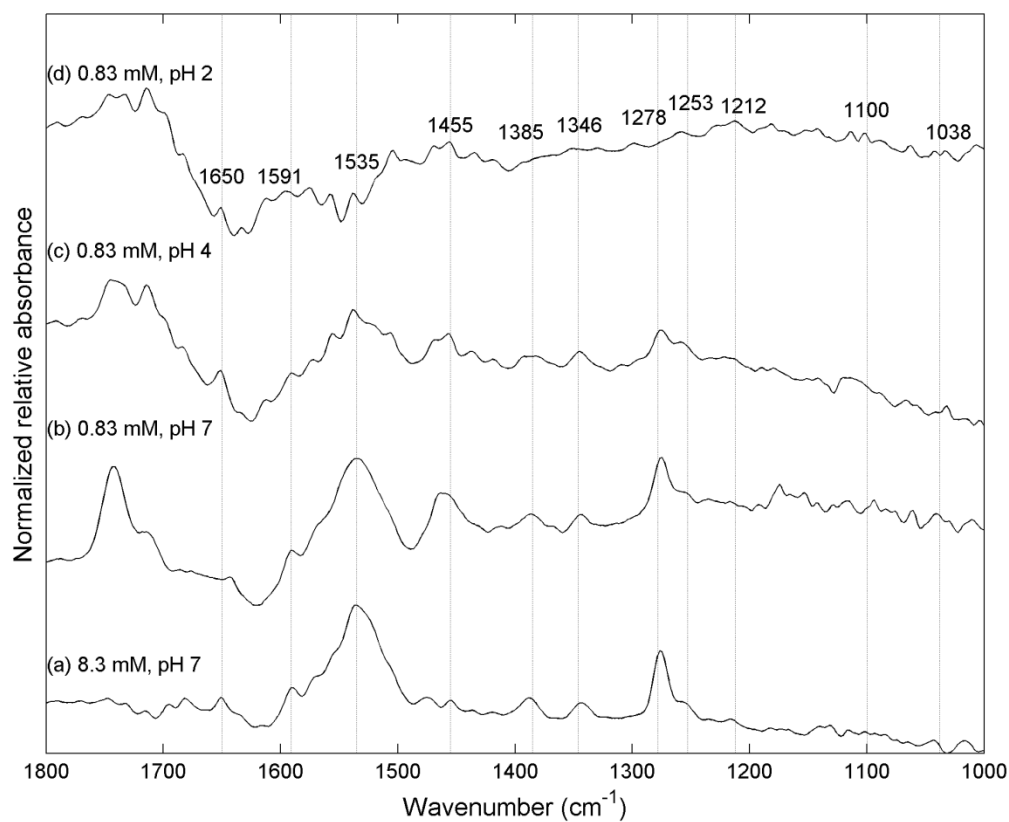


**Figure S4.6**. ATR-FTIR analysis of LAW$_{ox}$ (8.3 mM at pH 7 and 0.83 mM at pH 2, 4, 7) at static state by 400 scan.

Figure S4.7 shows that a reference spectrum of dissolved AHA$_{untre}$ and its interaction with goethite surface was obtained in the wavenumber region of 800 - 4000 cm$^{-1}$.
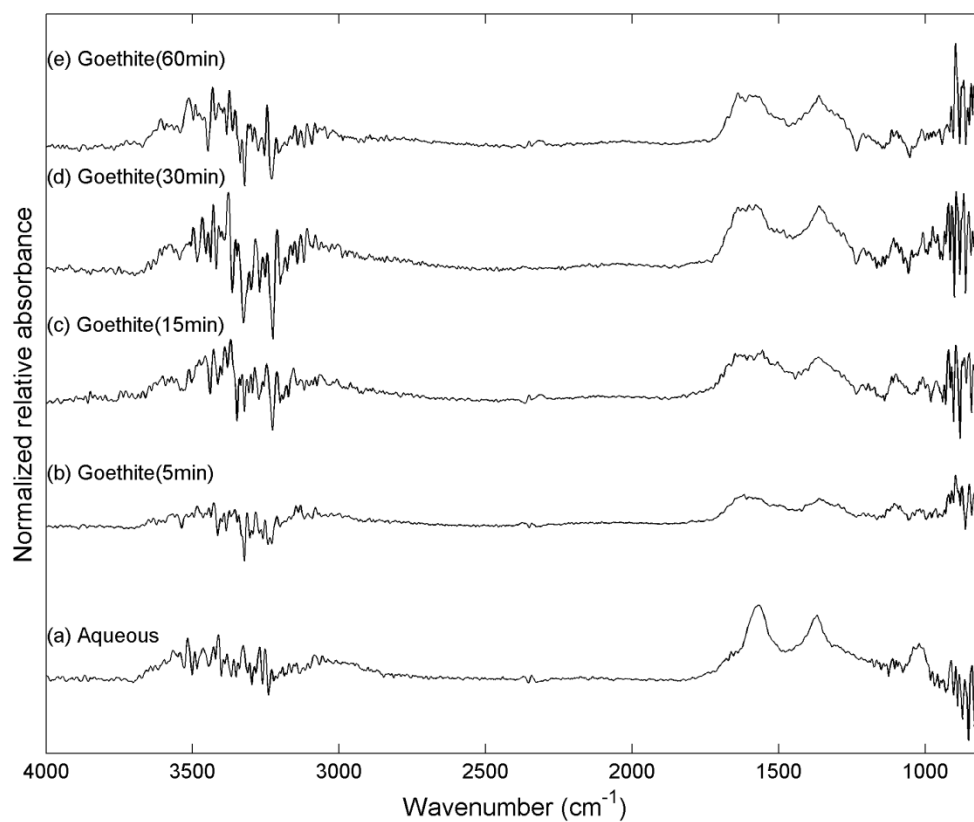


**Figure S4.7.** ATR-FTIR spectra (800-4000 cm$^{-1}$) of (a) 1000 mgDOC/L AHA$_{untre}$, pH 7 and its flow through interaction with goethite film acquired at (b) 5 min, (c) 15 min, (d) 30 min, and (e) 60 min.
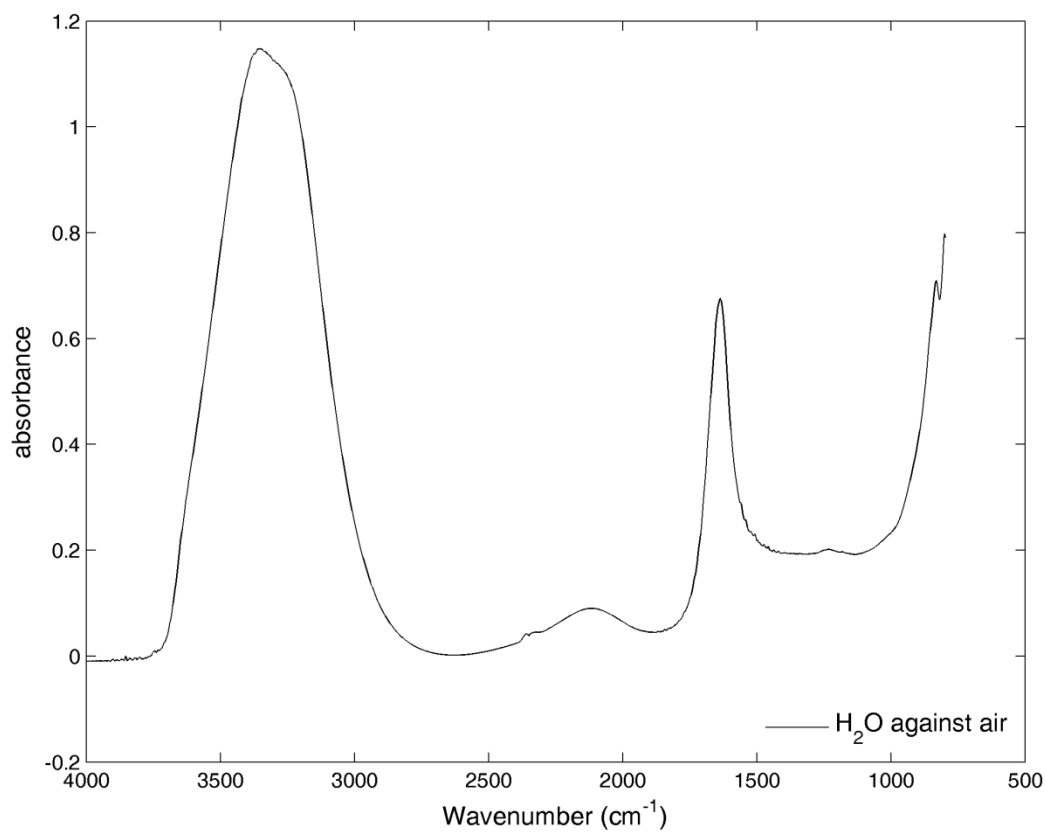
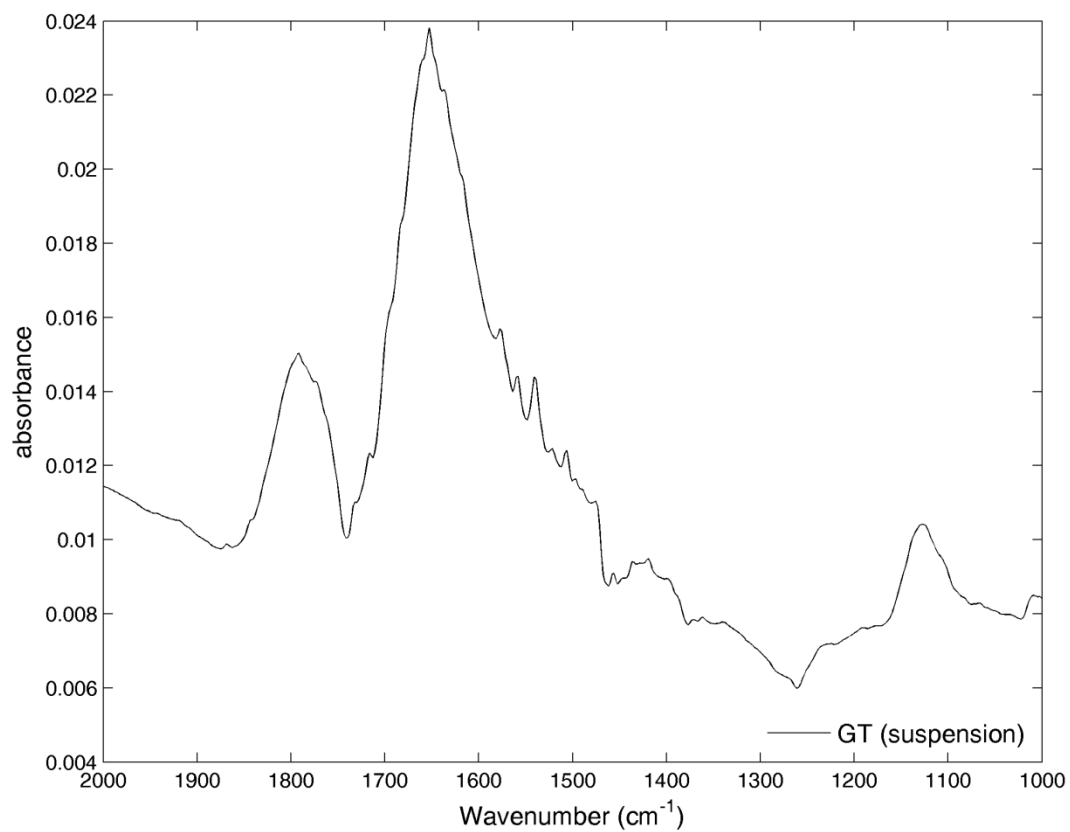**Figure S4.8.** ATR-FTIR spectra of Millipore water against air.

**Figure S4.9.** ATR-FTIR spectra of goethite suspension against water.

# References

1.  Pecher, K.; Haderlein, S. B.; Schwarzenbach, R. P., Reduction of Polyhalogenated Methanes by Surface-Bound Fe(II) in Aqueous Suspensions of Iron Oxides. Environmental Science & Technology 2002, 36, (8), 1734-1741.

2.  Luan, F.; Xie, L.; Li, J.; Zhou, Q., Abiotic reduction of nitroaromatic compounds by Fe(II) associated with iron oxides and humic acid. Chemosphere 2013, 91, (7), 1035-1041.

3.  Elsner, M.; Schwarzenbach, R. P.; Haderlein, S. B., Reactivity of Fe(II)-Bearing Minerals toward Reductive Transformation of Organic Contaminants. Environmental Science & Technology 2003, 38, (3), 799-807.

4.  Amstaetter, K.; Borch, T.; Larese-Casanova, P.; Kappler, A., Redox Transformation of Arsenic by Fe(II)-Activated Goethite (α-FeOOH). Environmental Science & Technology 2009, 44, (1), 102-108.

5.  Aeschbacher, M.; Brunner, S. H.; Schwarzenbach, R. P.; Sander, M., Assessing the Effect of Humic Acid Redox State on Organic Pollutant Sorption by Combined Electrochemical Reduction and Sorption Experiments. Environmental Science & Technology 2012, 46, (7), 3882-3890.

6.  Mladenov, N.; Zheng, Y.; Simone, B.; Bilinski, T. M.; McKnight, D. M.; Nemergut, D.; Radloff, K. A.; Rahman, M. M.; Ahmed, K. M., Dissolved Organic Matter Quality in a Shallow Aquifer of Bangladesh: Implications for Arsenic Mobility. Environmental Science & Technology 2015.

7.  Kappler, A.; Haderlein, S. B., Natural Organic Matter as Reductant for Chlorinated Aliphatic Pollutants. Environmental Science & Technology 2003, 37, (12), 2714-2719.

8.  Matthiessen, A., Kinetic aspects of the reduction of mercury ions by humic substances. J Anal Chem 1996, 354: 747—749.

9.  Tratnyek, P. G.; Scherer, M. M.; Deng, B.; Hu, S., Effects of Natural Organic Matter, Anthropogenic Surfactants, and Model Quinones on the Reduction of Contaminants by Zero-Valent Iron. Water Research 2001, 35, (18), 4435-4443.

10. Dunnivant, F. M.; Schwarzenbach, R. P.; Macalady, D. L., Reduction of substituted nitrobenzenes in aqueous solutions containing natural organic matter. Environmental Science & Technology 1992, 26, (11), 2133-2141.

11. Klausen, J.; Troeber, S. P.; Haderlein, S. B.; Schwarzenbach, R. P., Reduction of Substituted Nitrobenzenes by Fe(II) in Aqueous Mineral Suspensions. Environmental Science & Technology 1995, 29, (9), 2396-2404.

12. Doong, R.-A.; Chiang, H.-C., Transformation of Carbon Tetrachloride by Thiol Reductants in the Presence of Quinone Compounds. Environmental Science & Technology 2005, 39, (19), 7460-7468.

13. R.M.Cornmell; Schwertmann, U., The Iron Oxides 2003, 675.

14. Ruan, H. D.; Frost, R. L.; Kloprogge, J. T.; Duong, L., Infrared spectroscopy of goethite dehydroxylation: III. FT-IR microscopy of in situ study of the thermal transformation of goethite to hematite. Spectrochimica Acta Part A: Molecular and Biomolecular Spectroscopy 2002, 58, (5), 967-981.

15. Handler, R. M.; Beard, B. L.; Johnson, C. M.; Scherer, M. M., Atom Exchange between Aqueous Fe(II) and Goethite: An Fe Isotope Tracer Study. Environmental Science & Technology 2009, 43, (4), 1102-1107.

16. Frierdich, A. J.; Helgeson, M.; Liu, C.; Wang, C.; Rosso, K. M.; Scherer, M. M., Iron Atom Exchange between Hematite and Aqueous Fe(II). Environmental Science & Technology 2015.

17. Weng, L.; Van Riemsdijk, W. H.; Hiemstra, T., Humic Nanoparticles at the Oxide−Water Interface: Interactions with Phosphate Ion Adsorption. Environmental Science & Technology 2008, 42, (23), 8747-8752.

18. Weng; Van Riemsdijk, W. H.; Koopal, L. K.; Hiemstra, T., Adsorption of Humic Substances on Goethite: Comparison between Humic Acids and Fulvic Acids†. Environmental Science & Technology 2006, 40, (24), 7494-7500.

19. Wang, L.; Chin, Y.-P.; Traina, S. J., Adsorption of (poly)maleic acid and an aquatic fulvic acid by geothite. Geochimica et Cosmochimica Acta 1997, 61, (24), 5313-5324.

20. Saito, T.; Koopal, L. K.; van Riemsdijk, W. H.; Nagasaki, S.; Tanaka, S., Adsorption of Humic Acid on Goethite: Isotherms, Charge Adjustments, and Potential Profiles. Langmuir 2004, 20, (3), 689-700.

21. Gu, B.; Schmitt, J.; Chen, Z.; Liang, L.; McCarthy, J. F., Adsorption and desorption of natural organic matter on iron oxide: mechanisms and models. Environmental Science & Technology 1994, 28, (1), 38-46.

22. Evanko, C. R.; Dzombak, D. A., Influence of Structural Features on Sorption of NOM-Analogue Organic Acids to Goethite. Environmental Science & Technology 1998, 32, (19), 2846-2855.

23. Chassé, A. W.; Ohno, T., Higher Molecular Mass Organic Matter Molecules Compete with Orthophosphate for Adsorption to Iron (Oxy)hydroxide. Environmental Science & Technology 2016.

24. Antelo, J.; Arce, F.; Avena, M.; Fiol, S.; López, R.; Macías, F., Adsorption of a soil humic acid at the surface of goethite and its competitive interaction with phosphate. Geoderma 2007, 138, (1–2), 12-19.

25. Silvester, E.; Charlet, L.; Tournassat, C.; Géhin, A.; Grenèche, J.-M.; Liger, E., Redox potential measurements and Mössbauer spectrometry of FeII adsorbed onto FeIII (oxyhydr)oxides. Geochimica et Cosmochimica Acta 2005, 69, (20), 4801-4815.

26. Latta, D. E.; Bachman, J. E.; Scherer, M. M., Fe Electron Transfer and Atom Exchange in Goethite: Influence of Al-Substitution and Anion Sorption. Environmental Science & Technology 2012, 46, (19), 10614-10623.

27. Orsetti, S.; Laskov, C.; Haderlein, S. B., Electron Transfer between Iron Minerals and Quinones: Estimating the Reduction Potential of the Fe(II)-Goethite Surface from AQDS Speciation. Environmental Science & Technology 2013.

28. Handler, R. M.; Frierdich, A. J.; Johnson, C. M.; Rosso, K. M.; Beard, B. L.; Wang, C.; Latta, D. E.; Neumann, A.; Pasakarnis, T.; Premaratne, W. A. P. J.; Scherer, M. M., Fe(II)-Catalyzed Recrystallization of Goethite Revisited. Environmental Science & Technology 2014.

29. Klein, A. R.; Silvester, E.; Hogan, C. F., Mediated Electron Transfer between FeII Adsorbed onto Hydrous Ferric Oxide and a Working Electrode. Environmental Science & Technology 2014.

30. Elsner, M.; Haderlein, S. B.; Kellerhals, T.; Luzi, S.; Zwank, L.; Angst, W.; Schwarzenbach, R. P., Mechanisms and Products of Surface-Mediated Reductive Dehalogenation of Carbon Tetrachloride by Fe(II) on Goethite. Environmental Science & Technology 2004, 38, (7), 2058-2066.

31. Fieser, L. F.; Peters, M. A., THE POTENTIALS AND THE DECOMPOSITION REACTIONS OF ORTHO QUINONES IN ACID SOLUTION. Journal of the American Chemical Society 1931, 53, (2), 793-805.

32. Fieser, L. F., THE ALKYLATION OF HYDROXYNAPHTHOQUINONE I. ORTHO-ETHERS. Journal of the American Chemical Society 1926, 48, (11), 2922-2937.

33. Conant, J. B.; Fieser, L. F., REDUCTION POTENTIALS OF QUINONES. II. THE POTENTIALS OF CERTAIN DERIVATIVES OF BENZOQUINONE, NAPHTHOQUINONE AND ANTHRAQUINONE. Journal of the American Chemical Society 1924, 46, (8), 1858-1881.

34. Uchimiya, M., Reductive Transformation of 2,4-Dinitrotoluene: Roles of Iron and Natural Organic Matter. Aquatic Geochemistry 2010, 16, (4), 547-562.

35. Buchholz, A.; Laskov, C.; Haderlein, S. B., Effects of Zwitterionic Buffers on Sorption of Ferrous Iron at Goethite and Its Oxidation by CCl4. Environmental Science & Technology 2011, 45, (8), 3355-3360.

36. Aeschbacher, M.; Sander, M.; Schwarzenbach, R. P., Novel Electrochemical Approach to Assess the Redox Properties of Humic Substances. Environmental Science & Technology 2009, 44, (1), 87-93.

37. Sposito, G., The Surface Chemistry of Soils. Oxford University Press: New York, 1984.

38. Clark, W. M., Oxidation-Reduction Potentials of Organic Systems. Baltimore, Williams & Wilkins: 1960.

39. Thurman, E. M., Organic Geochemistry of Natural Waters. 1985.

40. Tan, K. H., Humic matter in soils and the environment: principles and controversies. New York, Marcel Deckker. 2003.

41. Waksman, S. A., Humus: Origin, Chemical Composition, and Importance in Nature. Williams & Wilkins: 1938.

42. Lovley, D. R.; Coates, J. D.; Blunt-Harris, E. L.; Phillips, E. J. P.; Woodward, J. C., Humic substances as electron acceptors for microbial respiration. Nature 1996, 382, (6590), 445-448.

43. Sunda, W. G.; Kieber, D. J., Oxidation of humic substances by manganese oxides yields low-molecular-weight organic substrates. Nature 1994, 367, (6458), 62-64.

44. Jiang, J.; Kappler, A., Kinetics of Microbial and Chemical Reduction of Humic Substances: Implications for Electron Shuttling. Environmental Science & Technology 2008, 42, (10), 3563-3569.

45. Aeschbacher, M.; Vergari, D.; Schwarzenbach, R. P.; Sander, M., Electrochemical Analysis of Proton and Electron Transfer Equilibria of the Reducible Moieties in Humic Acids. Environmental Science & Technology 2011, 45, (19), 8385-8394.

46. Gu, B.; Schmitt, J.; Chen, Z.; Liang, L.; McCarthy, J. F., Adsorption and desorption of different organic matter fractions on iron oxide. Geochimica et Cosmochimica Acta 1995, 59, (2), 219-229.

47. Hedges, J. I.; Oades, J. M., Comparative organic geochemistries of soils and marine sediments. Organic Geochemistry 1997, 27, (7–8), 319-361.

48. Kooner, Z. S., Comparative study of adsorption behavior of copper, lead, and zinc onto goethite in aqueous systems. Geo 1993, 21, (4), 242-250.

49. Forbes, E. A.; Posner, A. M.; Quirk, J. P., THE SPECIFIC ADSORPTION OF DIVALENT Cd, Co, Cu, Pb, AND Zn ON GOETHITE. Journal of Soil Science 1976, 27, (2), 154-166.

50. Bruemmer, G. W.; Gerth, J.; Tiller, K. G., Reaction kinetics of the adsorption and desorption of nickel, zinc and cadmium by goethite. I. Adsorption and diffusion of metals. Journal of Soil Science 1988, 39, (1), 37-52.

51. Ali, M. A.; Dzombak, D. A., Effects of simple organic acids on sorption of $Cu^{2+}$ and $Ca^{2+}$ on goethite. Geochimica et Cosmochimica Acta 1996, 60, (2), 291-304.

52. Scott, D. T.; McKnight, D. M.; Blunt-Harris, E. L.; Kolesar, S. E.; Lovley, D. R., Quinone Moieties Act as Electron Acceptors in the Reduction of Humic Substances by Humics-Reducing Microorganisms. Environmental Science & Technology 1998, 32, (19), 2984-2989.

53. Walpen, N.; Schroth, M. H.; Sander, M., Quantification of Phenolic Antioxidant Moieties in Dissolved Organic Matter by Flow-Injection Analysis with Electrochemical Detection. Environmental Science & Technology 2016.

54. Klüpfel, L.; Keiluweit, M.; Kleber, M.; Sander, M., Redox Properties of Plant Biomass-Derived Black Carbon (Biochar). Environmental Science & Technology 2014, 48, (10), 5601-5611.

55. Joshi, P.; Gorski, C. A., Anisotropic Morphological Changes in Goethite during $Fe^{2+}$-Catalyzed Recrystallization. Environmental Science & Technology 2016.

56. Fan, D.; Bradley, M. J.; Hinkle, A. W.; Johnson, R. L.; Tratnyek, P. G., Chemical Reactivity Probes for Assessing Abiotic Natural Attenuation by Reducing Iron Minerals. Environmental Science & Technology 2016.

57. Yang, Y.; Yan, W.; Jing, C., Dynamic Adsorption of Catechol at the Goethite/Aqueous Solution Interface: A Molecular-Scale Study. Langmuir 2012, 28, (41), 14588-14597.

58. Gulley-Stahl, H.; Hogan, P. A.; Schmidt, W. L.; Wall, S. J.; Buhrlage, A.; Bullen, H. A., Surface Complexation of Catechol to Metal Oxides: An ATR-FTIR, Adsorption, and Dissolution Study. Environmental Science & Technology 2010, 44, (11), 4116-4121.

59. Anschutz, A. J.; Penn, R. L., Reduction of crystalline iron(III) oxyhydroxides using hydroquinone: Influence of phase and particle size. Geochemical Transactions 2005, 6, (3), 60-60.

60. Bauer, I.; Kappler, A., Rates and Extent of Reduction of Fe(III) Compounds and $O_2$ by Humic Substances. Environmental Science & Technology 2009, 43, (13), 4902-4908.

61. Bauer, M.; Heitmann, T.; Macalady, D. L.; Blodau, C., Electron Transfer Capacities and Reaction Kinetics of Peat Dissolved Organic Matter. Environmental Science & Technology 2006, 41, (1), 139-145.

62. Nurmi, J. T.; Tratnyek, P. G., Electrochemical Properties of Natural Organic Matter (NOM), Fractions of NOM, and Model Biogeochemical Electron Shuttles. Environmental Science & Technology 2002, 36, (4), 617-624.

63. Perlinger, J. A.; Kalluri, V. M.; Venkatapathy, R.; Angst, W., Addition of Hydrogen Sulfide to Juglone. Environmental Science & Technology 2002, 36, (12), 2663-2669.

64. Uchimiya, M.; Stone, A., Reduction of Substituted p-Benzoquinones by FeII Near Neutral pH. Aquatic Geochemistry 2010, 16, (1), 173-188.

65. Kumbhar, A.; Padhye, S.; Ross, D., Cytotoxic properties of iron-hydroxynaphthoquinone complexes in rat hepatocytes. Biometals 1996, 9, (3), 235-240.

66. Padhye, S.; Garge, P.; Gupta, M. P., High-spin iron(II) complexes of ortho-functionalized paraquinones as models for quinone binding sites in reaction centres of photosynthetic bacteria. Inorganica Chimica Acta 1988, 152, (1), 37-40.

67. Halliwell, B.; Gutteridge, J. M., Oxygen toxicity, oxygen radicals, transition metals and disease. Biochem. J. 1984, 219, (1), 1-14.

68. Kessel, S. L.; Hendrickson, D. N., Binuclear ferric porphyrins bridged by the dianions of hydroquinones. Inorganic Chemistry 1980, 19, (7), 1883-1889.

69. Kessel, S. L.; Emberson, R. M.; Debrunner, P. G.; Hendrickson, D. N., Iron(III), manganese(III), and cobalt(III) complexes with single chelating o-semiquinone ligands. Inorganic Chemistry 1980, 19, (5), 1170-1178.

70. Kessel, S. L.; Hendrickson, D. N., Magnetic exchange interactions in binuclear transition-metal complexes. 16. Binuclear ferric complexes from the reaction of iron(II)(salen) with p-quinones. Inorganic Chemistry 1978, 17, (9), 2630-2636.

71. Stookey, L. L., Ferrozine---a new spectrophotometric reagent for iron. Analytical Chemistry 1970, 42, (7), 779-781.

72. Platte, J. A.; Marcy, V. M., Photometric Determination of Zinc with Zincon. Application to Water Containing Heavy Metals. Analytical Chemistry 1959, 31, (7), 1226-1228.

73. Schwarzenbach, R. P.; Stierli, R.; Lanz, K.; Zeyer, J., Quinone and iron porphyrin mediated reduction of nitroaromatic compounds in homogeneous aqueous solution. Environmental Science & Technology 1990, 24, (10), 1566-1574.

74. Larese-Casanova, P.; Kappler, A.; Haderlein, S. B., Heterogeneous oxidation of Fe(II) on iron oxides in aqueous systems: Identification and controls of Fe(III) product formation. Geochimica et Cosmochimica Acta 2012, 91, (0), 171-186.

75. Hider, R. C.; Mohd-Nor, A. R.; Silver, J.; Morrison, I. E. G.; Rees, L. V. C., Model compounds for microbial iron-transport compounds. Part 1. Solution chemistry and Mossbauer study of iron(II) and iron(III) complexes from phenolic and catecholic systems. Journal of the Chemical Society, Dalton Transactions 1981, 0, (2), 609-622.

76. Avdeef, A.; Sofen, S. R.; Bregante, T. L.; Raymond, K. N., Coordination chemistry of microbial iron transport compounds. 9. Stability constants for catechol models of enterobactin. Journal of the American Chemical Society 1978, 100, (17), 5362-5370.

77. Mentasti, E.; Pelizzetti, E.; Saini, G., Reactions between iron(III) and catechol (o-dihydroxybenzene). Part II. Equilibria and kinetics of the redox reaction in aqueous acid solution. Journal of the Chemical Society, Dalton Transactions 1973, 0, (23), 2609-2614.

78. Mentasti, E.; Pelizzetti, E., Reactions between iron(III) and catechol (o-dihydroxybenzene). part I. Equilibria and kinetics of complex formation in aqueous acid solution. Journal of the Chemical Society, Dalton Transactions 1973, 0, (23), 2605-2608.

79. Paul, T.; Liu, J.; Machesky, M. L.; Strathmann, T. J., Adsorption of zwitterionic fluoroquinolone antibacterials to goethite: A charge distribution-multisite complexation model. Journal of Colloid and Interface Science 2014, 428, 63-72.

80. Marsac, R.; Martin, S.; Boily, J.-F.; Hanna, K., Oxolinic Acid Binding at Goethite and Akaganéte Surfaces: Experimental Study and Modeling. Environmental Science & Technology 2015.

81. Gu, X.; Tan, Y.; Tong, F.; Gu, C., Surface complexation modeling of coadsorption of antibiotic ciprofloxacin and Cu(II) and onto goethite surfaces. Chemical Engineering Journal 2015, 269, 113-120.

82. Chen, C.; Dynes, J. J.; Wang, J.; Sparks, D. L., Properties of Fe-Organic Matter Associations via Coprecipitation versus Adsorption. Environmental Science & Technology 2014.

83. Fulda, B.; Voegelin, A.; Maurer, F.; Christl, I.; Kretzschmar, R., Copper Redox Transformation and Complexation by Reduced and Oxidized Soil Humic Acid. 1. X-ray Absorption Spectroscopy Study. Environmental Science & Technology 2013.

84. Hoffmann, M.; Mikutta, C.; Kretzschmar, R., Arsenite Binding to Natural Organic Matter: Spectroscopic Evidence for Ligand Exchange and Ternary Complex Formation. Environmental Science & Technology 2013.

85. Maurer, F.; Christl, I.; Fulda, B.; Voegelin, A.; Kretzschmar, R., Copper Redox Transformation and Complexation by Reduced and Oxidized Soil Humic Acid. 2. Potentiometric Titrations and Dialysis Cell Experiments. Environmental Science & Technology 2013.

86. Orsetti, S.; Marco-Brown, J. L.; Andrade, E. M.; Molina, F. V., Pb(II) Binding to Humic Substances: An Equilibrium and Spectroscopic Study. Environmental Science & Technology 2013.

87. Zhang, C.; Zhang, D.; Li, Z.; Akatsuka, T.; Yang, S.; Suzuki, D.; Katayama, A., Insoluble Fe-Humic Acid Complex as a Solid-Phase Electron Mediator for Microbial Reductive Dechlorination. Environmental Science & Technology 2014.

88. Catrouillet, C.; Davranche, M.; Dia, A.; Coz, M. B.-L.; Marsac, R.; Pourret, O.; Gruau, G., Geochemical modeling of Fe(II) binding to humic and fulvic acids. Chemical Geology, (0).

89. Philippe, A.; Schaumann, G. E., Interactions of Dissolved Organic Matter with Natural and Engineered Inorganic Colloids: A Review. Environmental Science & Technology 2014.

90. Orsetti, S.; Andrade, E. M.; Molina, F. V., Modeling Ion Binding to Humic Substances: Elastic Polyelectrolyte Network Model. Langmuir 2010, 26, (5), 3134-3144.

91. Yamamoto, M.; Nishida, A.; Otsuka, K.; Komai, T.; Fukushima, M., Evaluation of the binding of iron(II) to humic substances derived from a compost sample by a colorimetric method using ferrozine. Bioresource Technology 2010, 101, (12), 4456-4460.

92. Schlautman, M. A.; Morgan, J. J., Adsorption of aquatic humic substances on colloidal-size aluminum oxide particles: Influence of solution chemistry. Geochimica et Cosmochimica Acta 1994, 58, (20), 4293-4303.

93. Xue, Z.; Orsetti, S.; Marsac, R.; Lützenkirchen, J.; Haderlein, S. B., Effects of Sorbed Quinone/Hydroquinone on Electron Transfer and Apparent Redox Potential of Goethite. to be Submitted.

94. Tang, W.-W.; Zeng, G.-M.; Gong, J.-L.; Liang, J.; Xu, P.; Zhang, C.; Huang, B.-B., Impact of humic/fulvic acid on the removal of heavy metals from aqueous solutions using nanomaterials: A review. Science of The Total Environment 2014, 468–469, (0), 1014-1027.

95. Prado, A. G. S.; Torres, J. D.; Martins, P. C.; Pertusatti, J.; Bolzon, L. B.; Faria, E. A., Studies on copper(II)- and zinc(II)-mixed ligand complexes of humic acid. Journal of Hazardous Materials 2006, 136, (3), 585-588.

96. Tuchagues, J. P. M.; Hendrickson, D. N., Iron(III) complexes with semiquinone and hydroquinone ligands. Inorganic Chemistry 1983, 22, (18), 2545-2552.

97. Garge, P.; Chikate, R.; Padhye, S.; Savariault, J. M.; De Loth, P.; Tuchagues, J. P., Iron(II) complexes of ortho-functionalized naphthoquinones. 2. Crystal and molecular structure of bis(aquo)bis(lawsonato)iron(II) and intermolecular magnetic exchange interactions in bis(3-aminolawsonato)iron(II). Inorganic Chemistry 1990, 29, (18), 3315-3320.

98. Yamahara, R.; Ogo, S.; Masuda, H.; Watanabe, Y., (Catecholato)iron(III) complexes: structural and functional models for the catechol-bound iron(III) form of catechol dioxygenases. Journal of Inorganic Biochemistry 2002, 88, (3–4), 284-294.

99. Maurer, F.; Christl, I.; Kretzschmar, R., Reduction and Reoxidation of Humic Acid: Influence on Spectroscopic Properties and Proton Binding. Environmental Science & Technology 2010, 44, (15), 5787-5792.

100. Yu, Z.; Peiffer, S.; Göttlicher, J.; Knorr, K.-H., Electron transfer budgets and kinetics of abiotic oxidation and incorporation of aqueous sulfide by dissolved organic matter. Environmental Science & Technology 2015.

101. Struyk, Z.; Sposito, G., Redox properties of standard humic acids. Geoderma 2001, 102, (3–4), 329-346.

102. Naka, D.; Kim, D.; Strathmann, T. J., Abiotic Reduction of Nitroaromatic Compounds by Aqueous Iron(II)−Catechol Complexes. Environmental Science & Technology 2006, 40, (9), 3006-3012.

103. C., H. R.; Brendan., H.; R., M. j.; Mohd-Nor, A. R.; Silver, J., Model Compounds for Microbial Iron-transport Compounds.Part IV. Further Solution Chemistry and Miissbauer Studies on Iron(II)and Iron(III) Catechol Complexes. Inorganica Chimica Acta 1983, 80, 51-56.

104. Cox, D. D.; Benkovic, S. J.; Bloom, L. M.; Bradley, F. C.; Nelson, M. J.; Que, L.; Wallick, D. E., Catecholate LMCT bands as probes for the active sites of nonheme iron oxygenases. Journal of the American Chemical Society 1988, 110, (7), 2026-2032.

105. McBride, M. B., Adsorption and Oxidation of Phenolic Compounds by Iron and Manganese Oxides1. Soil Science Society of America Journal 1987, 51, (6), 1466-1472.

106. Kumbhar, A. S.; Padhye, S. B.; Jitender; Kale, R. K., Naturally Occurring Hydroxy Napthoquinones and Their Iron Complexes as Modulators of Radiation Induced Lipid Peroxidation in Synaptosomes. Metal-Based Drugs 1997, 4, (5), 279-285.

107. Valle-Bourrouet, G.; Ugalde-Saldívar, V. M.; Gómez, M.; Ortiz-Frade, L. A.; González, I.; Frontana, C., Magnetic interactions as a stabilizing factor of semiquinone species of lawsone by metal complexation. Electrochimica Acta 2010, 55, (28), 9042-9050.

108. Hanna, K.; Martin, S.; Quilès, F.; Boily, J. F., Sorption of Phthalic Acid at Goethite Surfaces under Flow-Through Conditions. Langmuir 2014, 30, (23), 6800-6807.

109. Yang, Y.; Du, J.; Jing, C., Dynamic adsorption process of phthalate at goethite/aqueous interface: An ATR-FTIR study. Colloids and Surfaces A: Physicochemical and Engineering Aspects 2014, 441, (0), 504-509.

110. Xue, Z.; Orsetti, S.; Haderlein, S. B., Effects of sorbed natural organic matter (NOM) on electron transfer at Fe(II)/goethite interface. to be Submitted.

111. Boily, J.-F.; Persson, P.; Sjöberg, S., Benzenecarboxylate surface complexation at the goethite (α-FeOOH)/water interface: II. Linking IR spectroscopic observations to mechanistic surface complexation models for phthalate, trimellitate, and pyromellitate. Geochimica et Cosmochimica Acta 2000, 64, (20), 3453-3470.

112. Berthomieu, C.; Nabedryk, E.; Mäntele, W.; Breton, J., Characterization by FTIR spectroscopy of the photoreduction of the primary quinone acceptor QA in photosystem II. FEBS Letters 1990, 269, (2), 363-367.

113. Nonella, M.; Mathias, G.; Tavan, P., Infrared Spectrum of p-Benzoquinone in Water Obtained from a QM/MM Hybrid Molecular Dynamics Simulation. The Journal of Physical Chemistry A 2003, 107, (41), 8638-8647.

114. Maximov, O. B.; Glebko, L. I., Quinoid groups in humic acids. Geoderma 1974, 11, (1), 17-28.

115. Al-Faiyz, Y. S. S., CPMAS 13C NMR characterization of humic acids from composted agricultural Saudi waste. Arabian Journal of Chemistry 2017, 10, Supplement 1, S839-S853.

116. Samios, S.; Lekkas, T.; Nikolaou, A.; Golfinopoulos, S., Structural investigations of aquatic humic substances from different watersheds. Desalination 2007, 210, (1), 125-137.

117. Sachs, S.; Bernhard, G., Humic acid model substances with pronounced redox functionality for the study of environmentally relevant interaction processes of metal ions in the presence of humic acid. Geoderma 2011, 162, (1–2), 132-140.

118. Shin, H.-S.; Monsallier, J. M.; Choppin, G. R., Spectroscopic and chemical characterizations of molecular size fractionated humic acid. Talanta 1999, 50, (3), 641-647.

119. Lumsdon, D. G.; Fraser, A. R., Infrared Spectroscopic Evidence Supporting Heterogeneous Site Binding Models for Humic Substances. Environmental Science & Technology 2005, 39, (17), 6624-6631.

120. Kang, S.; Xing, B., Humic Acid Fractionation upon Sequential Adsorption onto Goethite. Langmuir 2008, 24, (6), 2525-2531.

121. Hanna, K.; Quilès, F., Surface Complexation of 2,5-Dihydroxybenzoic Acid (Gentisic Acid) at the Nanosized Hematite−Water Interface: An ATR-FTIR Study and Modeling Approach. Langmuir 2011, 27, (6), 2492-2500.

122. Hanna, K.; Boily, J. F., Sorption of Two Naphthoic Acids to Goethite Surface under Flow through Conditions. Environmental Science & Technology 2010, 44, (23), 8863-8869.

123. Weng, L. P.; Koopal, L. K.; Hiemstra, T.; Meeussen, J. C. L.; Van Riemsdijk, W. H., Interactions of calcium and fulvic acid at the goethite-water interface. Geochimica et Cosmochimica Acta 2005, 69, (2), 325-339.

124. Duan, J.; Wang, J.; Graham, N.; Wilson, F., Coagulation of humic acid by aluminium sulphate in saline water conditions. Desalination 2002, 150, (1), 1-14.

125. Yoon, S.-H.; Lee, C.-H.; Kim, K.-J.; Fane, A. G., Effect of calcium ion on the fouling of nanofilter by humic acid in drinking water production. Water Research 1998, 32, (7), 2180-2186.

126. Tipping, E.; Hurley, M. A., A unifying model of cation binding by humic substances. Geochimica et Cosmochimica Acta 1992, 56, (10), 3627-3641.

127. Uchimiya, M.; Stone, A. T., Redox reactions between iron and quinones: Thermodynamic constraints. Geochimica et Cosmochimica Acta 2006, 70, (6), 1388-1401.

# Statement of Personal Contribution

Here, I state clearly that the general concept of this thesis was developed by Prof. Dr. Stefan Haderlein, Dr. Christine Laskov, Dr. Silvia Orsetti and me. All the experimental ideas were proposed by Prof. Dr. Stefan Haderlein, Dr. Silvia Orsetti and me. The detailed laboratory work and data analysis were conducted by myself. Prof. Dr. Stefan Haderlein and Dr. Silvia Orsetti financially supported my experimental work.

In Chapter 2, the initial idea was conceptualized by Prof. Dr. Stefan Haderlein, Dr. Silvia Orsetti and me. It was further supplemented by Dr. Rémi Marsac and Dr. Johannes Lützenkirchen. The experimental work was performed by myself. It contained the characterization of the redox species of lawsone, methods developed to determine their concentration, as well as sorption isotherms investigation under various conditions. And the dataset evaluation of lawsone sorption and the calculation of apparent reduction potential of goethite-Fe(II) surface were also done by me and discussed together with Prof. Dr. Stefan Haderlein and Dr. Silvia Orsetti. Furthermore, the sorption isotherm of oxidized lawsone on goethite-Fe(II) fitted by two Langmuir models was found and modelled by Dr. Rémi Marsac. The manuscript was prepared by me, together with Prof. Dr. Stefan Haderlein, Dr. Silvia Orsetti, Dr. Rémi Marsac and Dr. Johannes Lützenkirchen.

In Chapter 3, the initial idea behind this chapter was designed by Prof. Dr. Stefan Haderlein, Dr. Silvia Orsetti and me. The experimental work in the glovebox was carried out by myself. It contained the characterization of the redox species of Aldrich humic acid (AHA), $Fe(II)_{aq}$ concentration determination and investigating the AHA sorption isotherms. Only DOC measurements were performed by the technician Bernice Nisch in Prof. Dr. Peter Grathwohl's group. Additionally, the data analysis was done by me and discussed in detailed with Prof. Dr. Stefan Haderlein and Dr. Silvia Orsetti. The manuscript was written by me and later revised by Prof. Dr. Stefan Haderlein, Dr. Silvia Orsetti.

In Chapter 4, the initial idea present in this chapter was suggested by Prof. Dr. Stefan Haderlein, Dr. Silvia Orsetti and me. The experimental work about ATR-FTIR spectroscopy was carried out by myself in Lother-Meyer-Bau. The FTIR equipment belonged to Prof. Dr. Marcus Nowak's group. The technician Annette Flicker in this group provided me the introduction about the FTIR machine and maintained the equipment. Then the flow cell measurements of ATR-FTIR was established by me in Lother-Meyer-Bau. The following the IR spectroscopic measurements were conducted by myself. the data analysis was done by me and discussed in detailed with Prof. Dr. Stefan Haderlein and Dr. Silvia Orsetti. The manuscript was written by me and Prof. Dr. Stefan Haderlein, Dr. Silvia Orsetti. And Dr. Usman Muhammad gave fruitful of advice to improve the quality of the script.

# Acknowledgement

# Curriculum Vitae

## Personal data

| | |
|---|---|
| Name | Xue Zhengrong |
| Address | Leipart Str. 14, 81369, München, Germany |
| Birthday and place | 05.06.1986, Shanghai |
| Nationality | P.R. China |
| Institution | Faculty of science |
| | Department of Geoscience – Environmental Mineralogy Group |
| | Eberhard-Karls Universität Tübingen |
| | Telefon: +49-015784318022 |
| | E-Mail: xuezhengrong0459131@hotmail.com |

## Education

| | |
|---|---|
| Since 04/2012 | PhD study in Department of Geoscience – Environmental Mineralogy Group |
| | Universität Tübingen, Germany |
| 10.2009 – 10.2011 | Master degree in Applied Environmental Geoscience. |
| | Universität Tübingen, Germany |
| 03.2007 - 09.2008 | Bachelor degree in Environment Engineering and Technology |
| | Fachhochschule Lübeck, Germany |
| 09.2004 - 03.2007 | Bachelor degree in Chemical Engineering and Technology |
| | East China University of Science and Technology, China |
| Courses Taken | Aqueous and Environmental chemistry, Hydrogeology, Environmental modeling (MATLAB), Aqueous chemistry modeling (PHREEQC), Contaminant hydrogeology, Environmental isotope chemistry, Geotechnical engineering, Lab course environmental chemistry, Air pollution and control, Waste water treatment. Bachelor/Master thesis. |

## Knowledge Background

| | |
|---|---|
| Analytical techniques | Water and mineral analyze, field sampling, work in oxic and anoxic condition (glovebox), UV, DOC, Fluorescence spectropy, HPLC/MS, GC-MS, ATR-FTIR technique |
| Language | Fluent in German and English |
| Computer skills | Good at Matlab, Phreeqc |

## Awards

| | |
|---|---|
| Sep.2005 | Scholarship of East china University of Science and Technology |
| Sep.2006 | Scholarship of East china University of Science and Technology |

## Conferences attended

| | |
|---|---|
| 27-29.05.2013 | Junger Umweltwissenschaftler 2013 |
| | Poster contributions |